Coherent Diffraction Imaging

Ross Harder aka "The Imposter"

34-ID-C

Advanced Photon Source

~~https://tinyurl.com/y2qtrz7c~~

Acknowledgments:

Prof. Ian Robinson (BNL)

Dr. Xiaojing Huang (BNL)

Dr. Jesse Clark (~~PULSE institute, SLAC~~ Amazon)

Prof. Oleg Shpyrko (UCSD)

Dr. Andrew Ulvestad (~~ANL – MSD~~Tesla)

Dr. Ian McNulty (~~ANL – CNM~~ MaxIV)

Dr. Junjing Deng (ANL – APS)

Compact Objects (CDI)

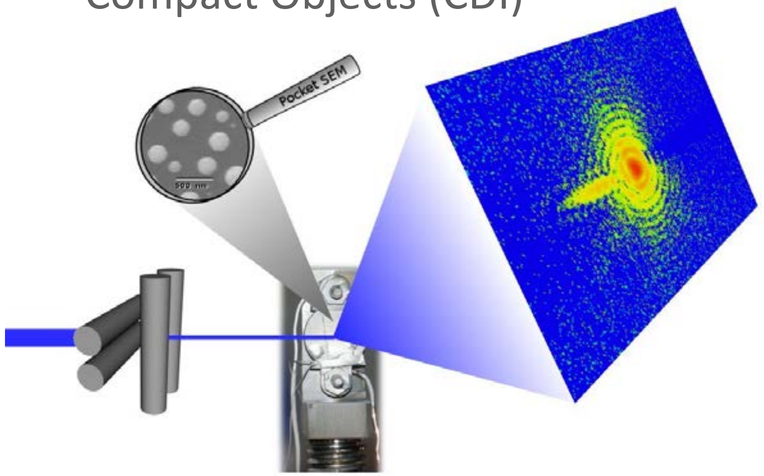

Non-compact samples (Ptychography)

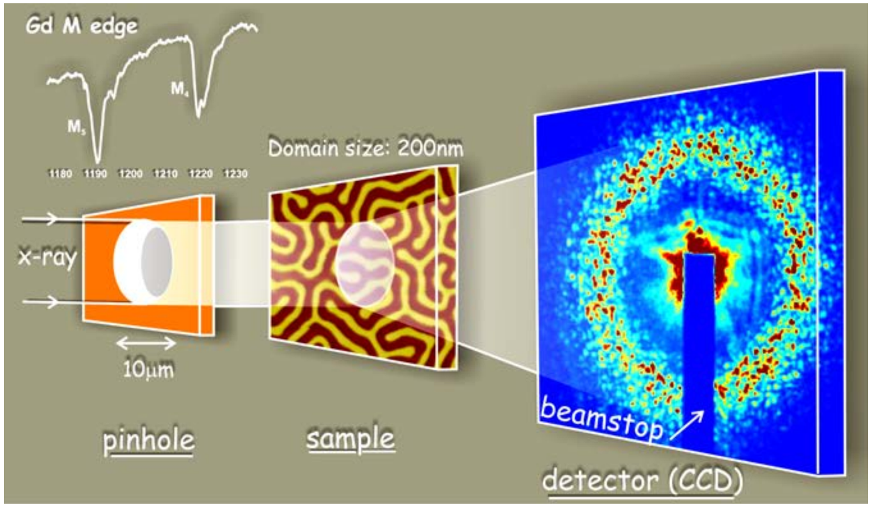

Argonne NATIONAL LABORATORY

COHERENCE

$$\Gamma(\mathbf{r}_1, \mathbf{r}_2; \tau) = \left\langle E^*(\mathbf{r}_1, t)E(\mathbf{r}_2, t + \tau)\right\rangle$$

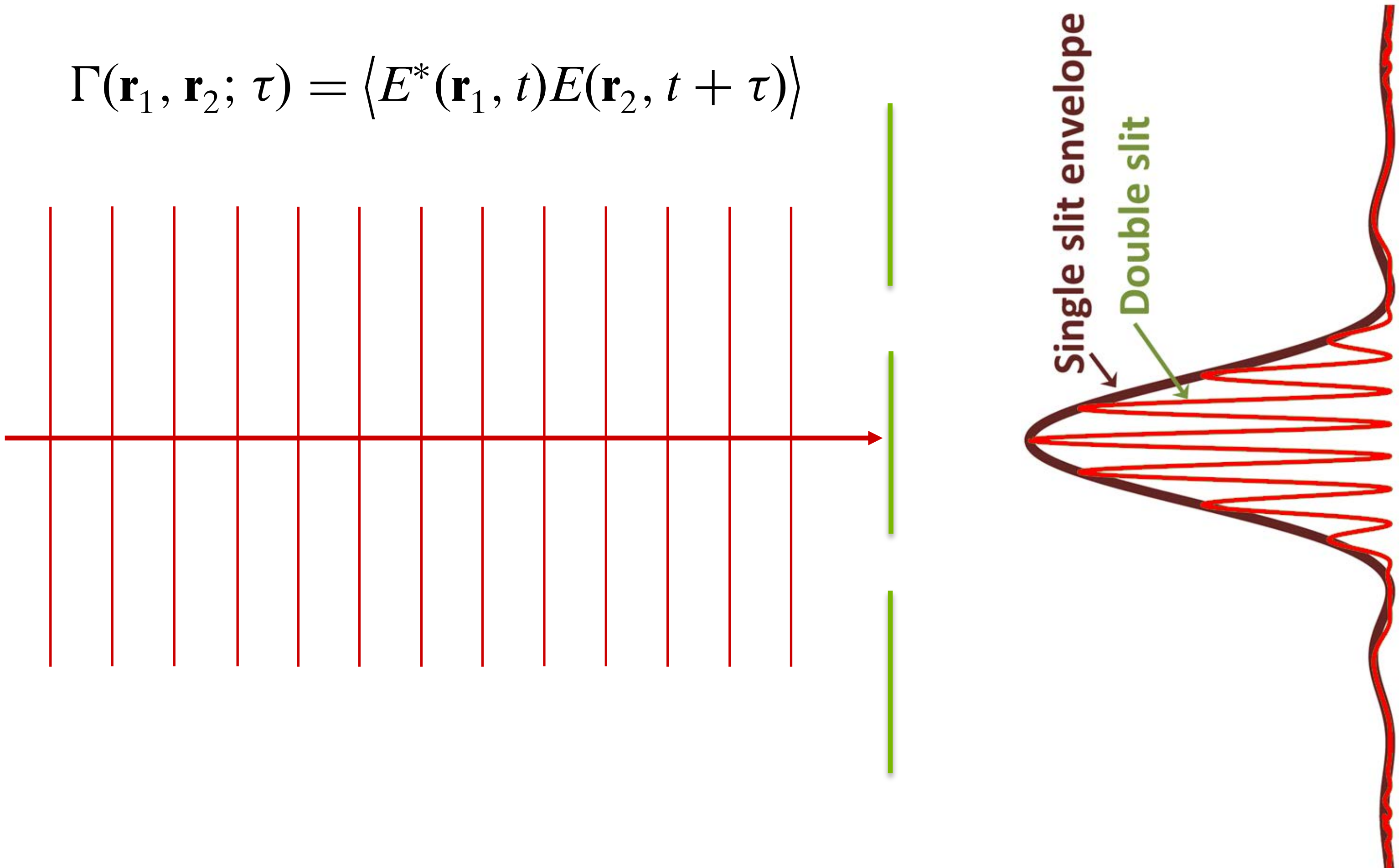

Visibility of fringes is a direct measure of the coherence of a beam.
If beam is coherent across the spacing of the slits a Fourier Transform of the slit structure is observed downstream.

COHERENCE

longitudinal coherence

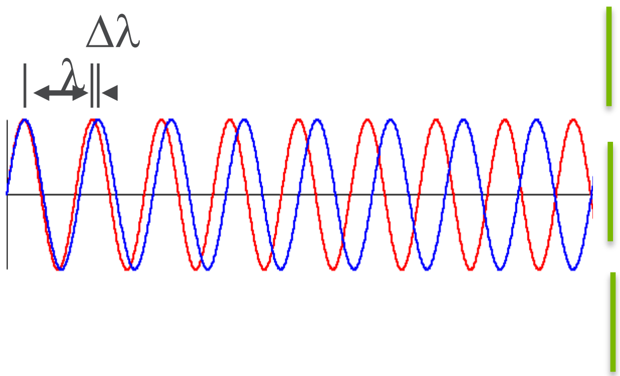

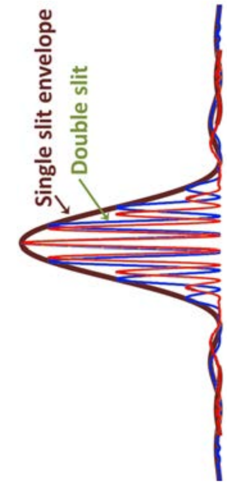

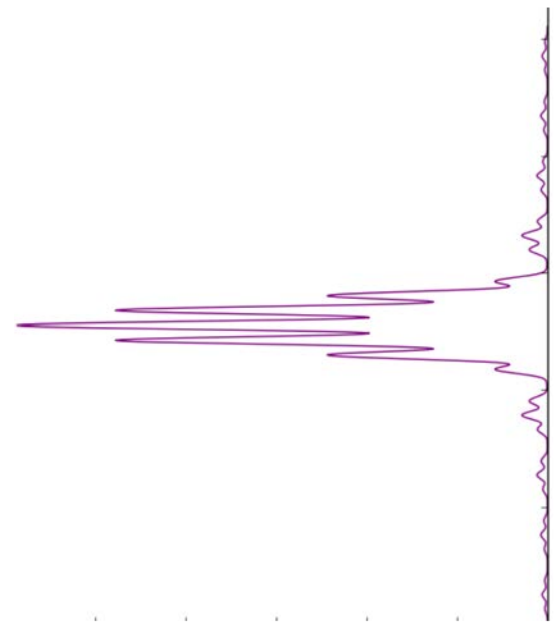

transverse coherence

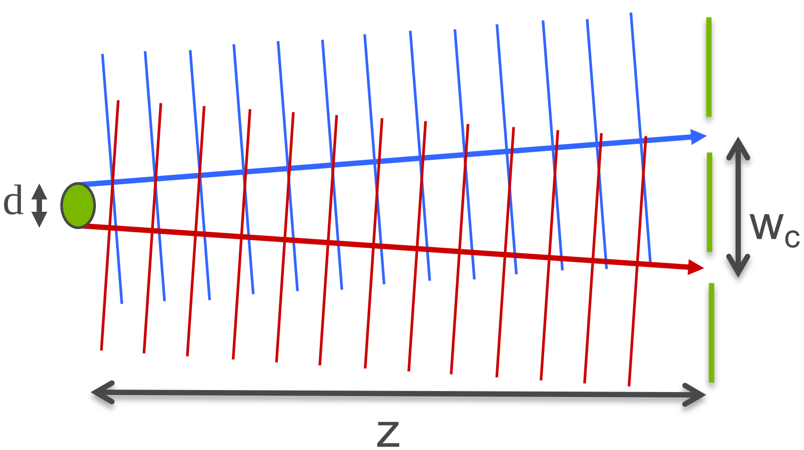

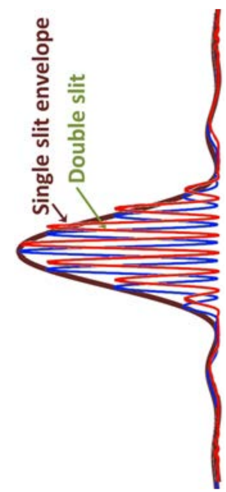

COHERENCE

longitudinal coherence

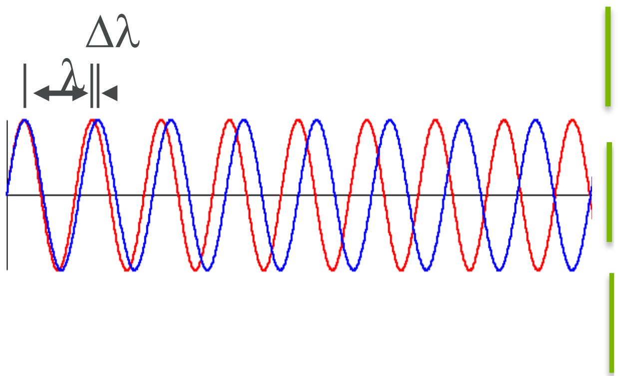

$$l_c \sim \frac{\lambda^2}{\Delta\lambda}$$

$$\tau_c \sim \frac{\lambda^2}{c\Delta\lambda}$$

Si (111)
0.5 um or 1.5 fs

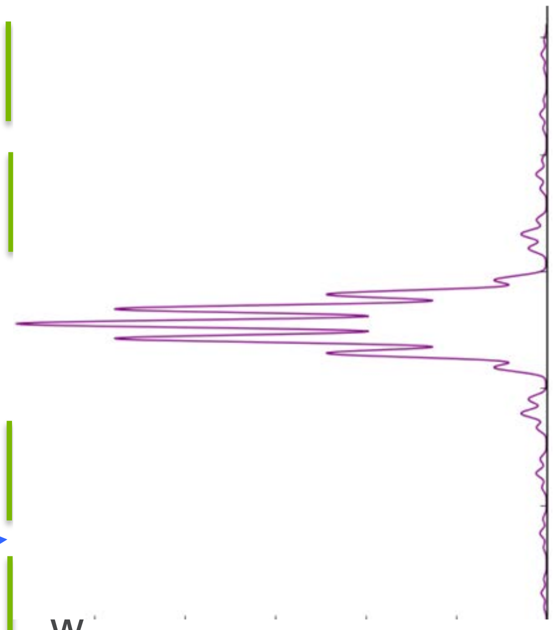

transverse coherence

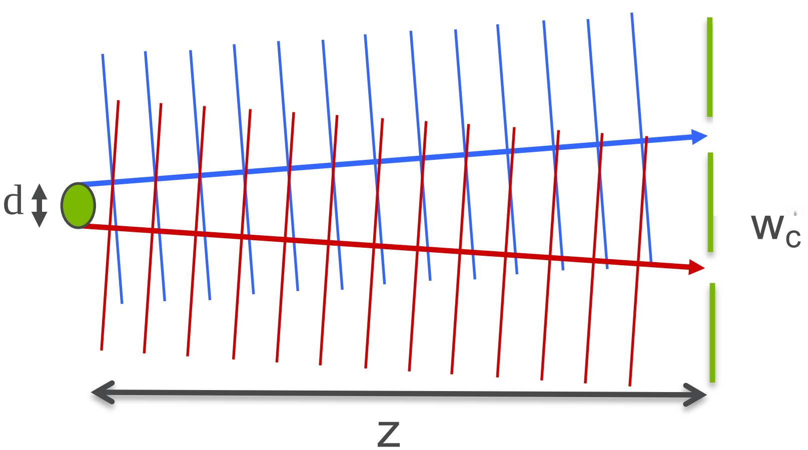

$$w_c \sim \frac{\lambda z}{d}$$

34-ID-C 50m
25x70 um @ 9 keV

Courtesy Prof. Oleg Shpyrko (UCSD)

Coherence: Laser Speckle

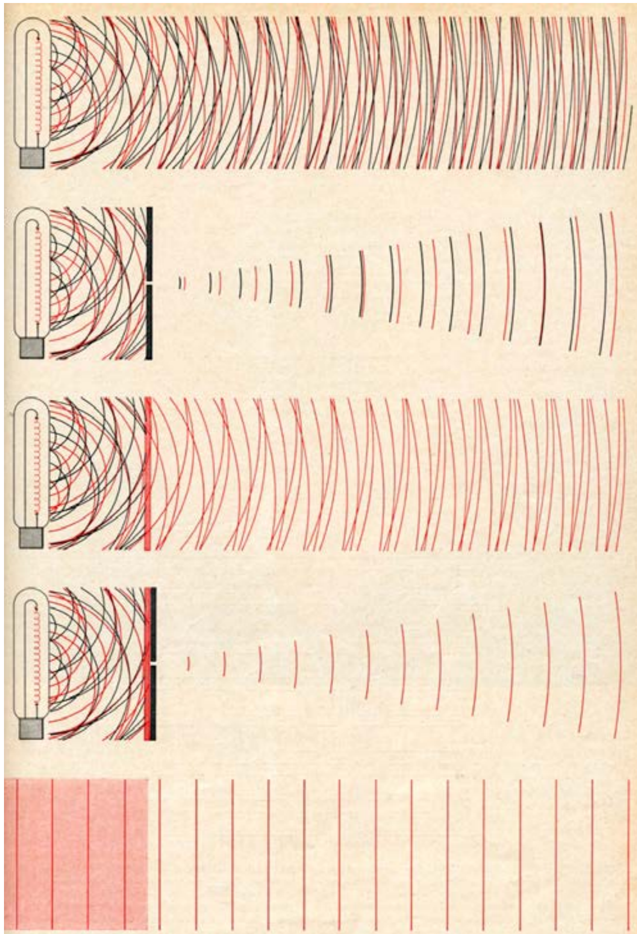

A. L. Schawlow "Laser Light"
Scientific American, 219 (3), p. 120, (1968)

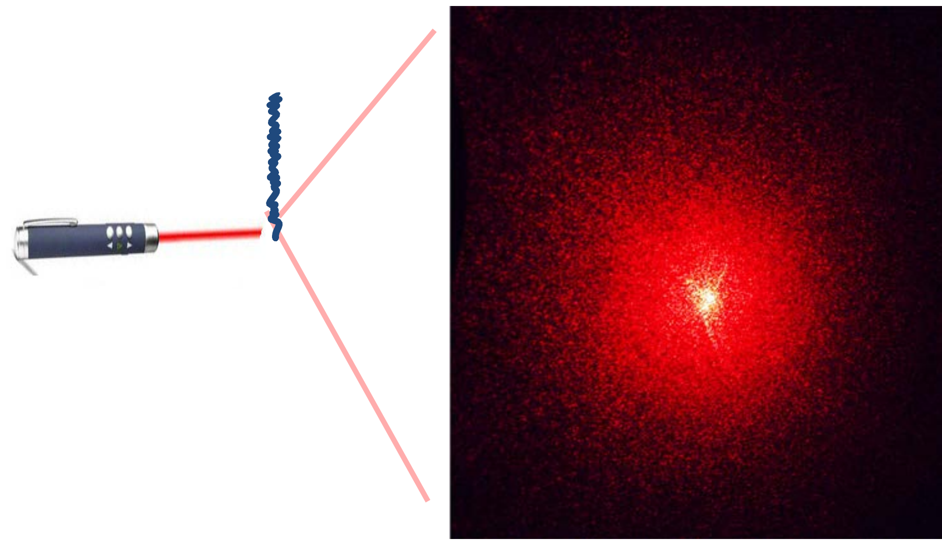

Laser Speckle: Interference pattern arising from randomly distributed scatterers

Argonne NATIONAL LABORATORY

SIMPLEST SPECKLE EXPERIMENT: TWINKLE, TWINKLE LITTLE STAR

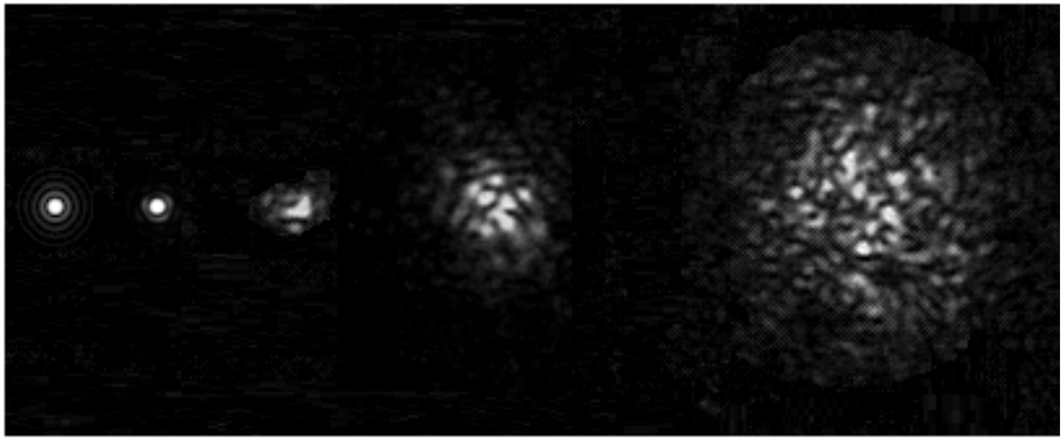

$(D/r_0) \rightarrow$ 0.5 1 3 6 12

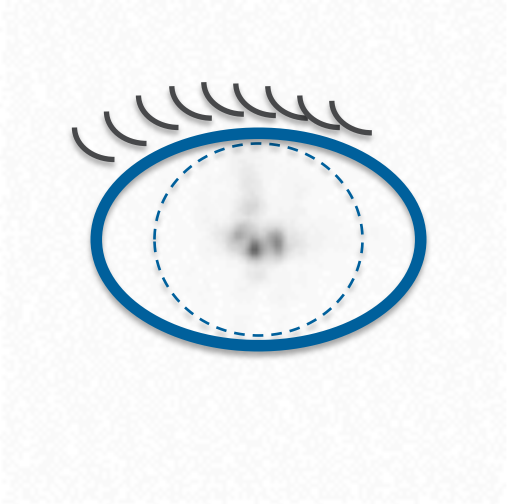

Stars are big, but very far away. As a result, their light has a high transverse coherence. As the light propagates through the atmosphere our eye detects a portion of the coherent diffraction

Courtesy Prof. Oleg Shpyrko (UCSD)

First Speckle: Exner, 1877

(using candle light)

First Speckle Photo: von Laue, 1914

(using arc discharge lamp)

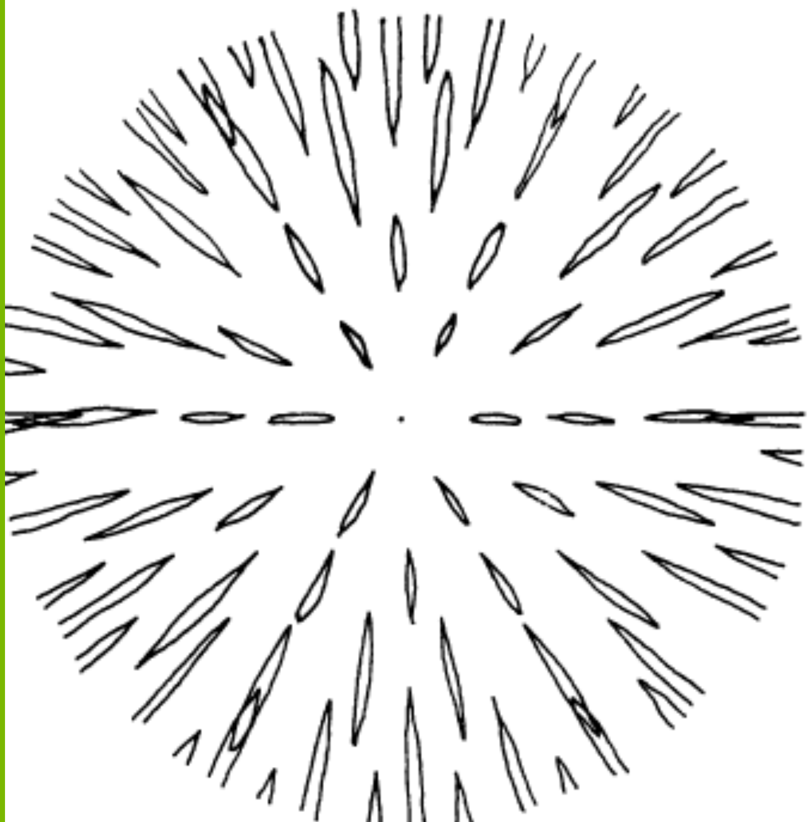

K. Exner: Sitzungsber. Kaiserl. Akad. Wiss. (Wien) 76, 522 (1877)

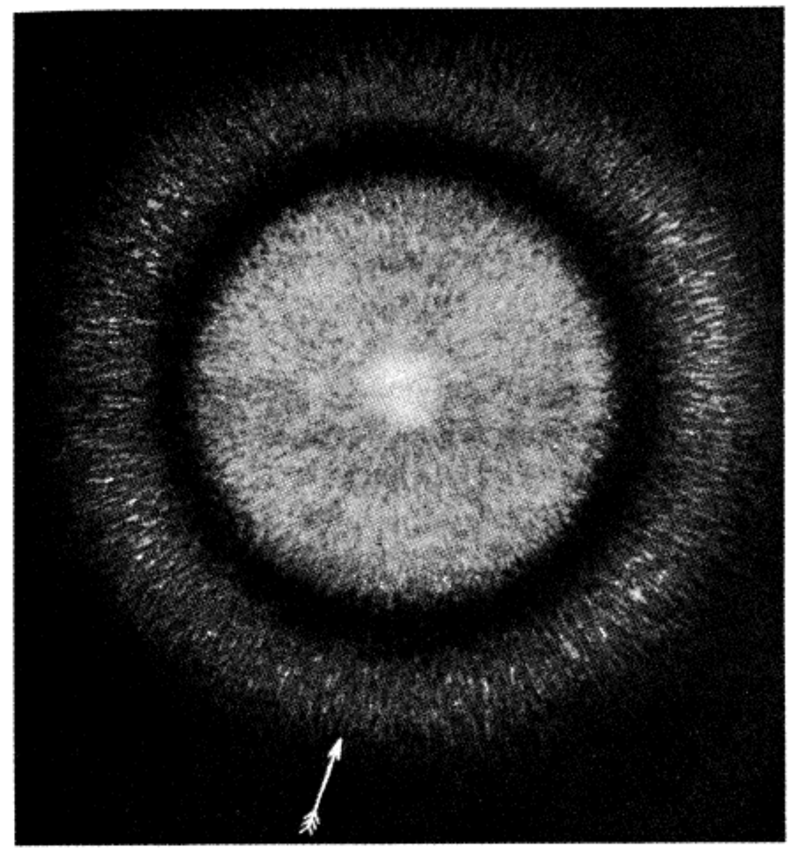

M. von Laue: Sitzungsber. Akad. Wiss. (Berlin) 44, 1144 (1914)

Argonne NATIONAL LABORATORY

Courtesy Prof. Oleg Shpyrko (UCSD)

First X-ray Speckle:

M. Sutton et al., *Nature* **352**, 608-610 (1991)

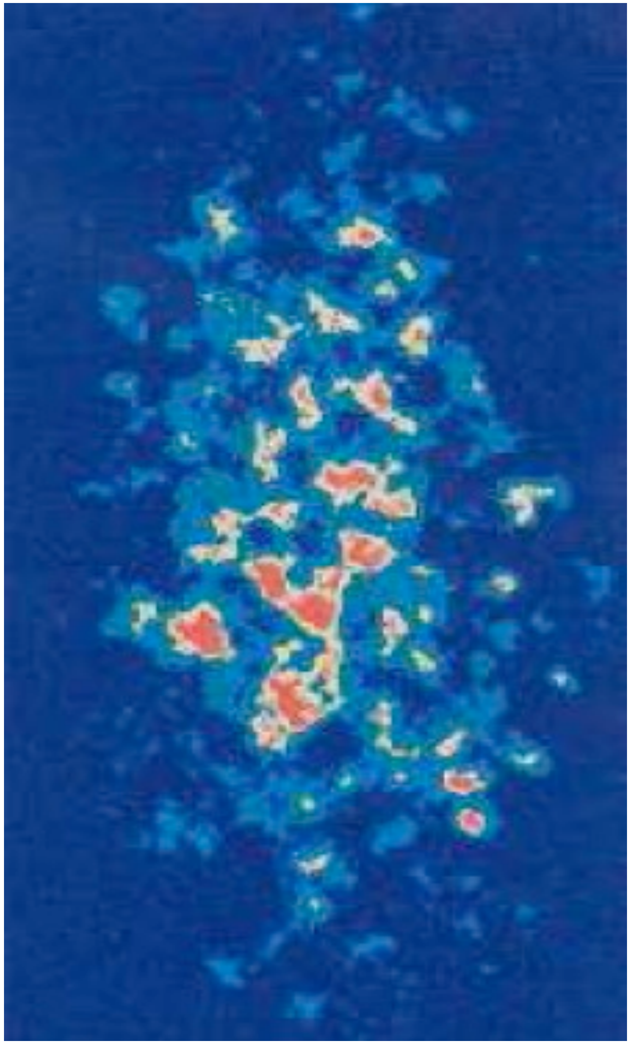

$$I \propto |F(q)|^2$$

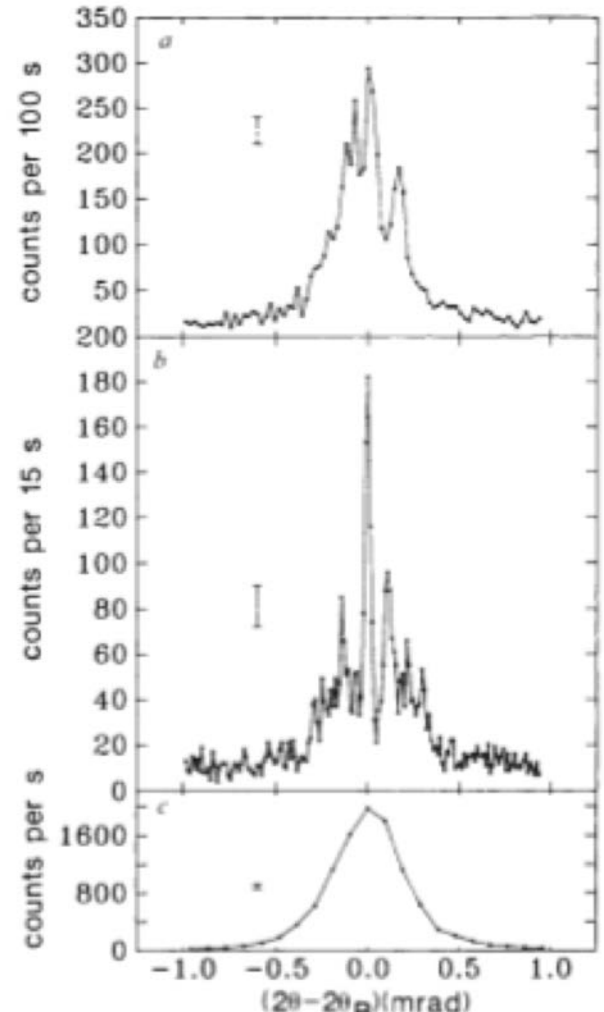

FIG. 4 Speckle patterns measured using *a*, 2.5-μm, *b*, 5 μm and *c*, 50-μm collimating pinholes. The analysing pinholes used were 50, 25 and 100 μm, respectively. Representative error bars are indicated, and the solid lines simply connect the data points. The (001) Bragg angle, $2\theta_B$, is ~23.9°.

Courtesy Prof. Oleg Shpyrko (UCSD)

WHY USE SYNCHROTRON RADIATION?

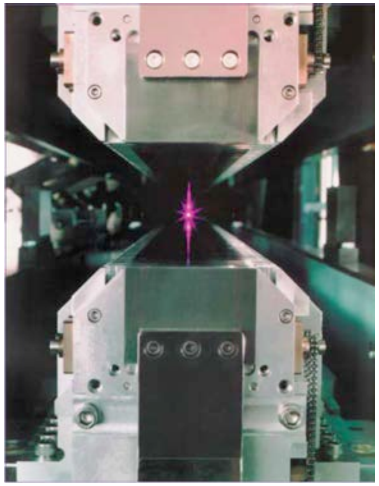

Synchrotron sources offer:

- Brightnesss (small source, collimated)
- Tunability (IR to hard x-rays)
- Polarization (linear, circular)
- Time structure (short pulses)

Source brightness is the key figure of merit for coherent imaging

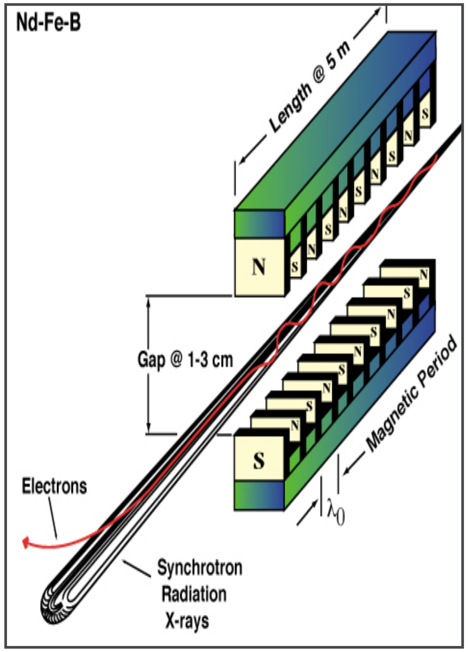

B = photons/source area, divergence, bandwidth

$F_c \sim \lambda^2 B$

Argonne NATIONAL LABORATORY

COHERENT X-RAY REFERENCES

- Vartanyants, I A, and A Singer. 2010 “Coherence Properties of Hard X-Ray Synchrotron Sources and X-Ray Free-Electron Lasers.” *New Journal of Physics* 12 (3): 035004.
- Singer, Andrej, and Ivan A Vartanyants. 2014. “Coherence Properties of Focused X-Ray Beams at High-Brilliance Synchrotron Sources.” *Journal of Synchrotron Radiation* 21 (1). International Union of Crystallography: 5–15. doi:10.1038/nnano.2008.246.
- Nugent, Keith. 2009. “Coherent Methods in the X-Ray Sciences.” *Advances in Physics* 59 (1): 1–99. doi:doi: 10.1080/00018730903270926.

Courtesy Prof. Oleg Shpyrko (UCSD)

X-RAYS, TWO EXTREMES FOR STRUCTURAL STUDY:

X-ray Imaging (Shadowgraphs)

- Inhomogeneous, non-periodic materials
- Limited spatial resolution (~0.001 mm)

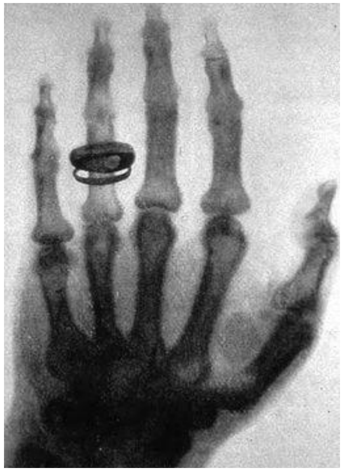

Roentgen, Nobel 1900

X-ray Diffraction (Scattering)

Coherent Imaging is scattering

- Is particularly sensitive to periodicity in the sample (Crystals)
- Atomic resolution (unit cell)

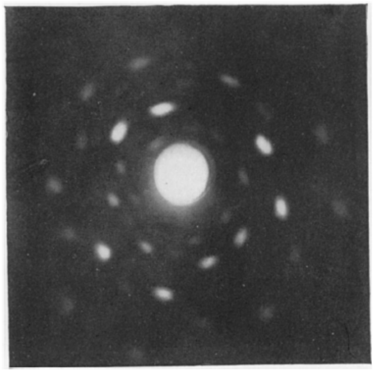

Von Laue, Nobel 1914
Bragg & Bragg, Nobel 1915

Argonne NATIONAL LABORATORY

IMAGING REGIMES WITH COHERENT X-RAYS

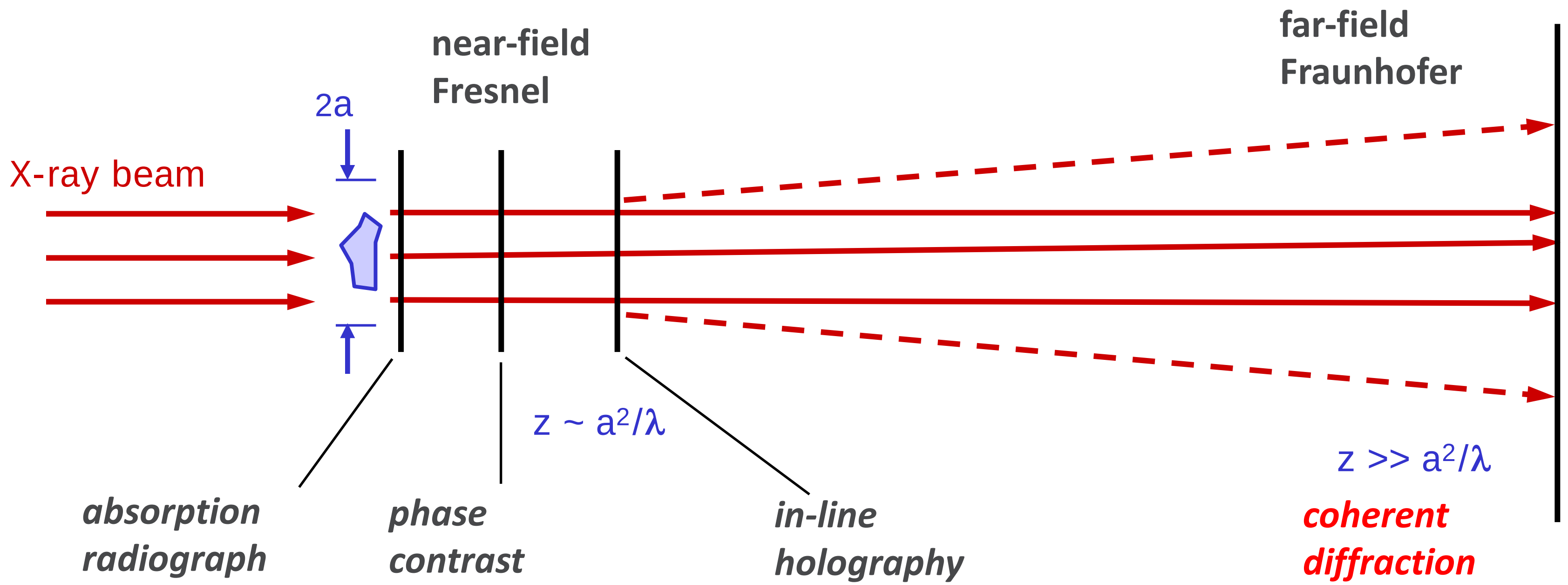

Kagoshima (1999)

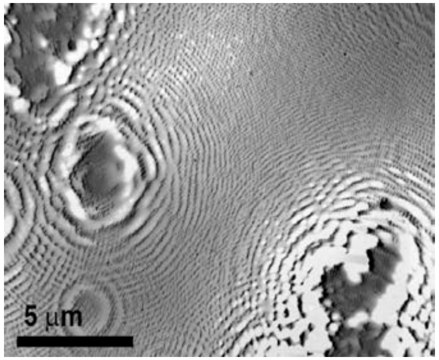

Jacobsen (1990)

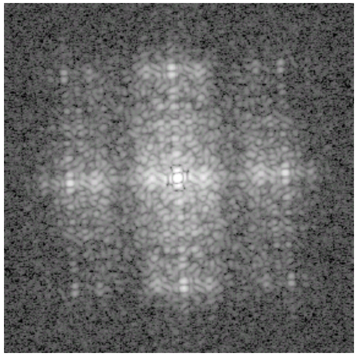

Miao (1999)

REFRACTIVE INDEX AND CONTRAST IN THE X-RAY REGION

$$n = 1 - \delta - i\beta = 1 - \frac{r_e}{2\pi}\lambda^2 \sum_i n_i f_i(0)$$

$$A = A_0 \exp(-inkt)$$
$$k = 2\pi / \lambda$$

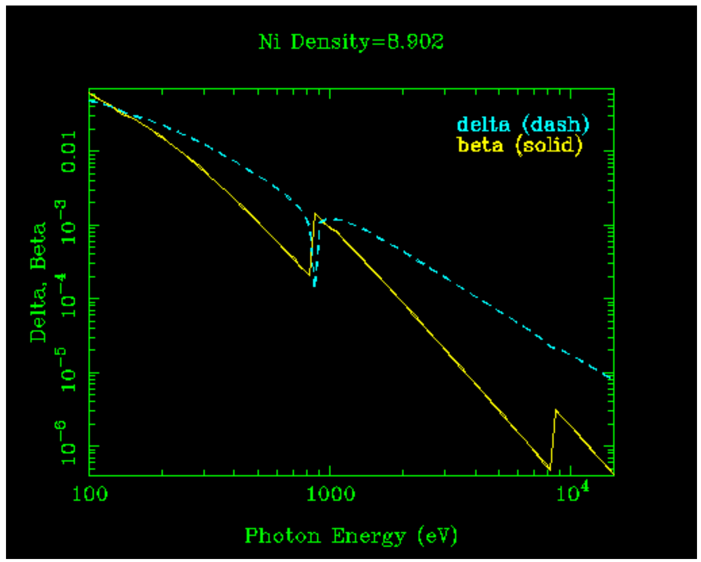

- Absorption contrast: sensitive to *Im(n)*

  $\sim 4\pi\beta(x,y)t/\lambda$

- Phase contrast: sensitive to *Re(n)*

  $\sim 2\pi\delta(x,y)t/\lambda$

PHYSICAL REVIEW B **85**, 020104(R) (2012)

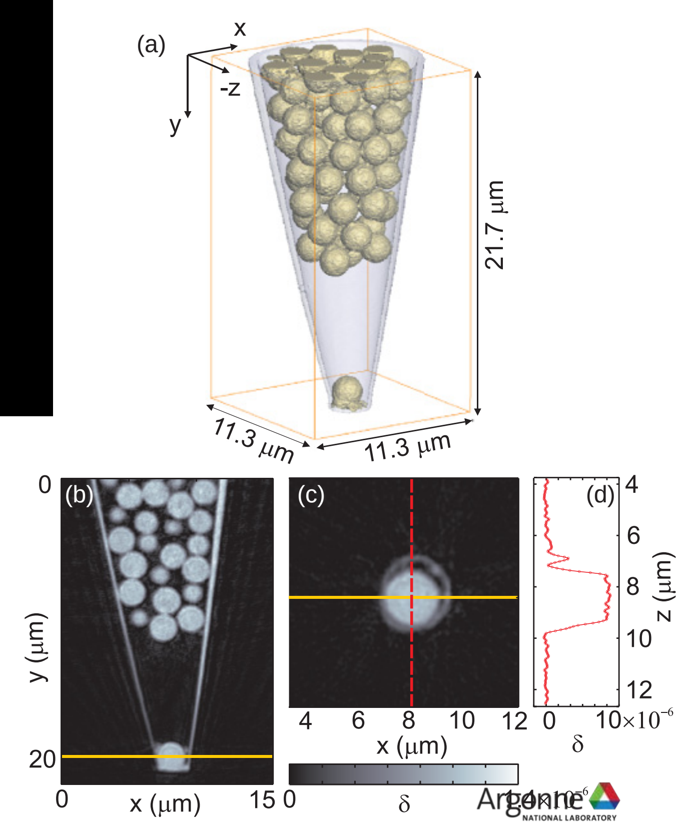

Diaz, Ana, et al, 2012. "Quantitative X-Ray Phase Nanotomography." *Physical Review B* 85.

REFRACTIVE INDEX AND CONTRAST IN THE X-RAY REGION

$$n = 1 - \delta - i\beta = 1 - \frac{r_e}{2\pi}\lambda^2 \sum_i n_i f_i(0)$$

$$A = A_0 \exp(-inkt)$$

$$k = 2\pi/\lambda$$

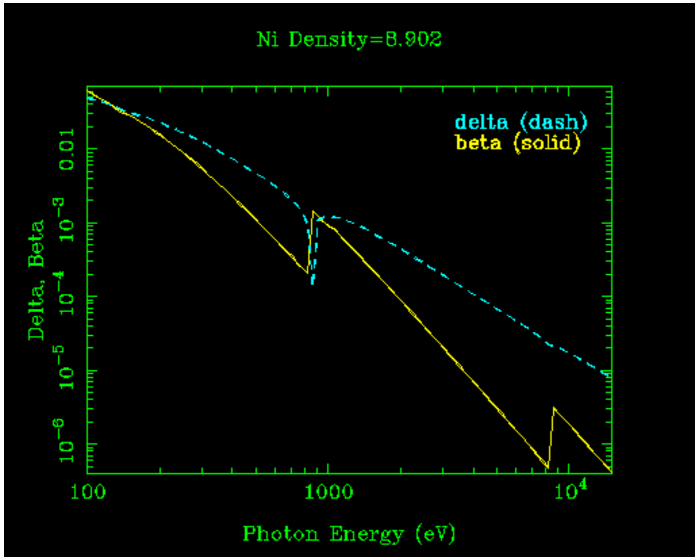

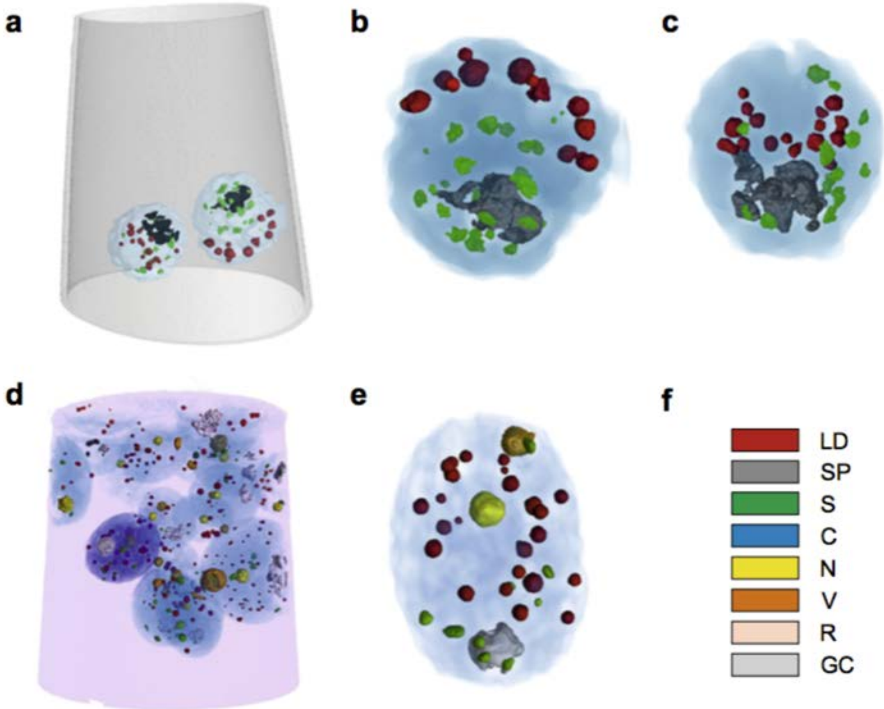

A. Diaz,et al., Journal of Structural Biology, vol. 192, no. 3, pp. 461–469, Oct. 2015.

Absorption contrast:

sensitive to *Im(n)*

$\sim 4\pi\beta(x,y)t/\lambda$

Phase contrast:

sensitive to *Re(n)*

$\sim 2\pi\delta(x,y)t/\lambda$

POLARIZED X-RAYS GIVE SENSITIVITY TO ELECTRON SPIN in PtCo

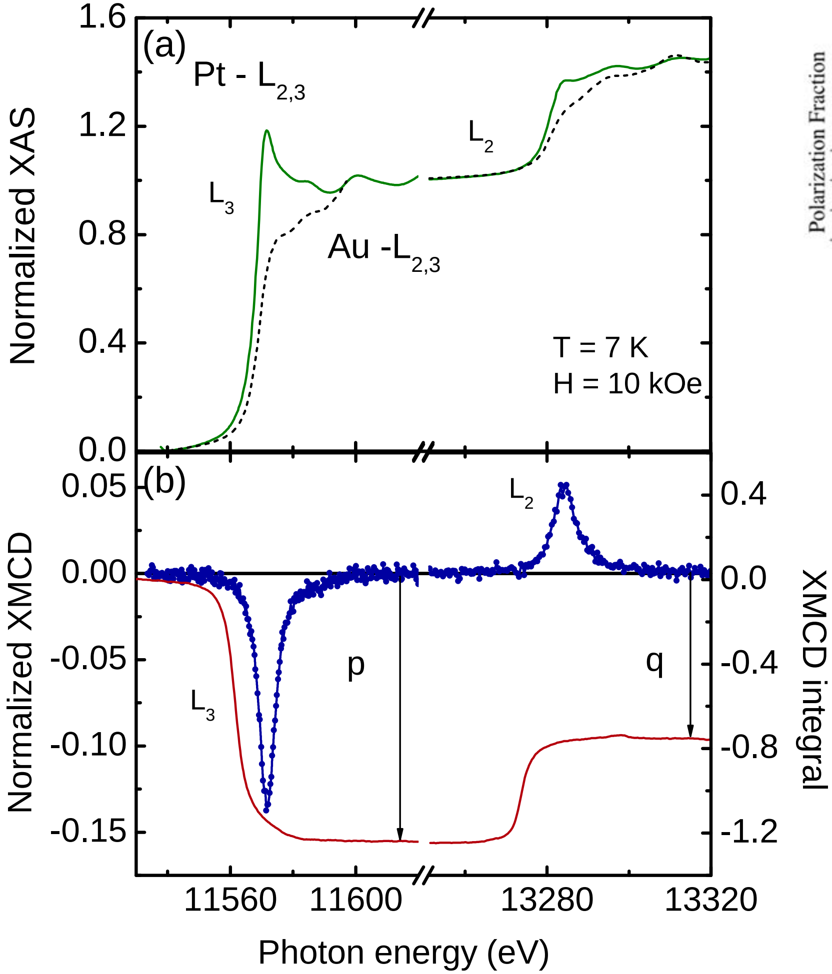

Figueroa, A. I., et al. (2014). *Physical Review B*, *90*(17), 174421

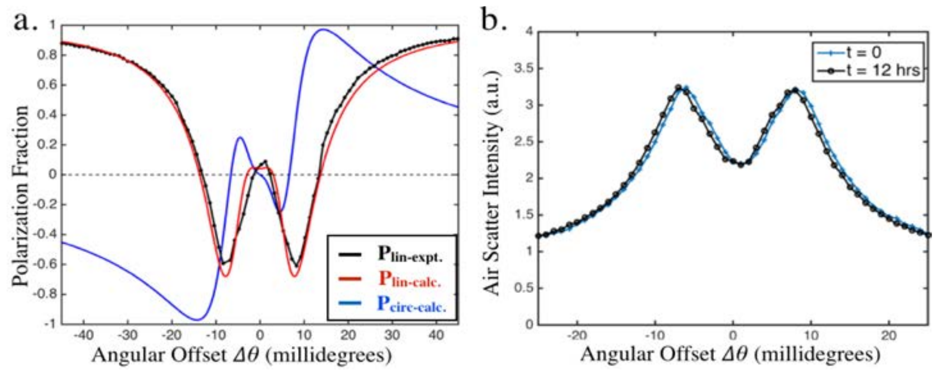

LCP @ 11.565keV

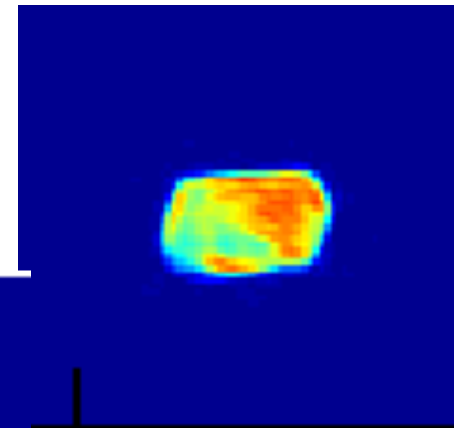

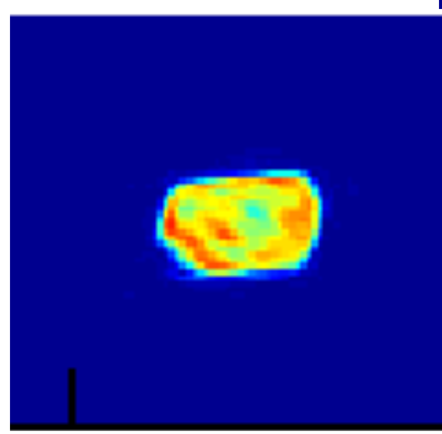

RCP @ 11.565keV

CDI IN BRAGG GEOMETRY: IMAGING DISPLACEMENT FIELD (STRAIN)

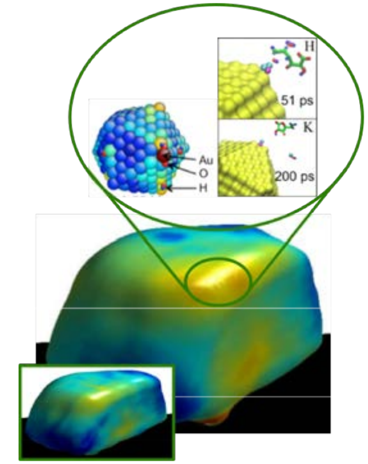

Displacement field u(r):

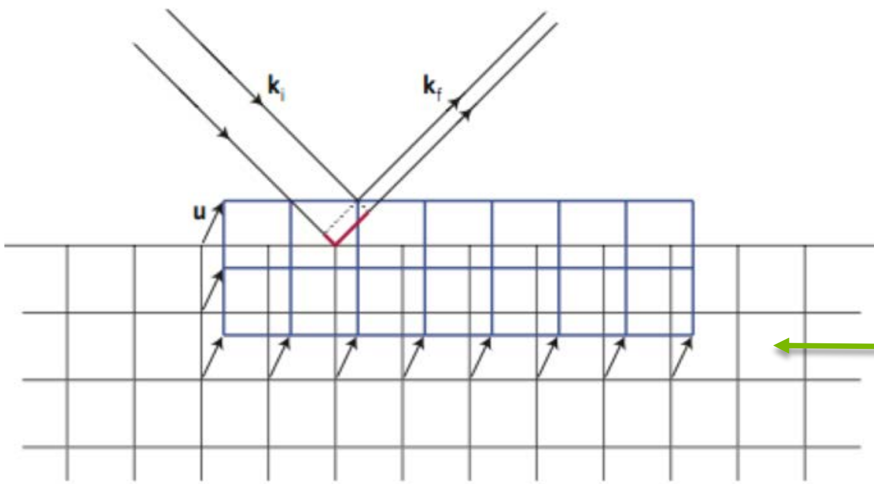

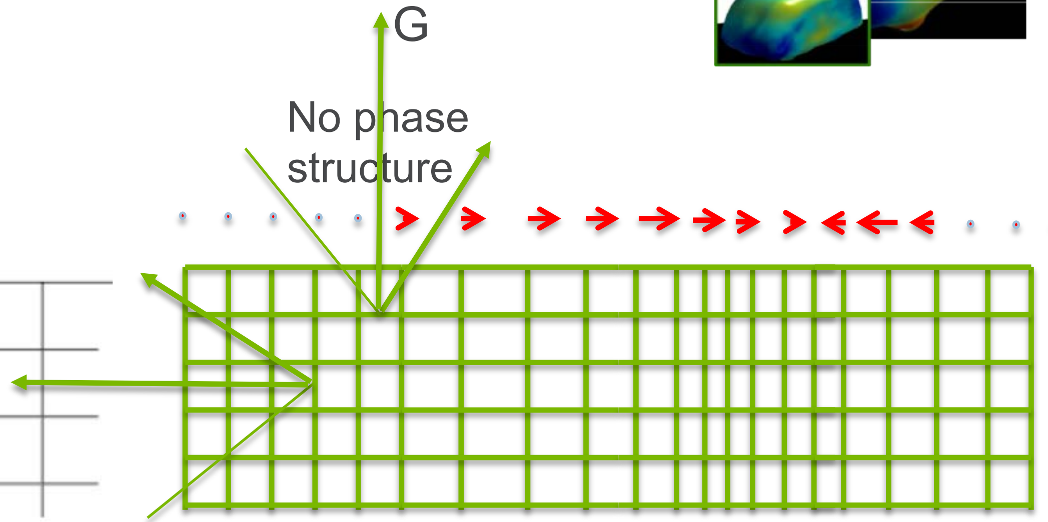

Coherent X-ray Diffraction measures:

$$\widetilde{\rho}(\mathbf{r}) = \rho_{\mathbf{G}_{hkl}}(\mathbf{r})\exp\left[-i\mathbf{G}_{hkl}\cdot\mathbf{u}(\mathbf{r})\right]$$

Strain is a gradient of u(r), the phase component of the complex-valued density

Courtesy Prof. Oleg Shpyrko (UCSD)

TRADITIONAL MICROSCOPY:

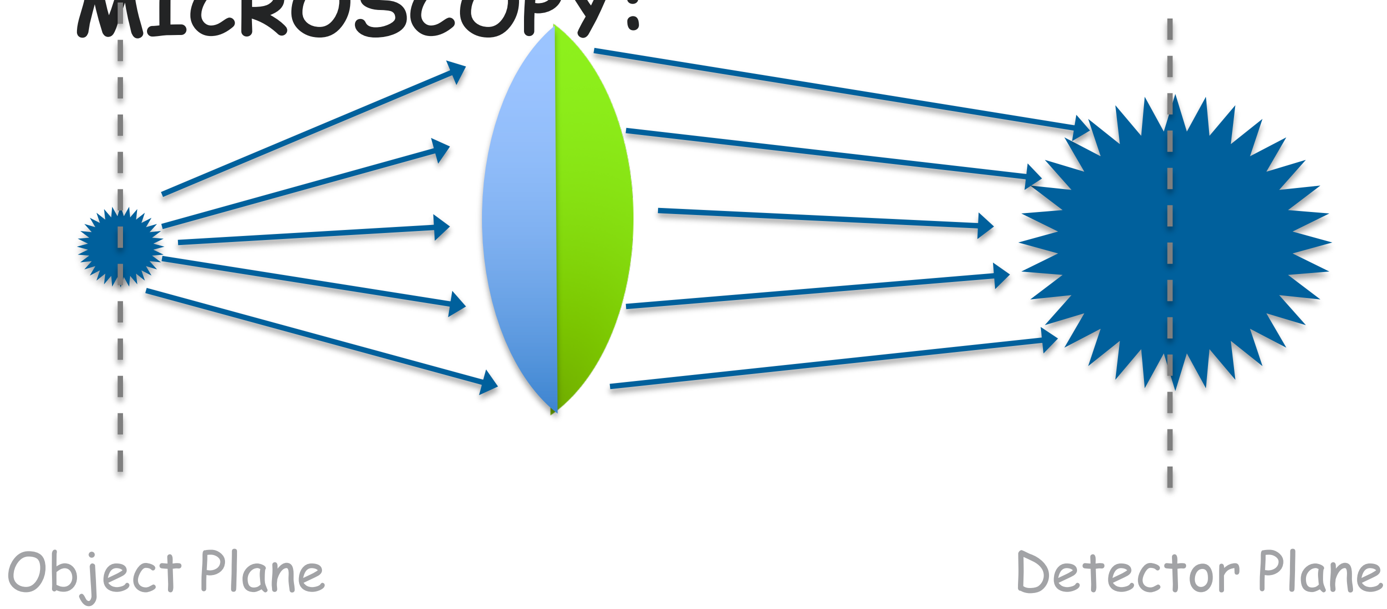

Lens-less Imaging:

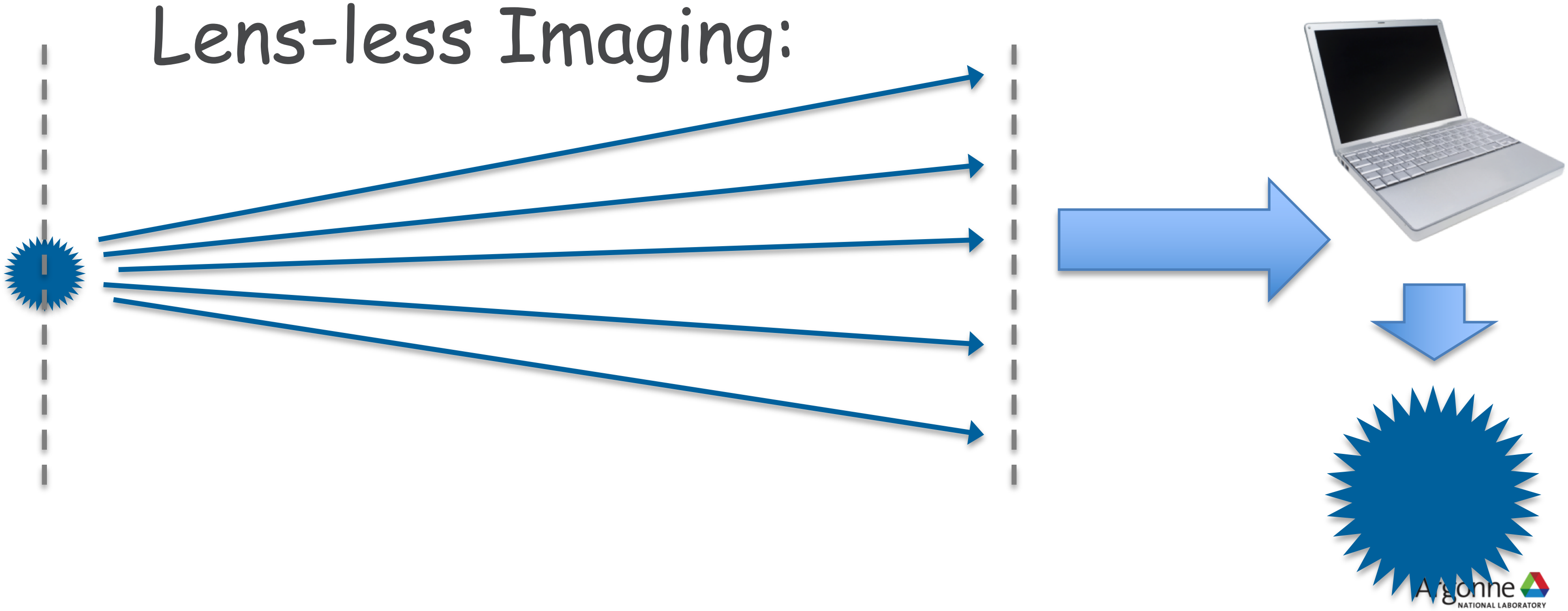

Courtesy Prof. Oleg Shpyrko (UCSD)

FIRST DEMONSTRATION OF CDI WITH X-RAYS

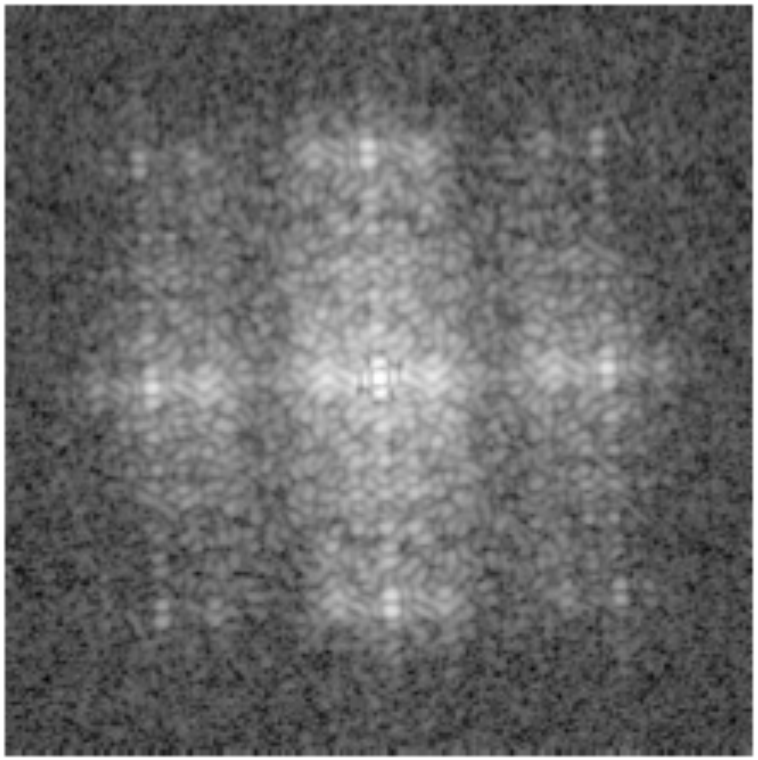

diffraction pattern

reconstruction

J. Miao, Nature 400, 342 (1999)

COHERENT DIFFRACTIVE IMAGING:

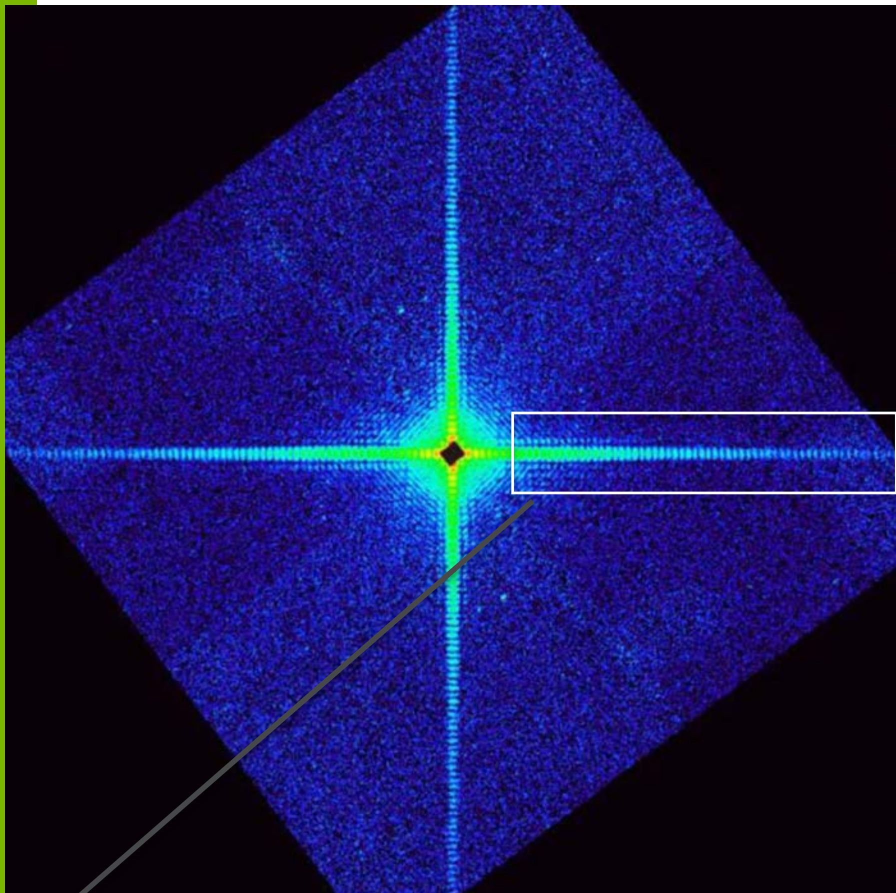

Y. Takahashi et al.,
Phys. Rev. B 82, 214102 (2010)

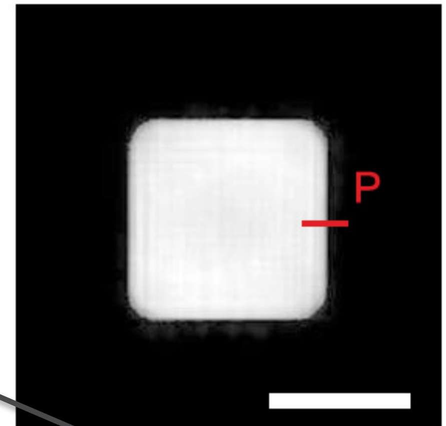

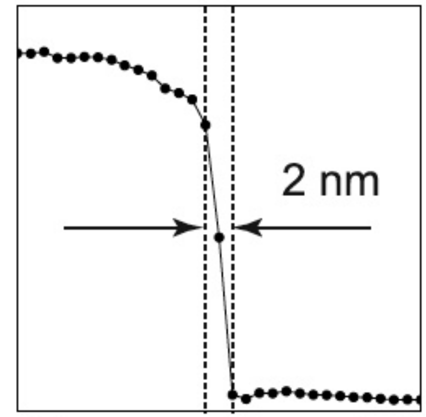

Line scan through P

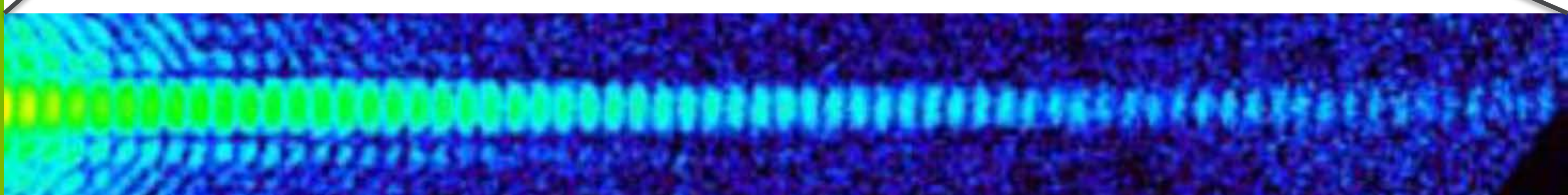

LARGE-FORMAT, SINGLE-PHOTON SENSITIVE X-RAY CCD CAMERAS OPENED THE DOOR TO COHERENT X-RAY IMAGING

Fairchild Peregrine 486 CCD Camera

- **4K x 4K pixel array (61.4 mm square area)**
- **15 μm pixels, 100% fill factor**
- **Back-illuminated for up to 80% QE**
- **Readout noise < 5 e- at 50 Kpixels/s**
- **Dynamic range > 86 dB in MPP**
- **6 s readout with four on-chip amplifiers**
- **Pixel binning for more rapid readout**
- **Peltier-cooled to -50 C for low dark current**

Hi Resolution Imaging (CCD)?

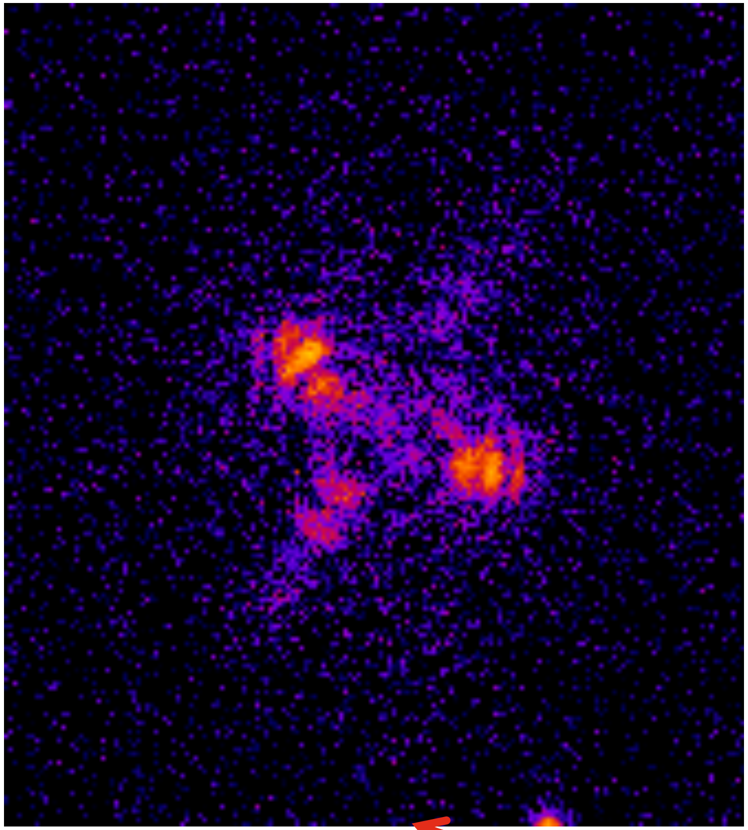

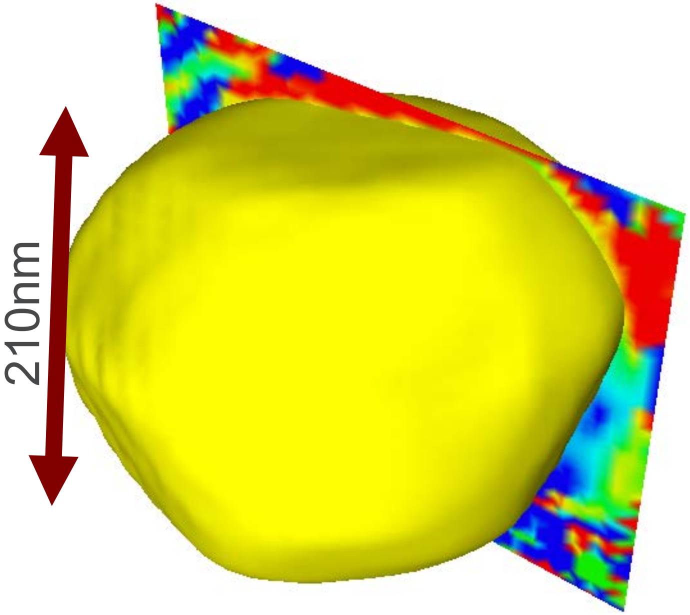

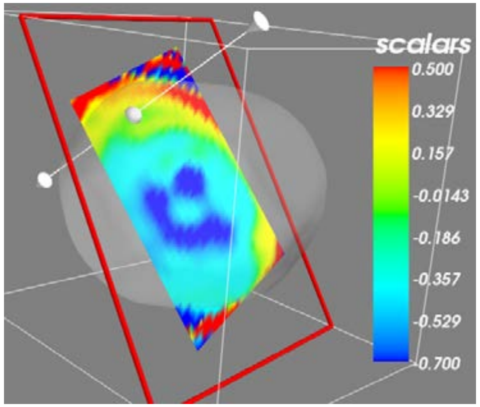

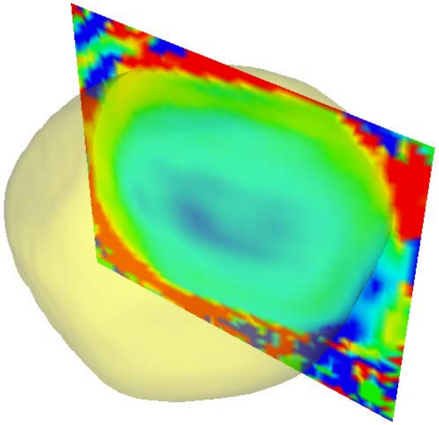

~7nm data

At APS 34-ID-C:
9.25 hours of scanning
38 minutes of x-ray exposure

Rainbow color map (still) considered harmful
http://ieeexplore.ieee.org/document/4118486/

PIXEL ARRAY DETECTORS: REVOLUTIONIZING COHERENT IMAGING

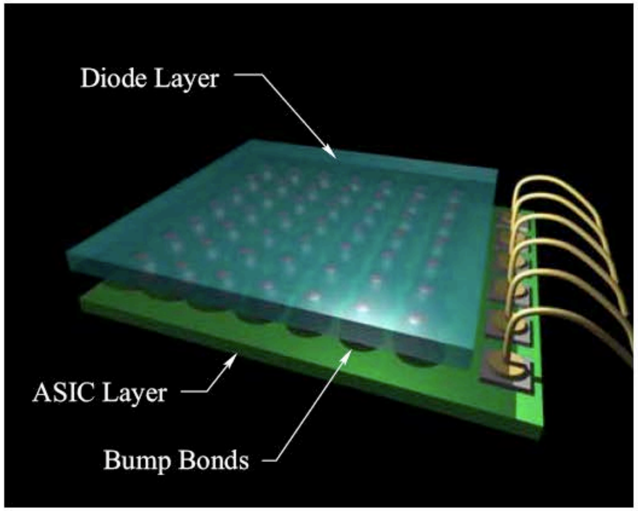

D. Schuette, S. Gruner (Cornell)

A Three Layer Hybrid Device

- Diode layer → converts x-rays to photocurrent.
- ASIC layer → custom signal processing electronics.
- A layer of metallic interconnects (bump bonds) between corresponding pixels on the diode and ASIC layers.

Pilatus 6M detector (PSI/Dectris)

PADs can be read out in ~1 ms (CCDs take seconds!)

PAD pixels are 55-150 μm. (CCDs are 12-24 μm)

Hi Resolution Imaging (PAD)?

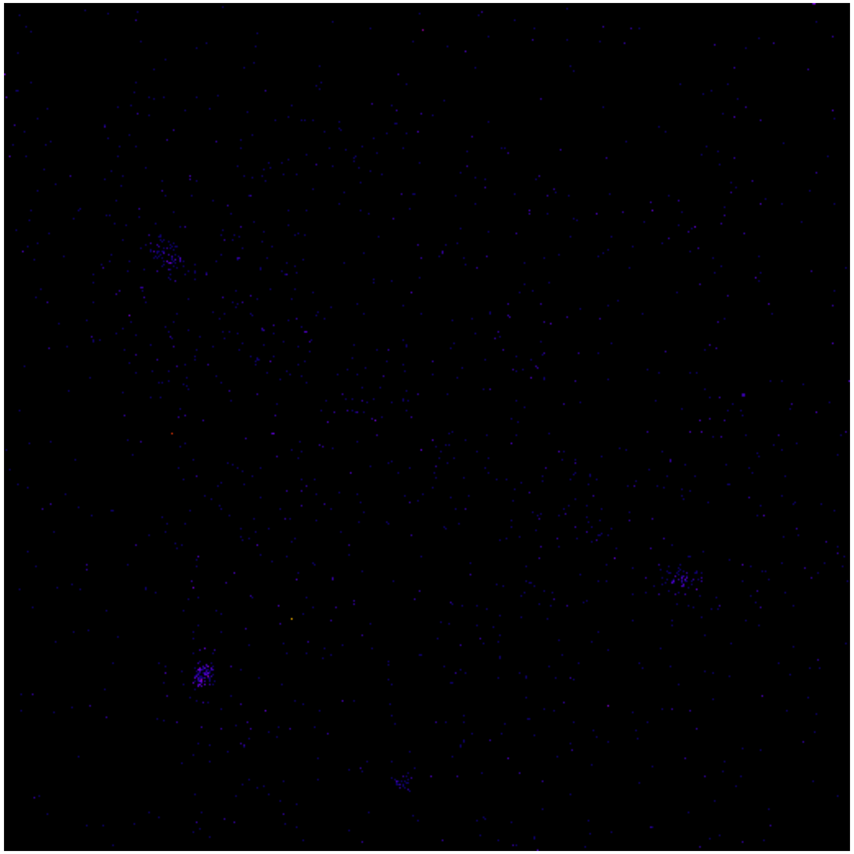

Quad Timepix GaAs sensor

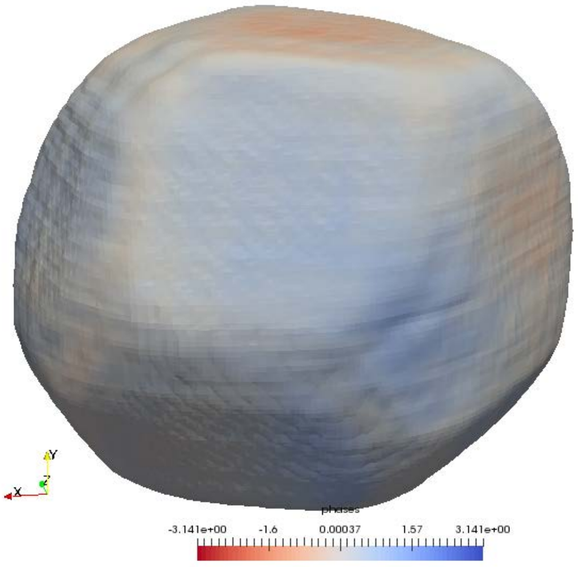

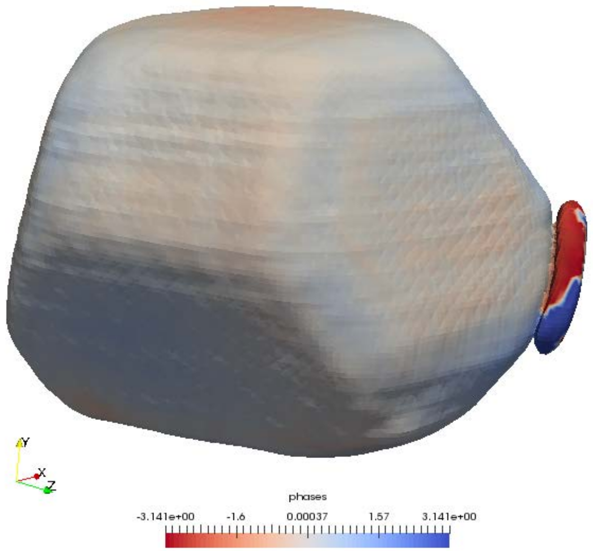

700nm gold crystal
3 degree rocking curve
25 minute measurement
15 sec movie (1X APS-U measurement)

Coherent Diffraction from Crystals

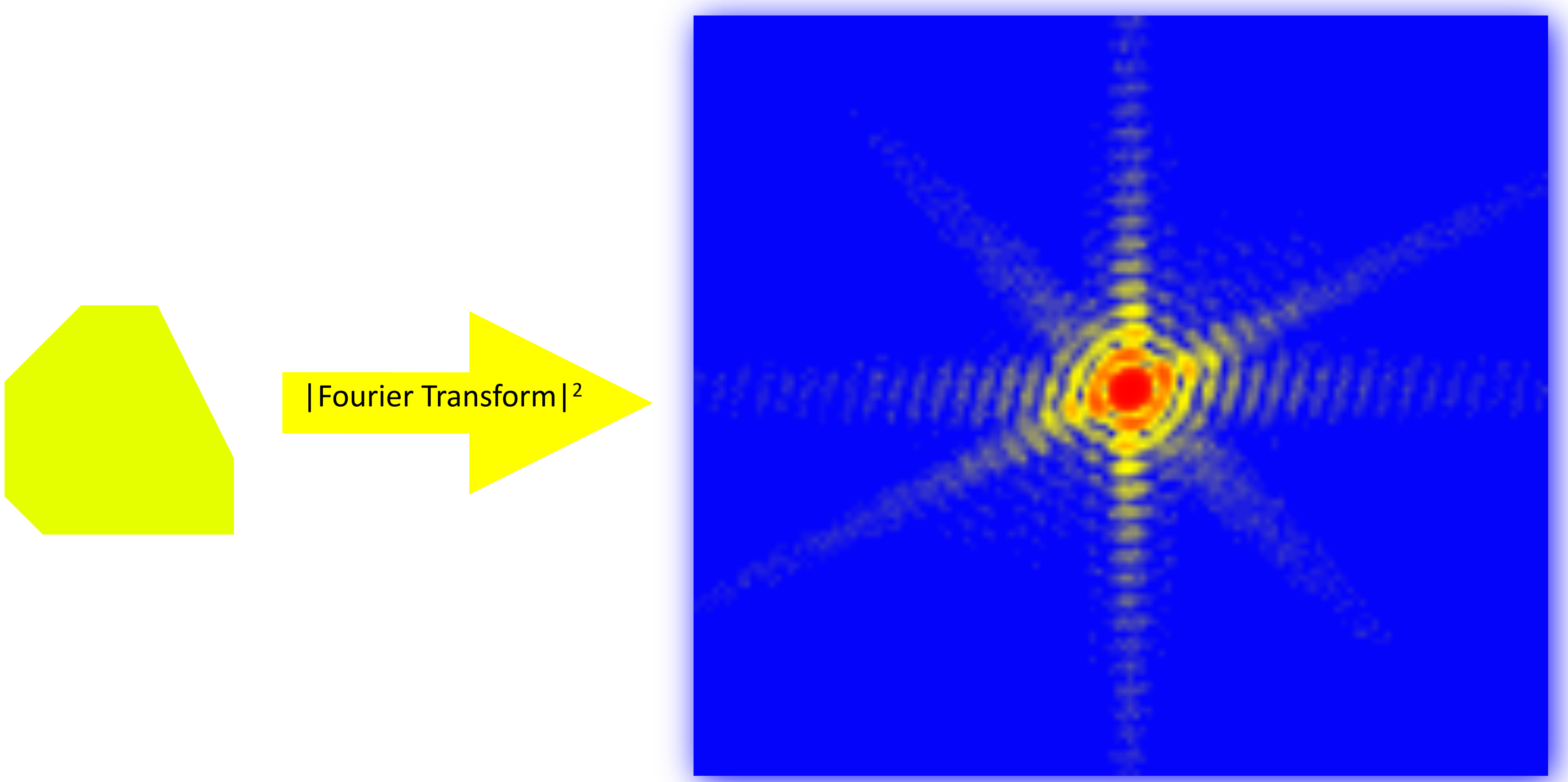

Coherent Diffraction from Crystals

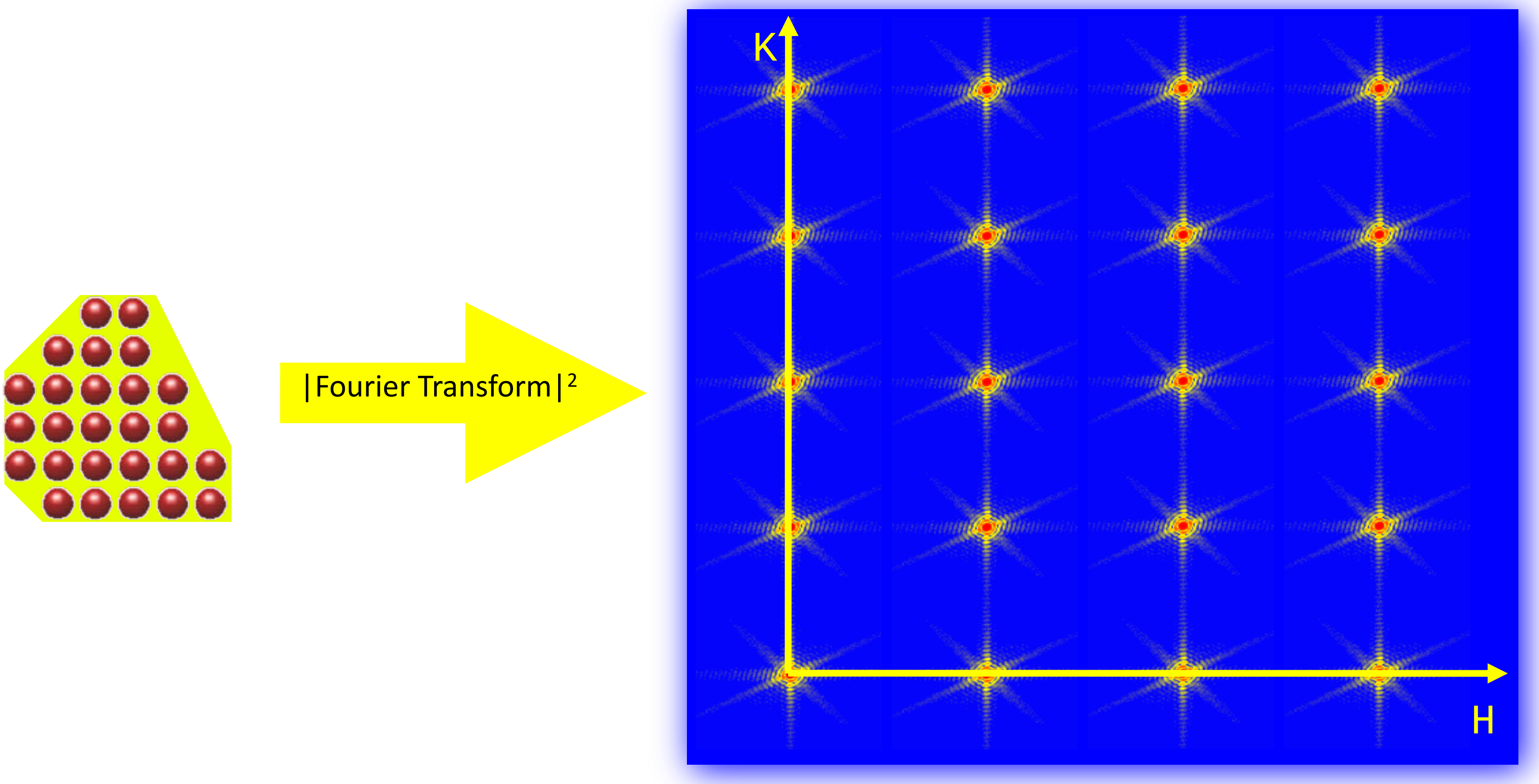

Measuring 3D CXD

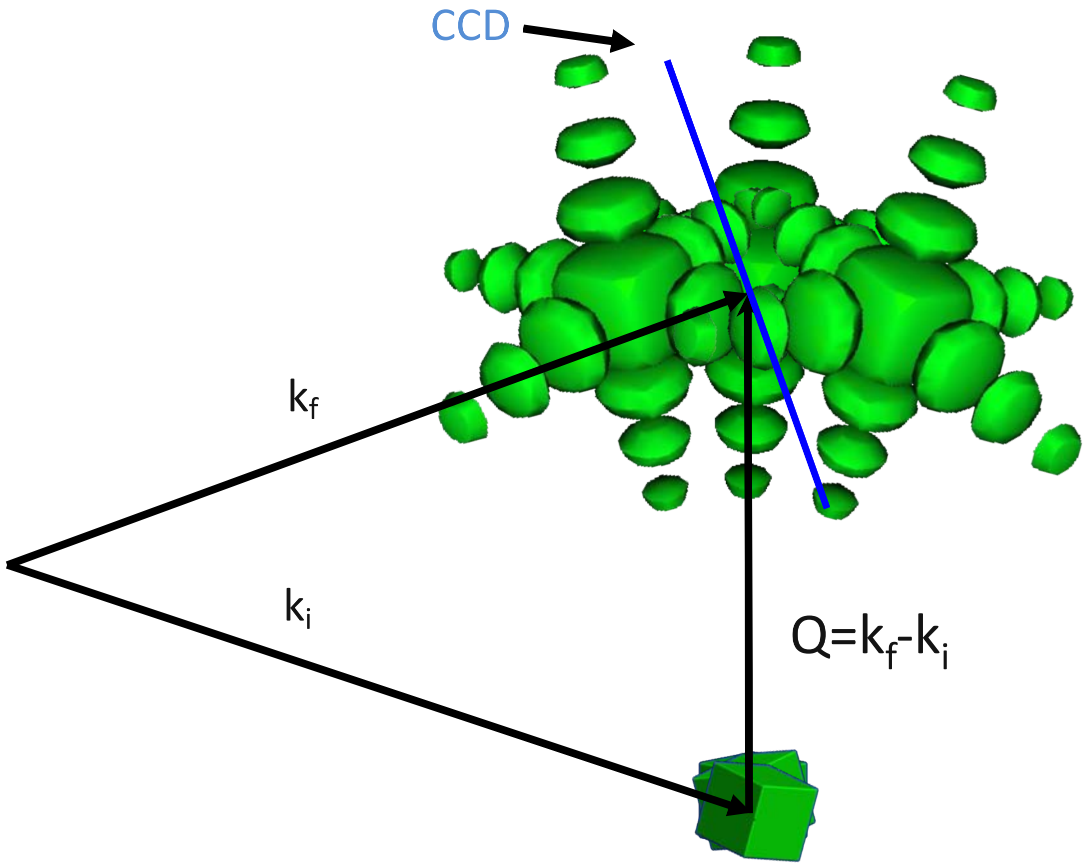

Silver Nano Cube (111)

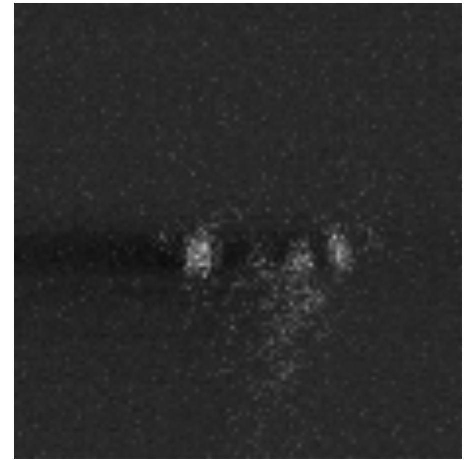

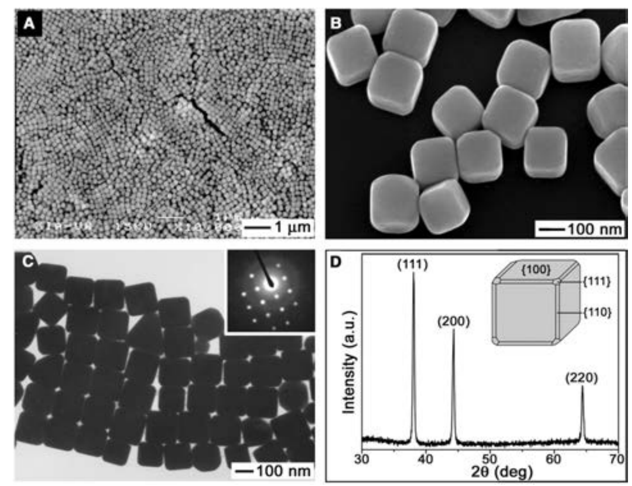

Yugang Sun and Younan Xia, Science 298 2177 (2003)

3D Ag Nano Cube

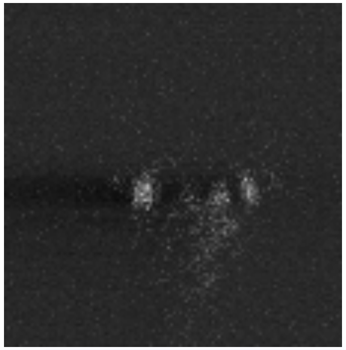

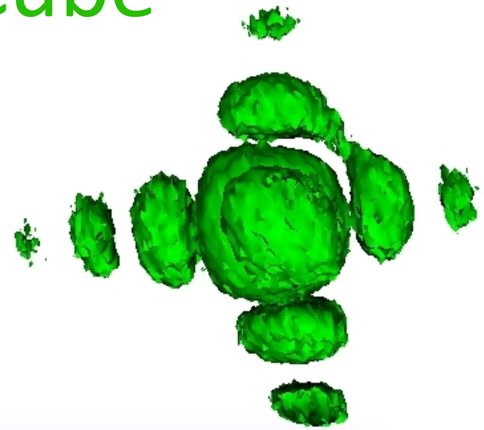

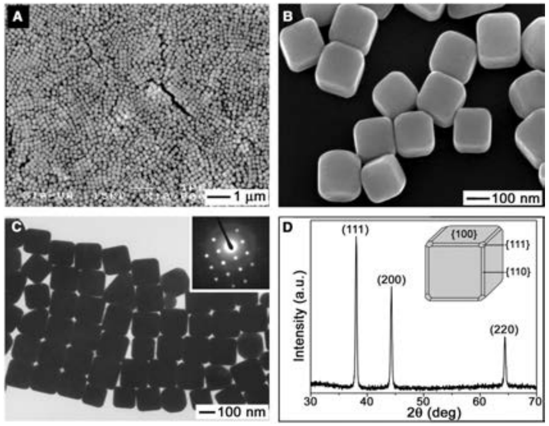

Yugang Sun and Younan Xia, Science 298 2177 (2003)

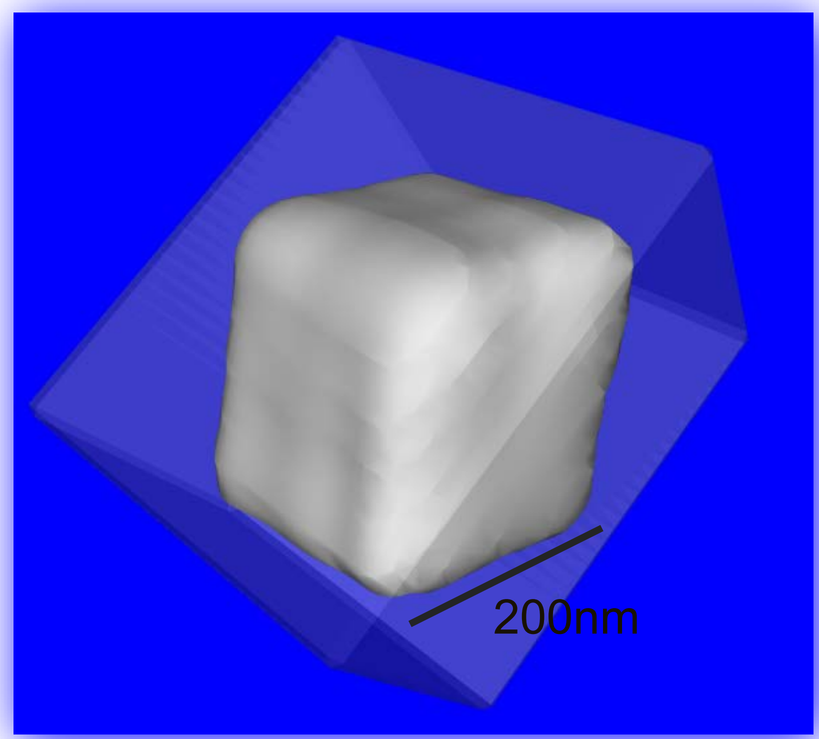

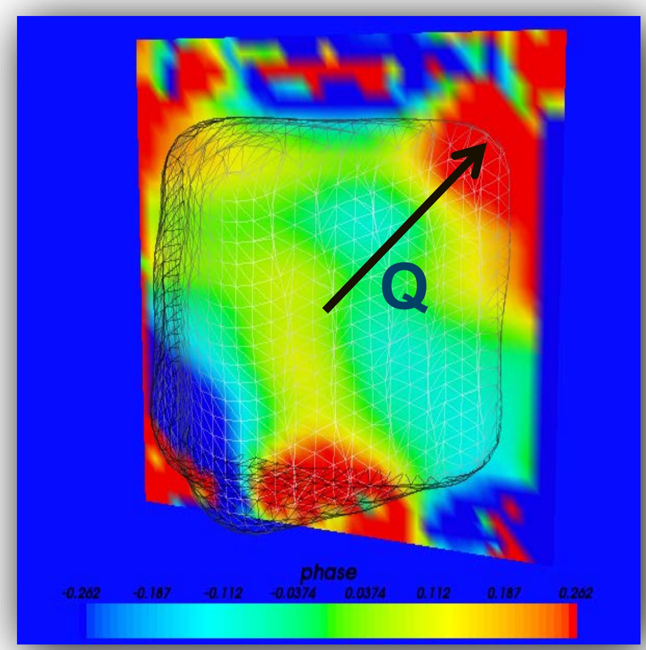

APS 34-ID-C

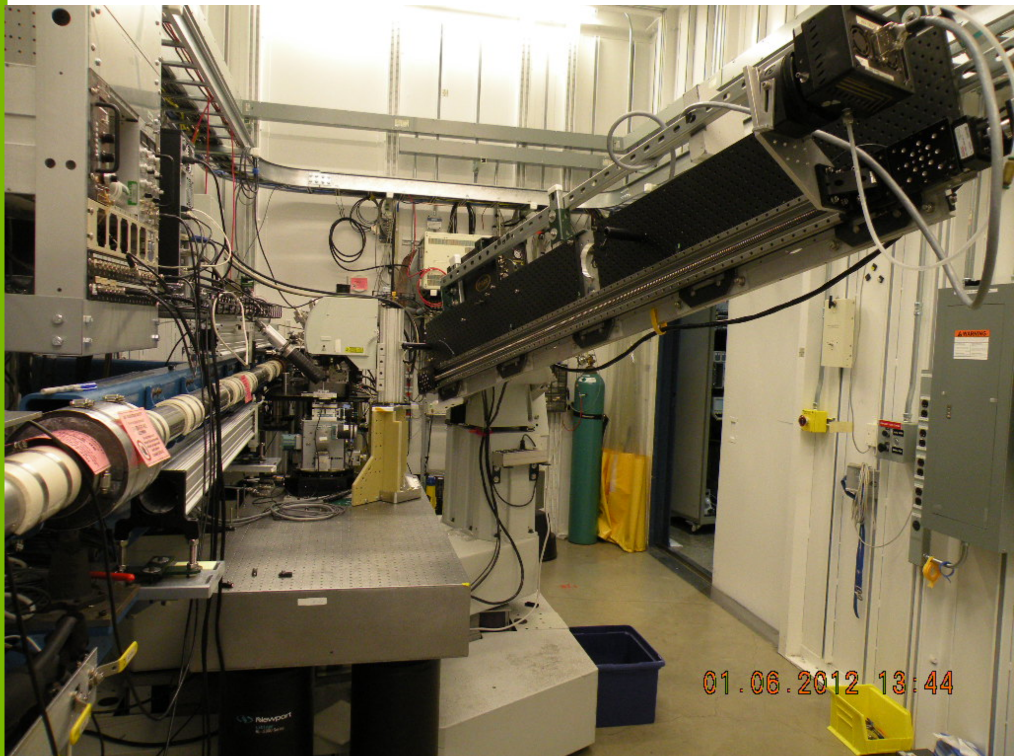

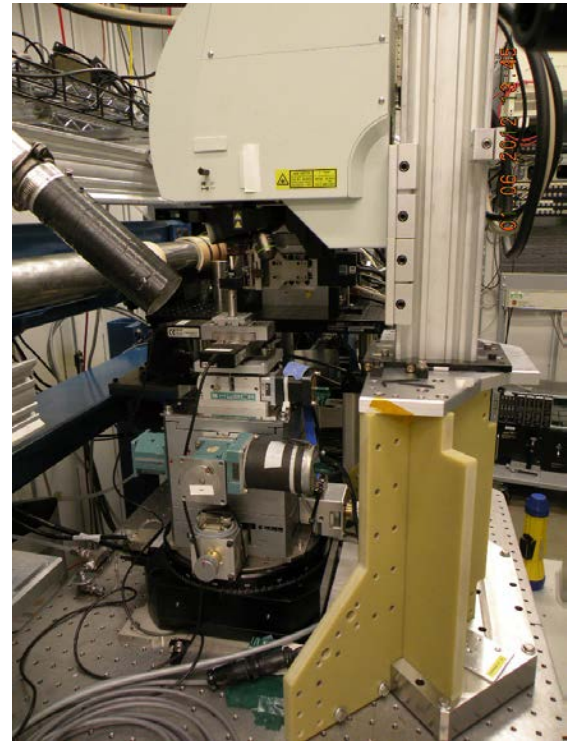

Precision scanning stage

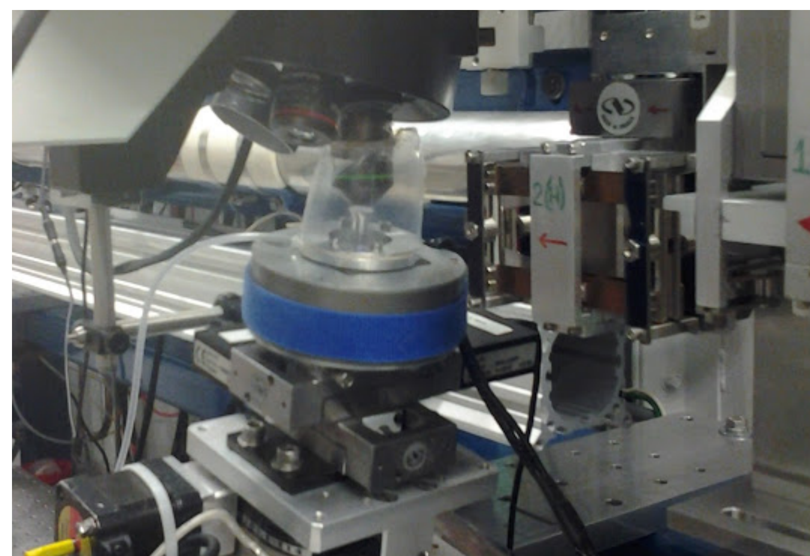

ORIGINAL PHASE RETRIEVAL PAPER (BY D. SAYRE):

NOT $\rho=\rho^2$ Acta Cryst. (1952). 5, 60

Acta Cryst. (1952). **5**, 843

Some implications of a theorem due to Shannon. By D. Sayre, *Johnson Foundation for Medical Physics, University of Pennsylvania, Philadelphia 4, Pennsylvania, U.S.A.*

(*Received 3 July* 1952)

Shannon (1949), in the field of communication theory, has given the following theorem: If a function $d(x)$ is known to vanish outside the points $x = \pm a/2$, then its Fourier transform $F(X)$ is completely specified by the values which it assumes at the points $X = 0, \pm 1/a, \pm 2/a, \ldots$. In fact, the continuous $F(X)$ may be filled in merely by laying down the function $\sin \pi aX/\pi aX$ at each of the above points, with weight equal to the value of $F(X)$ at that point, and adding.

Now the electron-density function $d(x)$ describing a single unit cell of a crystal vanishes outside the points $x = \pm a/2$, where a is the length of the cell. The reciprocal-lattice points are at $X = 0, \pm 1/a, \pm 2/a, \ldots$, and hence the experimentally observable values of $F(X)$ would suffice, by the theorem, to determine $F(X)$ everywhere, if the phases were known. (In principle, the necessary points extend indefinitely in reciprocal space, but by using, say, Gaussian atoms both $d(x)$ and $F(X)$ can be effectively confined to the unit cell and the observable region, respectively.)

For centrosymmetrical structures, to be able to fill in the $|F|^2$ function would suffice to yield the structure, for sign changes could occur only at the points where $|F|^2$ vanishes. The structure corresponding to the $|F|^2$ function is the Patterson of a single unit cell. This has twice the width of the unit cell, and hence to fill in the $|F|^2$ function would require knowledge of $|F|^2$ at the half-integral, as well as the integral h's. This is equivalent to a statement made by Gay (1951).

I think the conclusions which may be stated at this point are:

1. Direct structure determination, for centrosymmetric structures, could be accomplished as well by finding the sizes of the $|F|^2$ at half-integral h as by the usual procedure of finding the signs of the F's at integral h.

2. In work like that of Boyes-Watson, Davidson & Perutz (1947) on haemoglobin, where $|F|^2$ was observed at non-integral h, it would suffice to have only the values at half-integral h.

The extension to three dimensions is obvious.

References

Boyes-Watson, J., Davidson, E. & Perutz, M. F. (1947). *Proc. Roy. Soc.* A, **191**, 83.

Gay, R. (1951). Paper presented at the Second International Congress of Crystallography, Stockholm.

Shannon, C. E. (1949). *Proc. Inst. Radio Engrs., N.Y.* **37**, 10.

Critical sampling

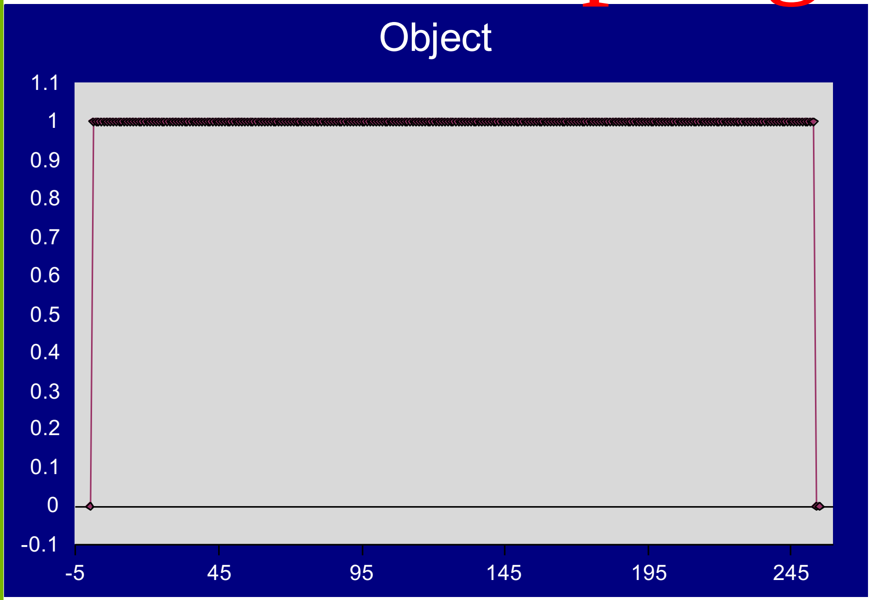

N unknown densities
N/2 equations

$$\left|A_q\right| = \left|\sum_{0}^{N} \rho_n e^{-iqr_n}\right|$$

Nyquist Freq = 1/(2*bandwidth)
Intensity is under sampled

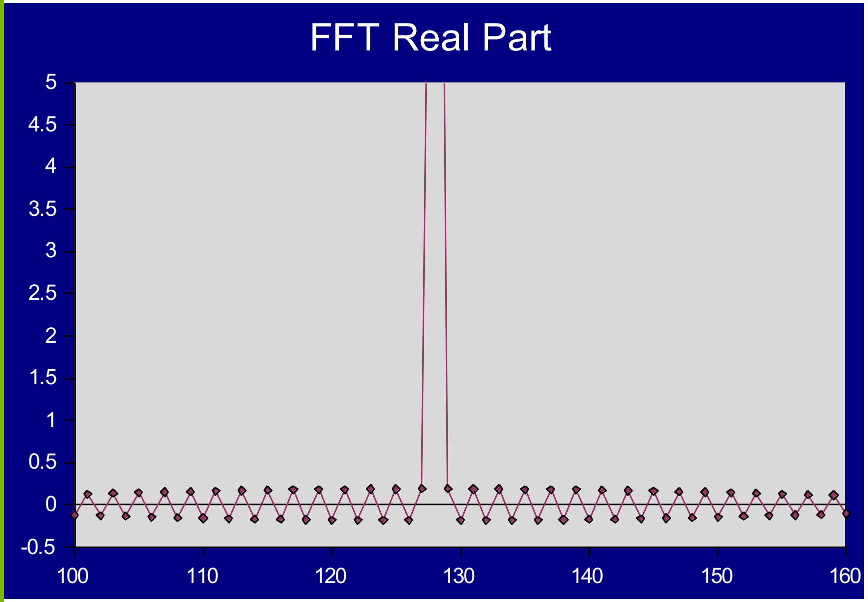

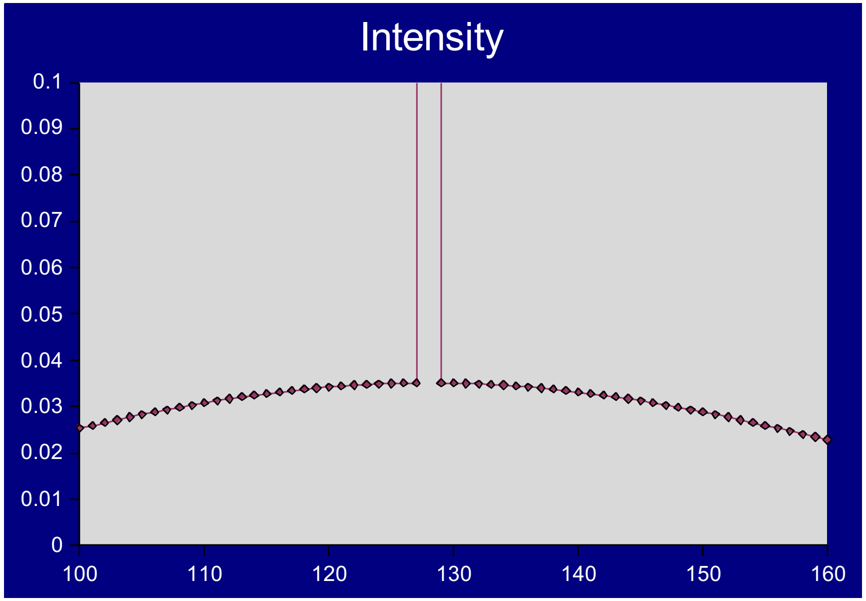

Oversampling 2x

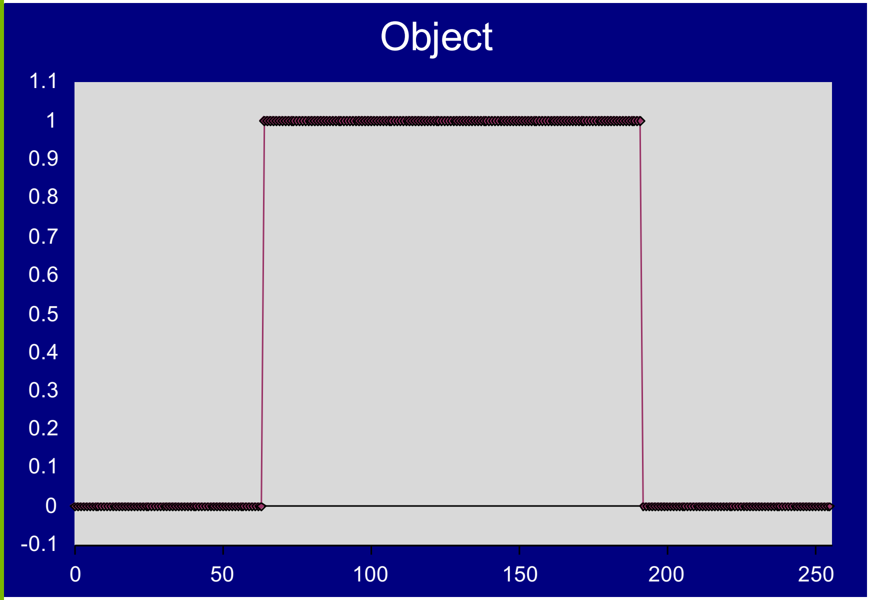

N/2 equations

N/2 Unknown densities

N/2 Known Densities(zero)

$$|A_q| = \left|\sum_0^N \rho_n e^{-iqr_n}\right|$$

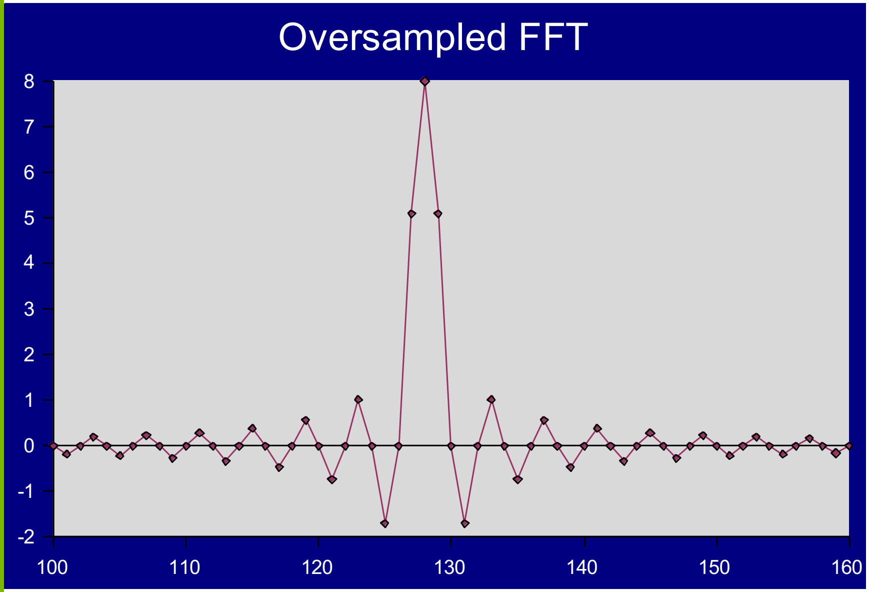

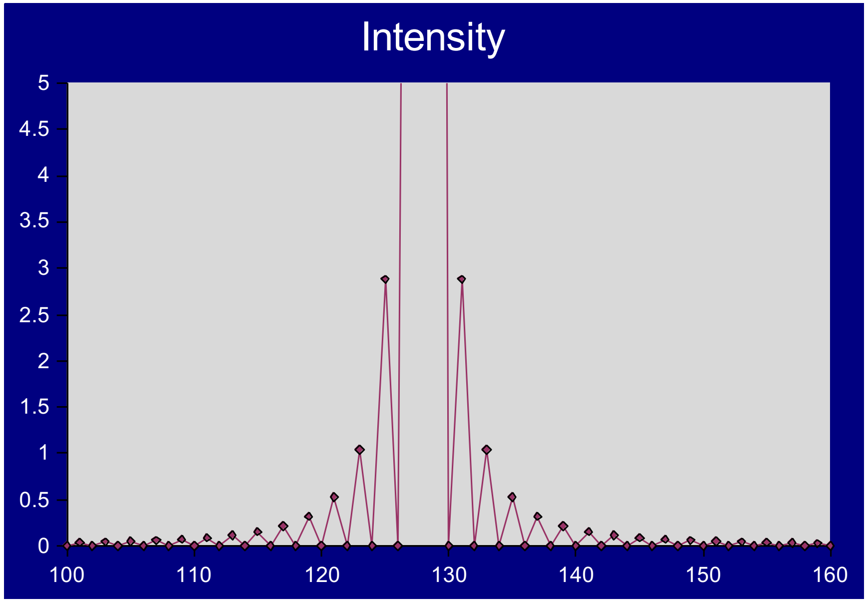

Input Output Algorithms

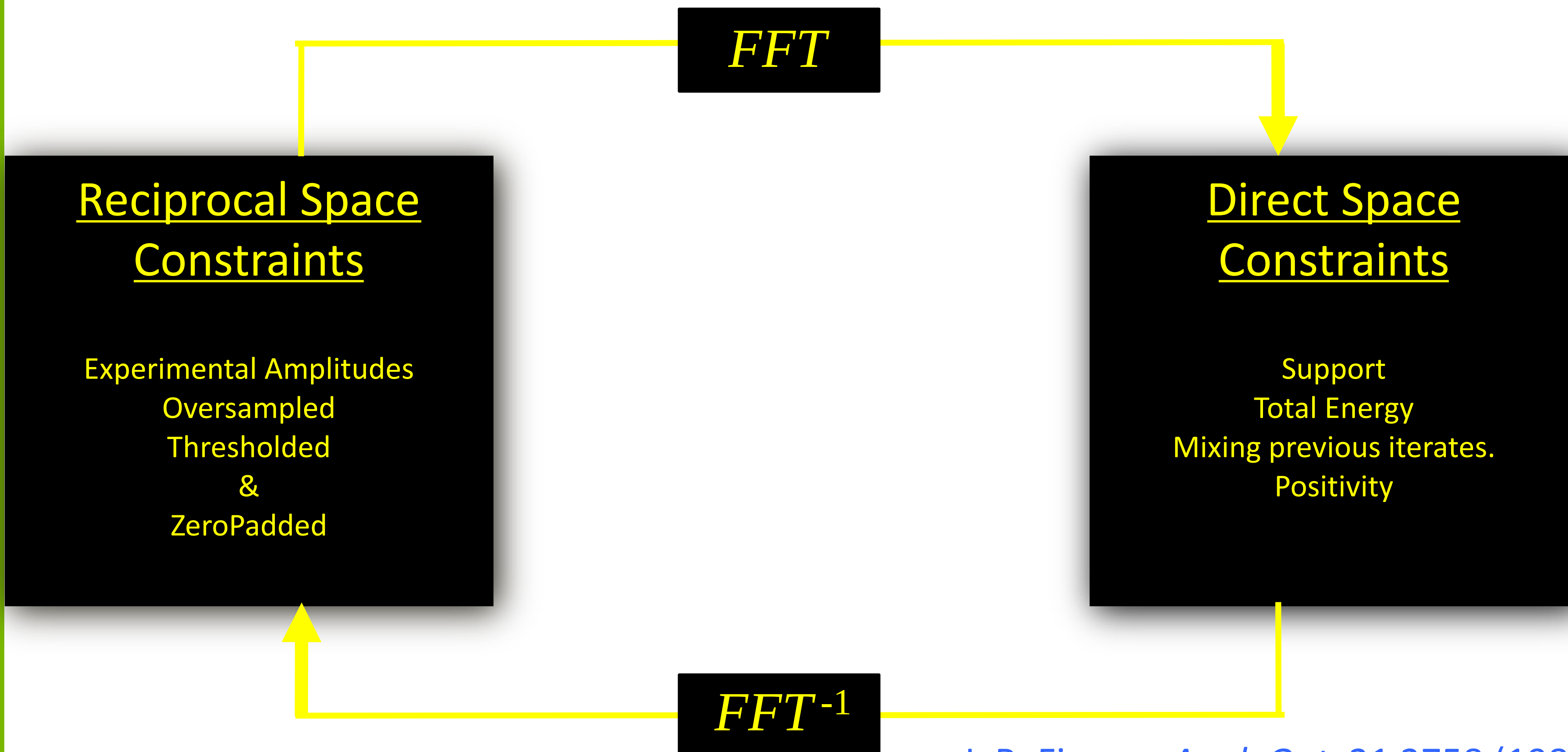

J. R. Fienup *Appl. Opt.* 21 2758 (1982)
Collins *Nature* 298, 49 (1982)
R. W. Gerchberg and W. O. Saxton *Optik* 35 237 (1972)
Fienup, James R. 2013. "Phase Retrieval Algorithms: a Personal Tour." *Applied Optics* 52 (1): 45–56.

Input Output Algorithms

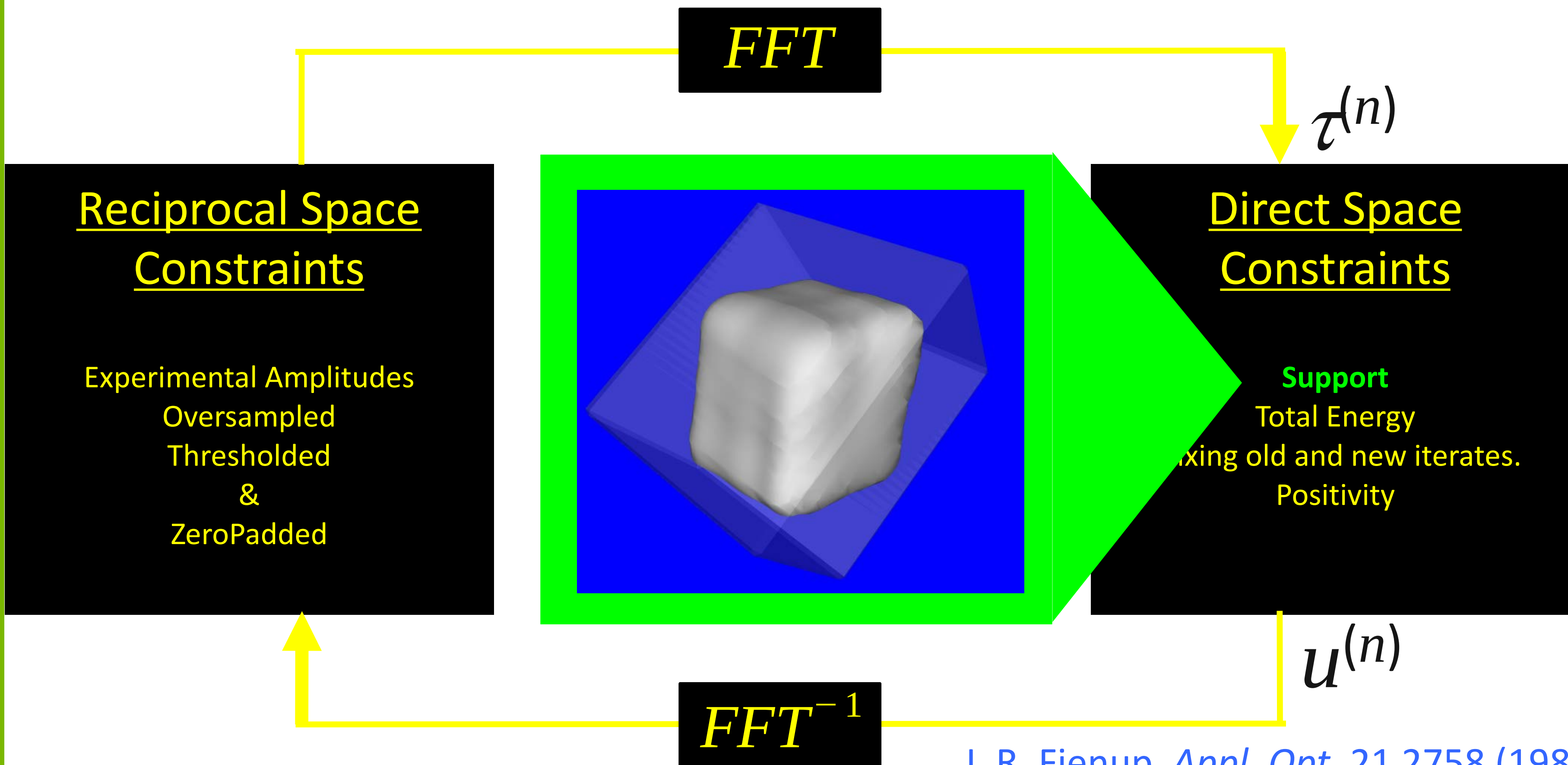

J. R. Fienup *Appl. Opt.* 21 2758 (1982)
Collins *Nature* 298, 49 (1982)
R. W. Gerchberg and W. O. Saxton *Optik* 35 237 (1972)
Fienup, James R. 2013. “Phase Retrieval Algorithms: a Personal Tour.” *Applied Optics* 52 (1): 45–56.

Input Output Algorithms

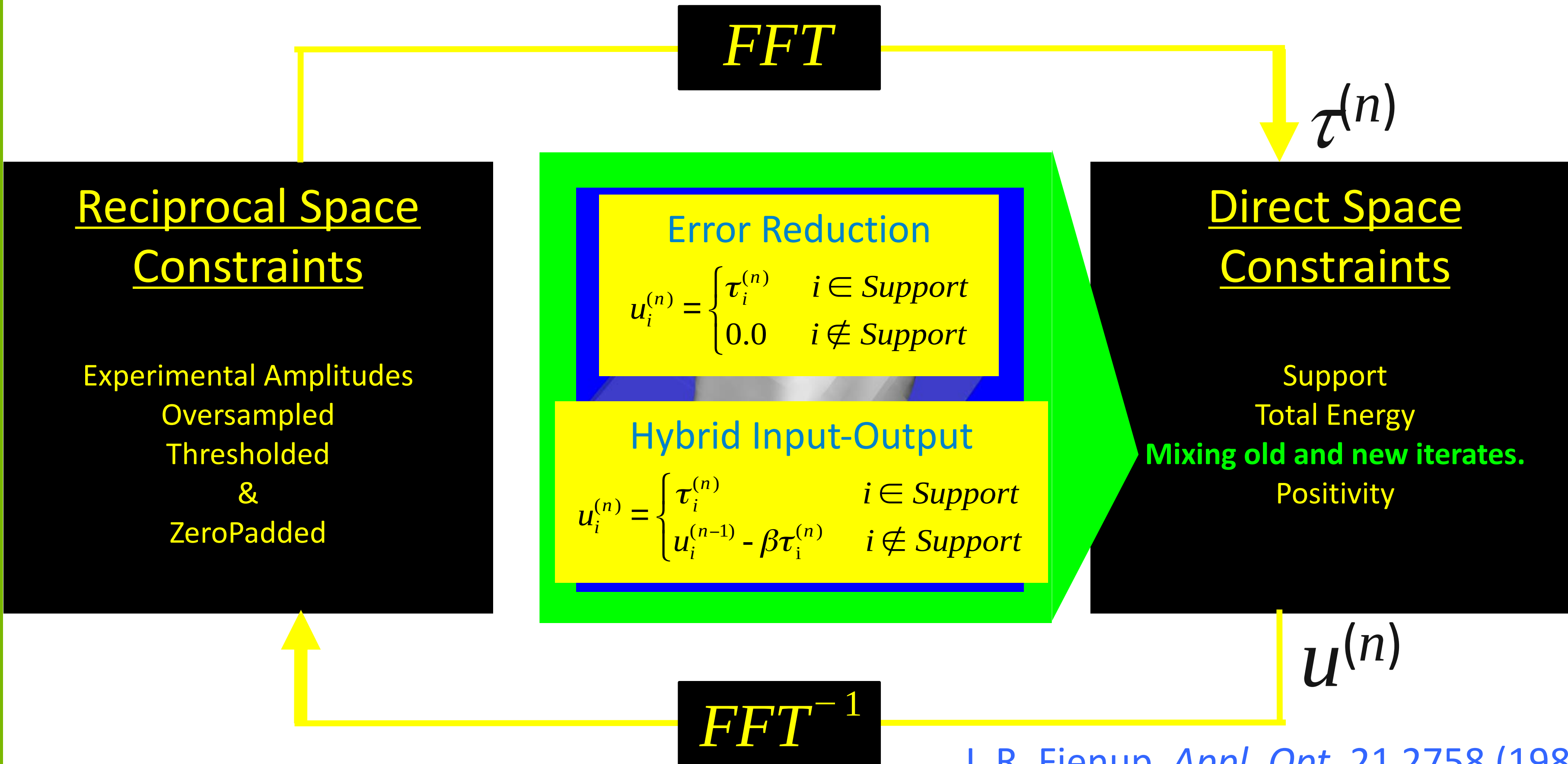

J. R. Fienup *Appl. Opt.* 21 2758 (1982)
Collins *Nature* 298, 49 (1982)
R. W. Gerchberg and W. O. Saxton *Optik* 35 237 (1972)
Fienup, James R. 2013. “Phase Retrieval Algorithms: a Personal Tour.” *Applied Optics* 52 (1): 45–56.

Input Output Algorithms

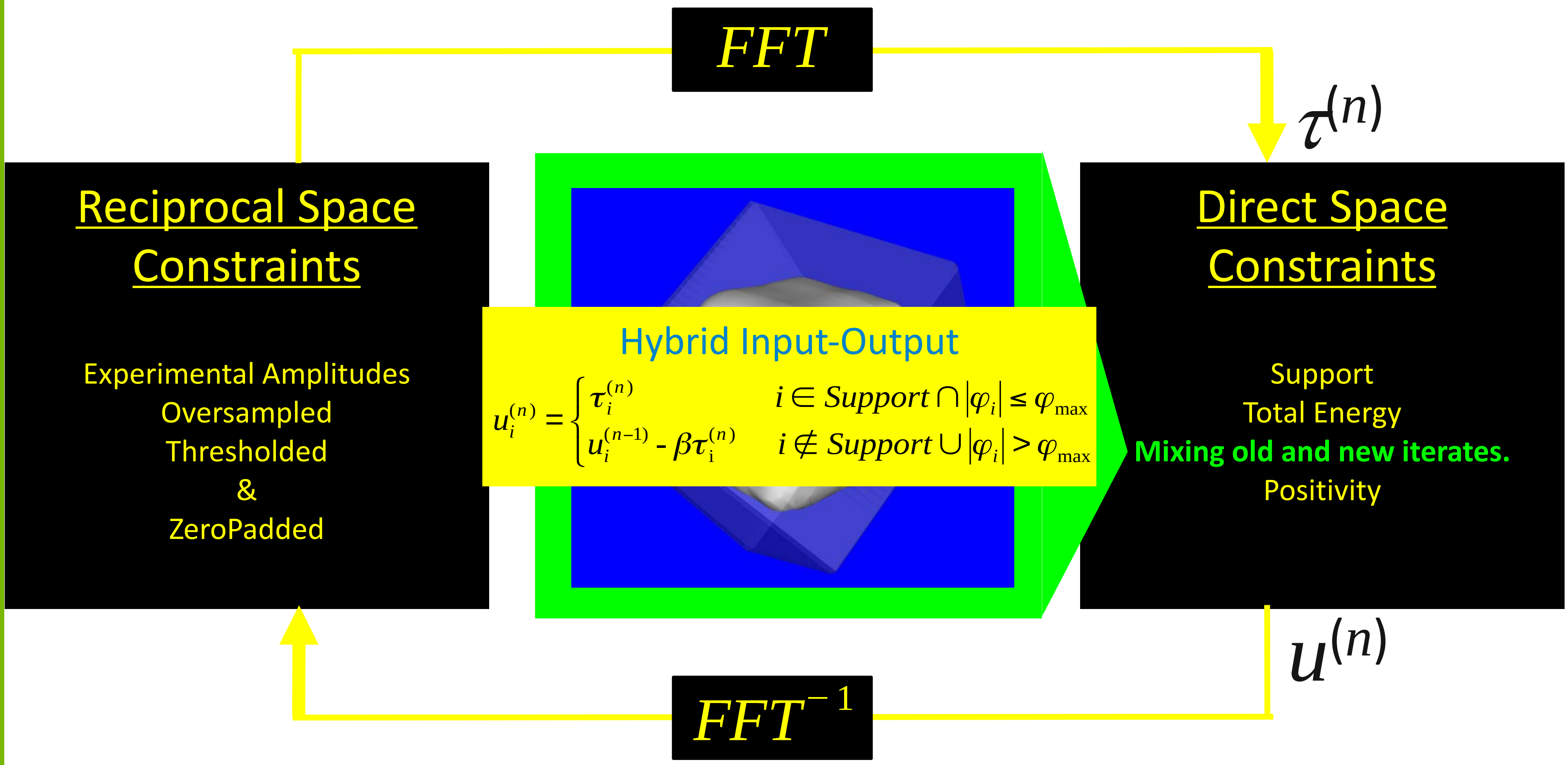

Harder, R., Liang, M., Sun, Y., Xia, Y., & Robinson, I. K. (2010). Imaging of complex density in silver nanocubes by coherent x-ray diffraction. *New Journal of Physics*, *12*(3), 035019.
Huang, X., Harder, R., Xiong, G., Shi, X., & Robinson, I. (2011). Propagation uniqueness in three-dimensional coherent diffractive imaging. *Physical Review B*, *83*(22), 224109.

Input Output Algorithms

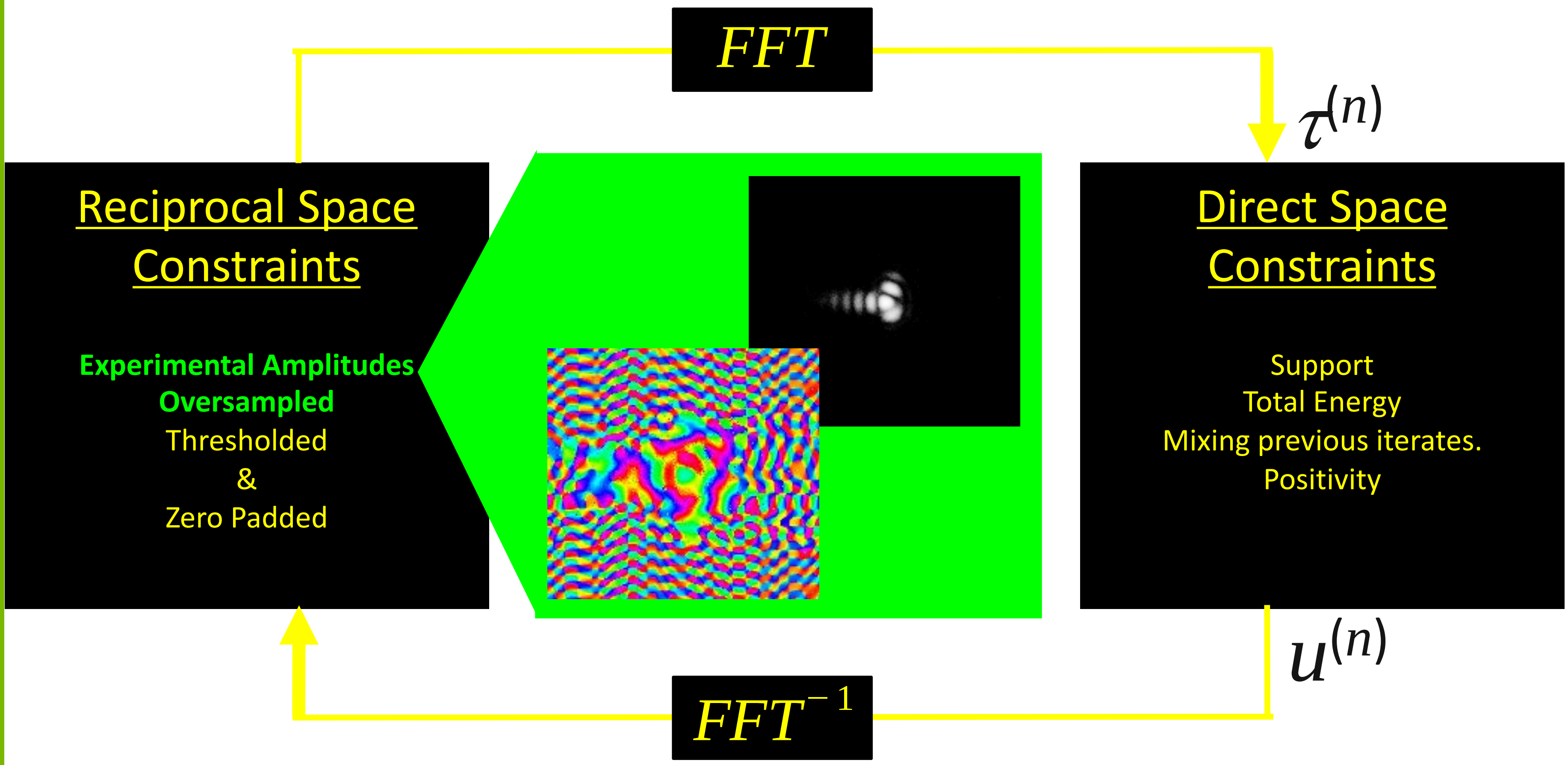

Harder, R., Liang, M., Sun, Y., Xia, Y., & Robinson, I. K. (2010). Imaging of complex density in silver nanocubes by coherent x-ray diffraction. *New Journal of Physics*, *12*(3), 035019.
Huang, X., Harder, R., Xiong, G., Shi, X., & Robinson, I. (2011). Propagation uniqueness in three-dimensional coherent diffractive imaging. *Physical Review B*, *83*(22), 224109.

Monitor Reciprocal Space Error

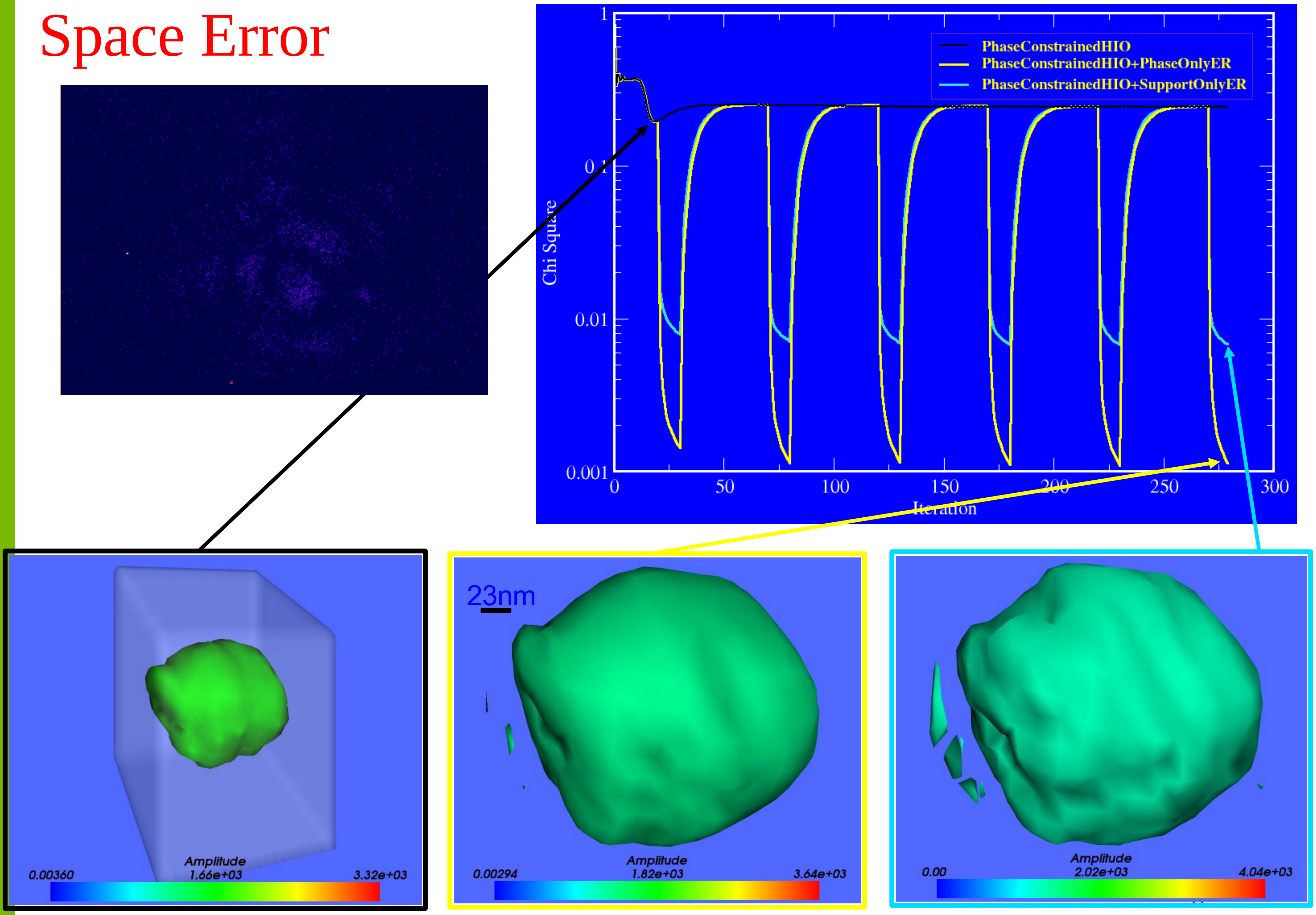

GENETIC/GUIDED ALGORITHM

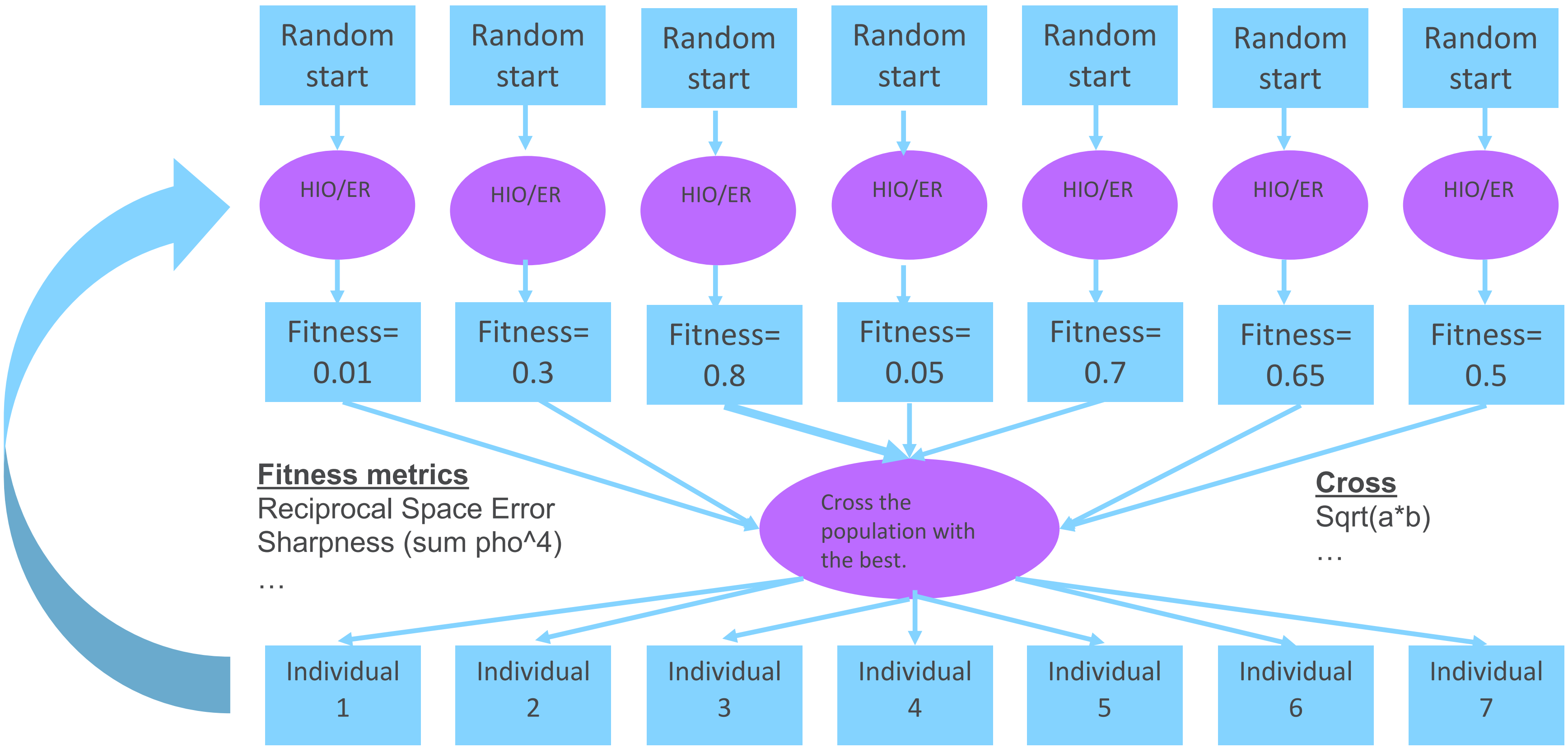

Clark, J. N., Ihli, J., Schenk, A. S., Kim, Y.-Y., Kulak, A. N., Campbell, J. M., et al. (2015). Three-dimensional imaging of dislocation propagation during crystal growth and dissolution. *Nature Materials*, *14*(8), 780–784. http://doi.org/10.1038/nmat4320

Clark, J. N., Huang, X., Harder, R., & Robinson, I. K. (2012). High-resolution three-dimensional partially coherent diffraction imaging. *Nature Communications*, *3*, 993–. http://doi.org/10.1038/ncomms1994

ROSS J. HARDER (XSD)
MATHEW J. CHERUKARA (XSD)
YOUSSEF NASHED (MCS)
TOM PETERKA (MCS)
PRASANNA BALAPRAKASH (MCS)
S. SANKARANARAYANAN (CNM)
BADRI NARAYANAN (MSD)

Argonne NATIONAL LABORATORY

TRAINING THE NEURAL NETWORK

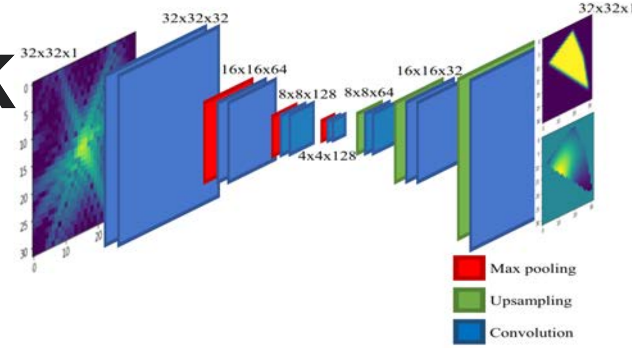

Deep neural networks

sBCDI-NN

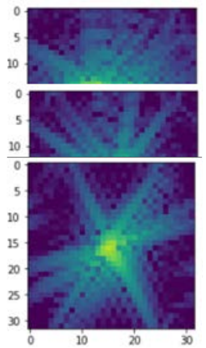

Reciprocal space intensity → Encoder1 → Decoder1 → Real space intensity

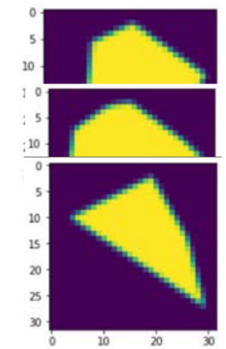

Training:
180,000 examples generated
20,000 held back for validation
1,000 used for testing

pBCDI-NN

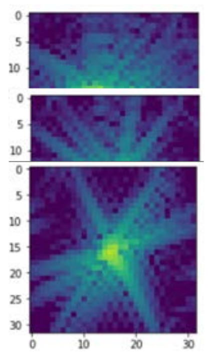

Reciprocal space intensity → Encoder2 → Decoder2 → Real space phase

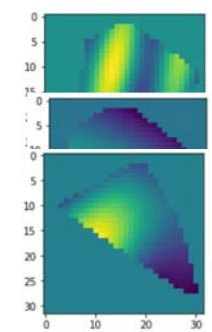

Cherukara, M. J., Nashed, Y. S. G., & Harder, R. J. (2018). *Scientific Reports*, *8*(1), 16520. http://doi.org/10.1038/s41598-018-34525-1

NEURAL NETWORK THAT LEARNS IMAGE RECONSTRUCTION

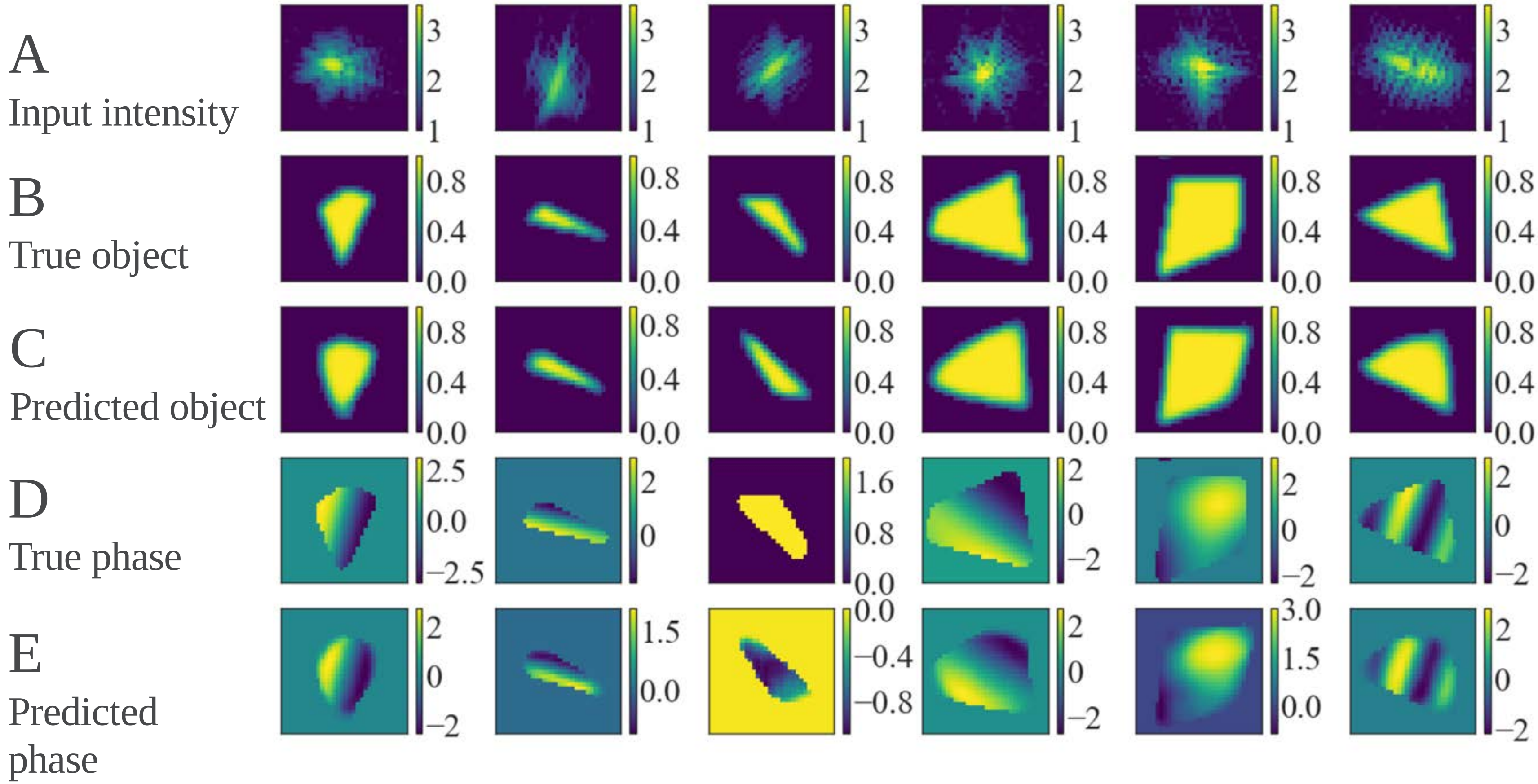

3D Ag Nano Cube

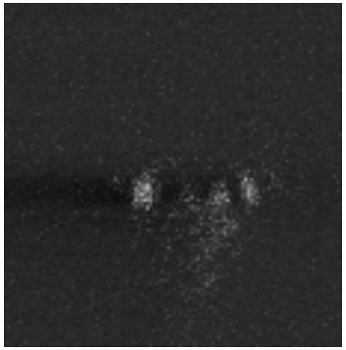

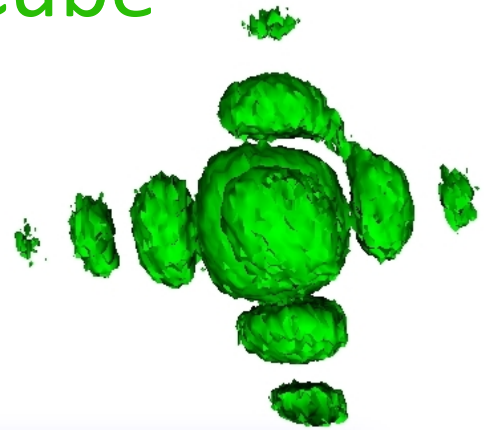

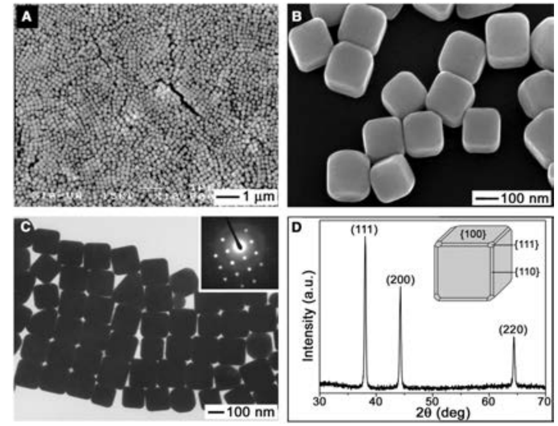

Yugang Sun and Younan Xia, Science 298 2177 (2003)

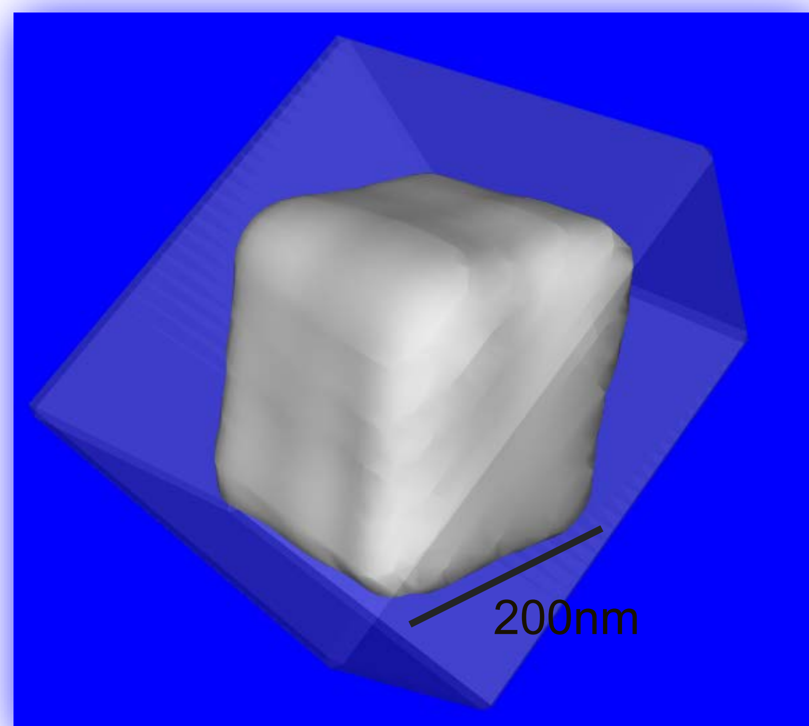

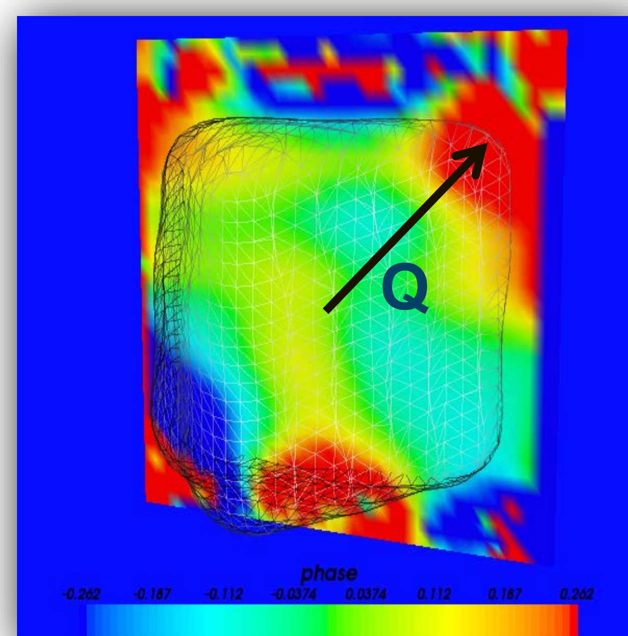

3D Strain Map in ZnO

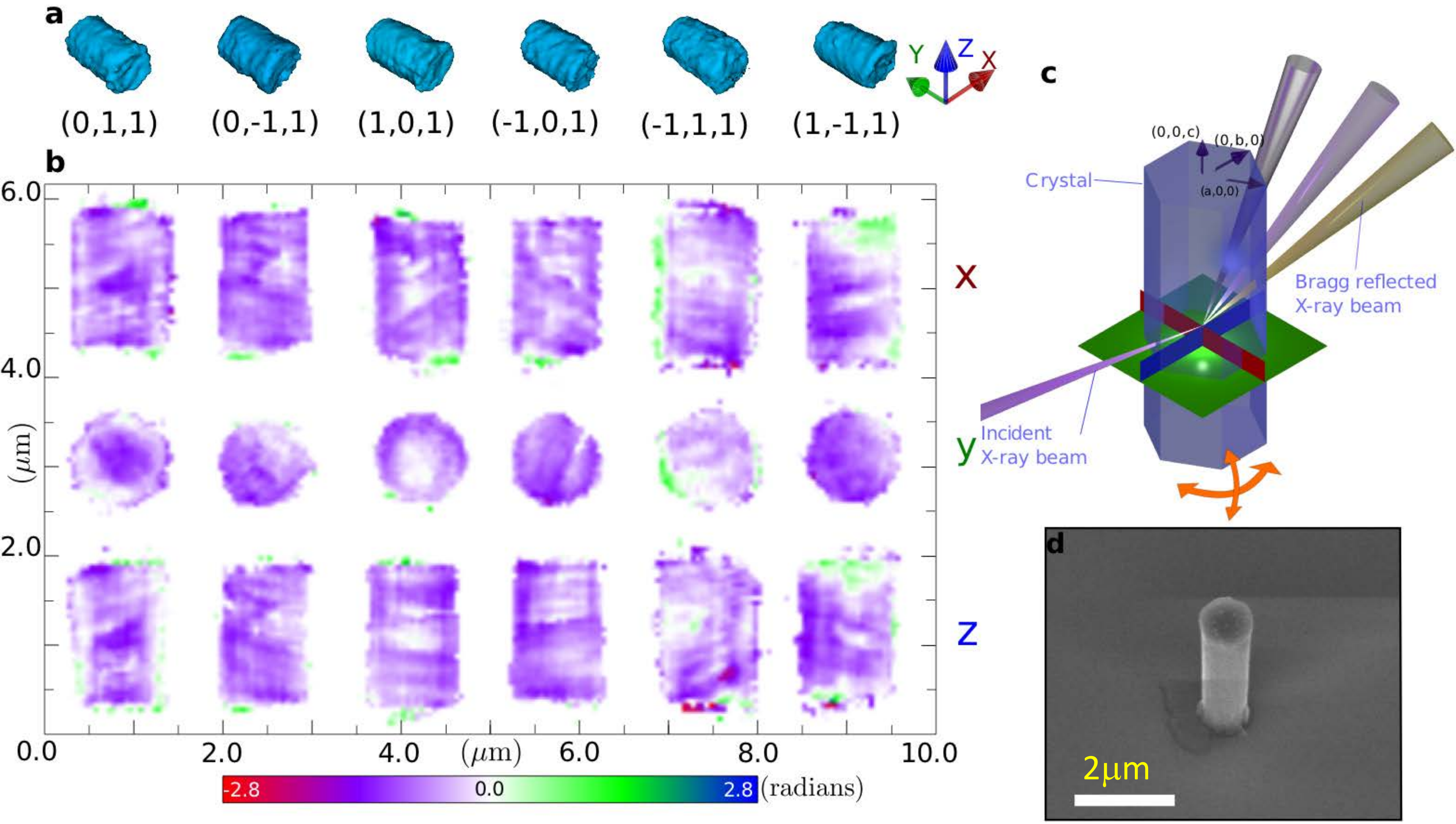

Nature Materials ***9, 120 - 124 (2010)***

3D Strain Map in ZnO

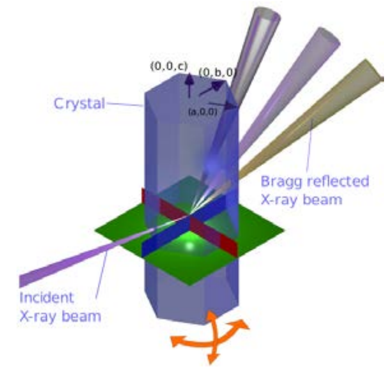

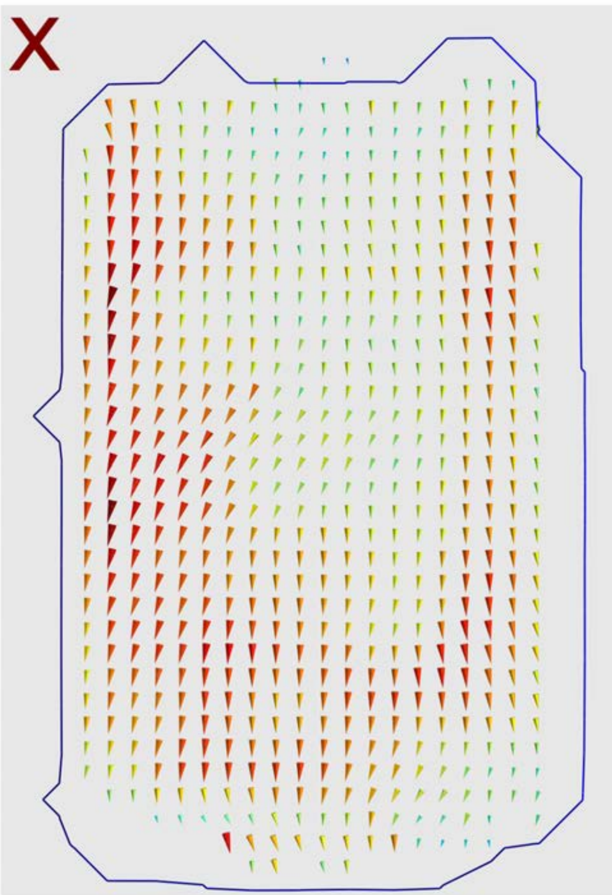

$$u_j = \xi_{ji} q_{ki} \phi_k; \qquad \xi_{ji} = (q_{kj} q_{ki})^{-1}$$

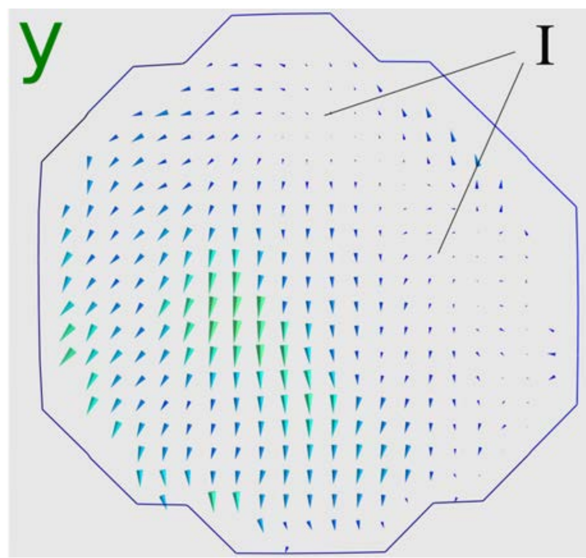

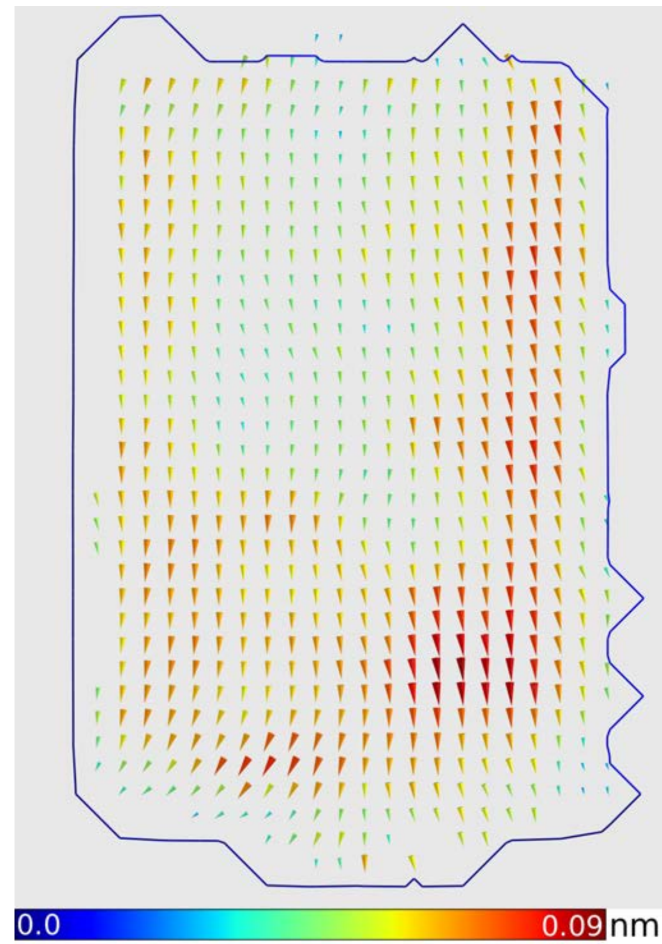

Nature Materials ***9, 120 - 124 (2010)***

3D Strain Map in ZnO

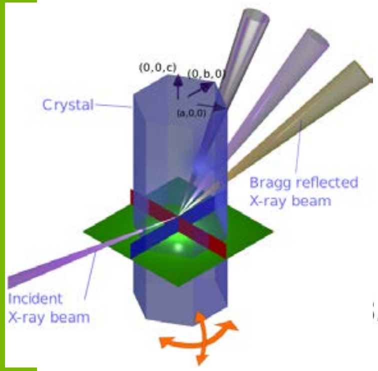

$$\epsilon_{ij} = \frac{1}{2}\left(\frac{\partial u_j}{\partial x_i} + \frac{\partial u_i}{\partial x_j}\right), \qquad \tau_{ij} = \left(\frac{\partial u_j}{\partial x_i} - \frac{\partial u_i}{\partial x_j}\right)$$

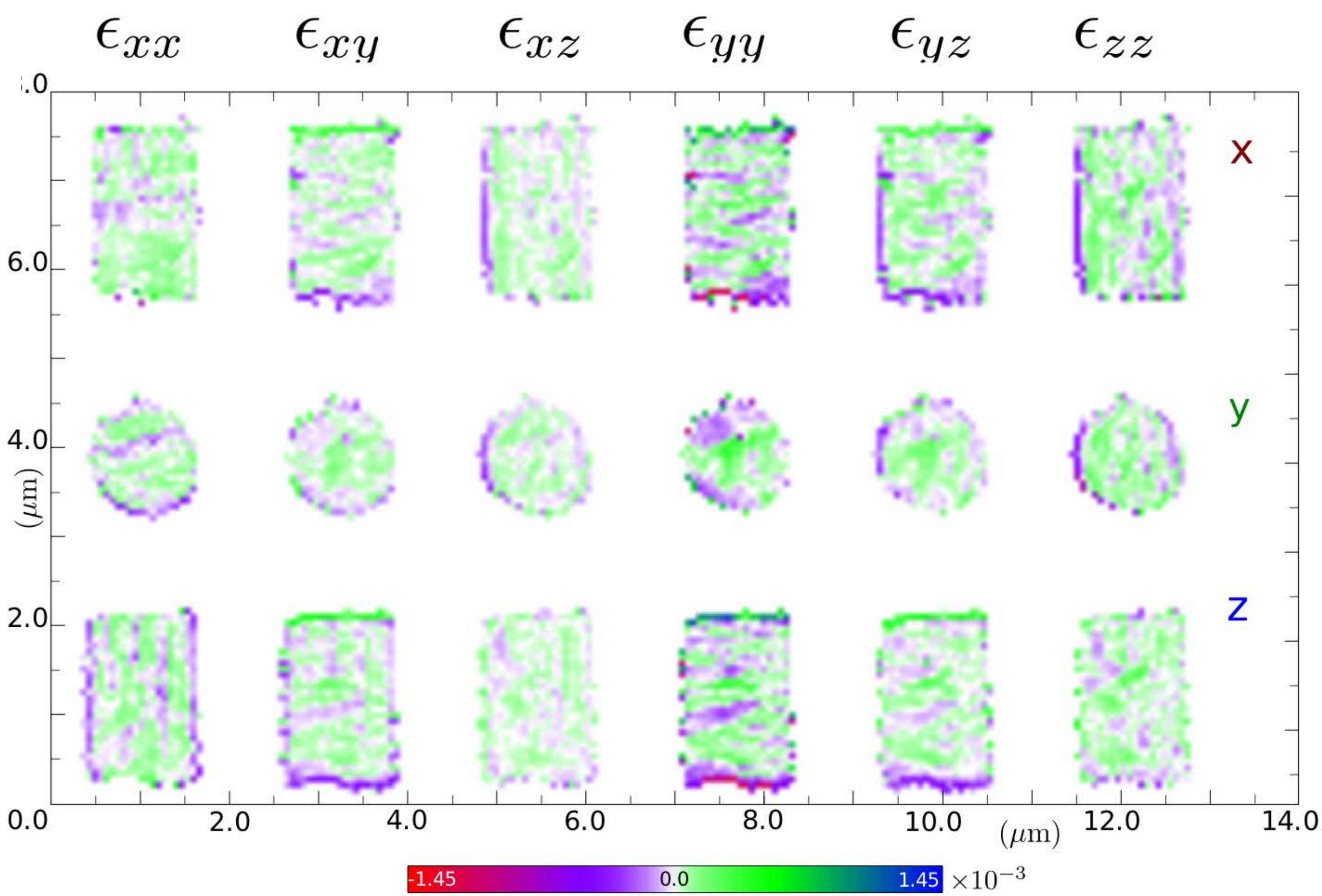

Nature Materials ***9, 120 - 124 (2010)***

Patterned Gold Nanocystal Samples

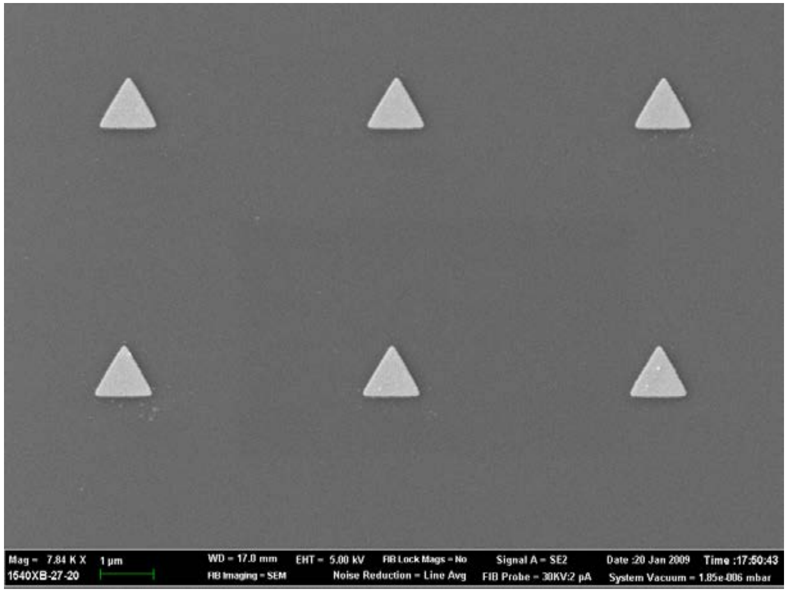

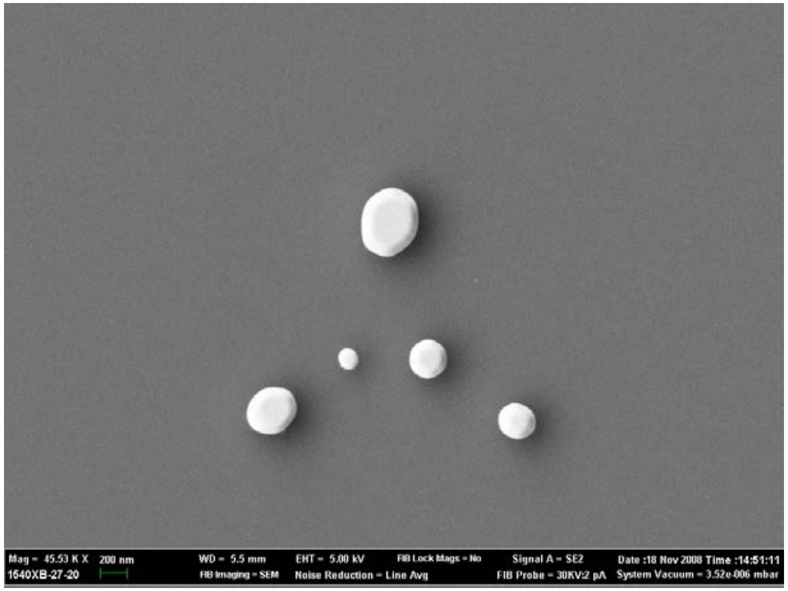

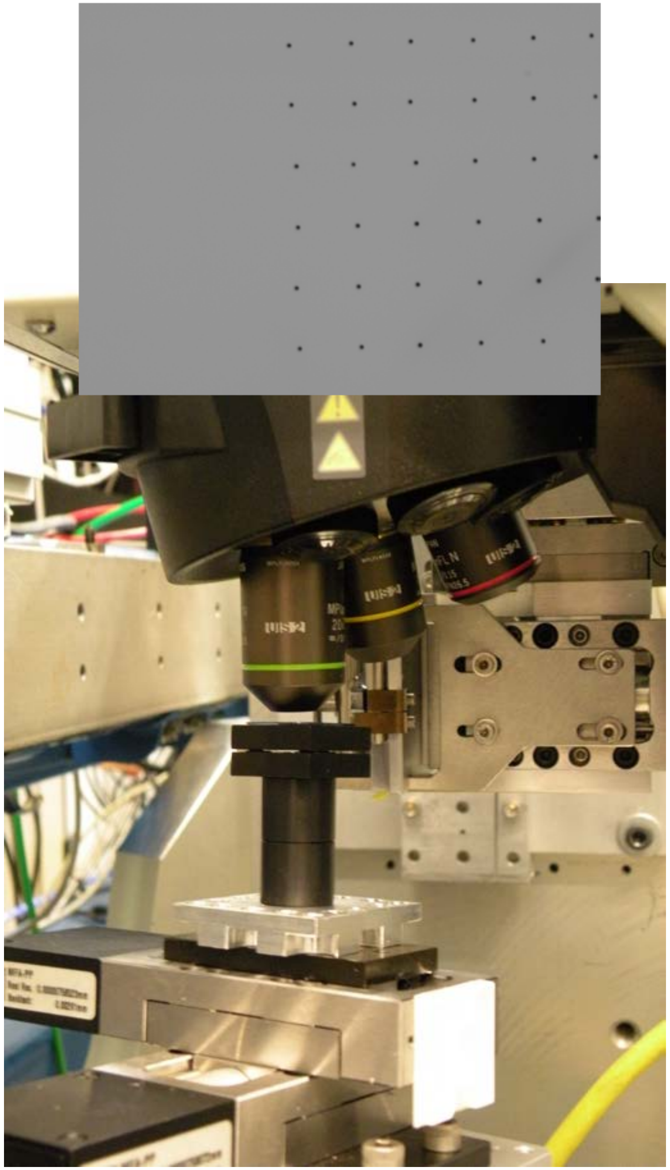

Argonne NATIONAL LABORATORY

Multiple reflection reconstructions

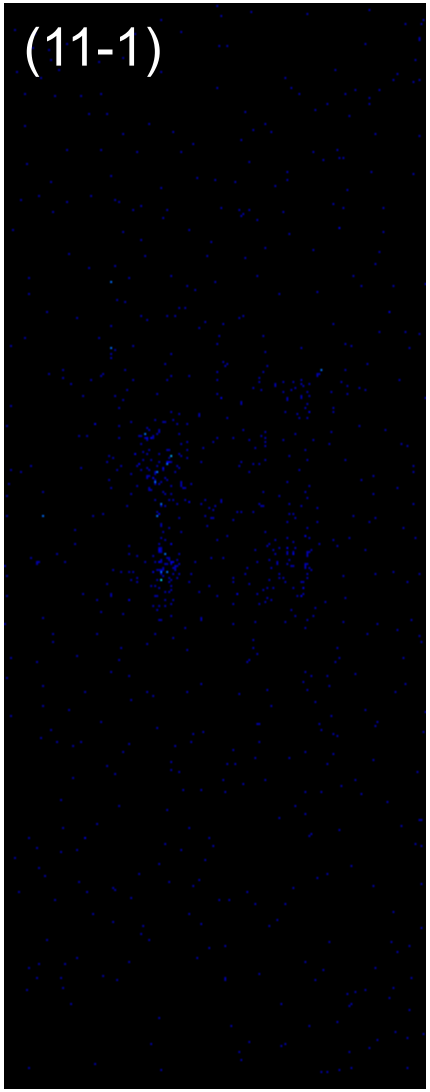

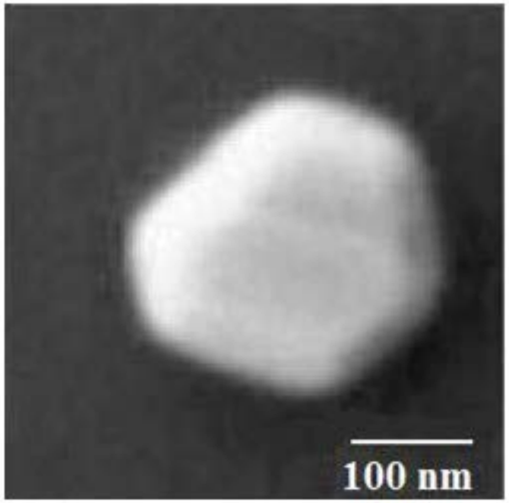

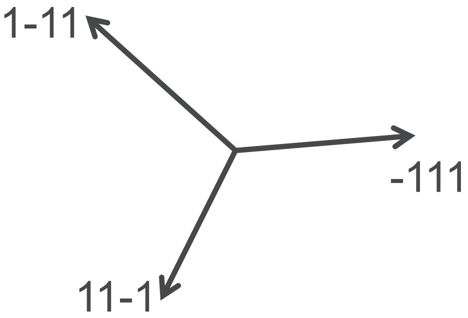

Multiple reflection reconstructions

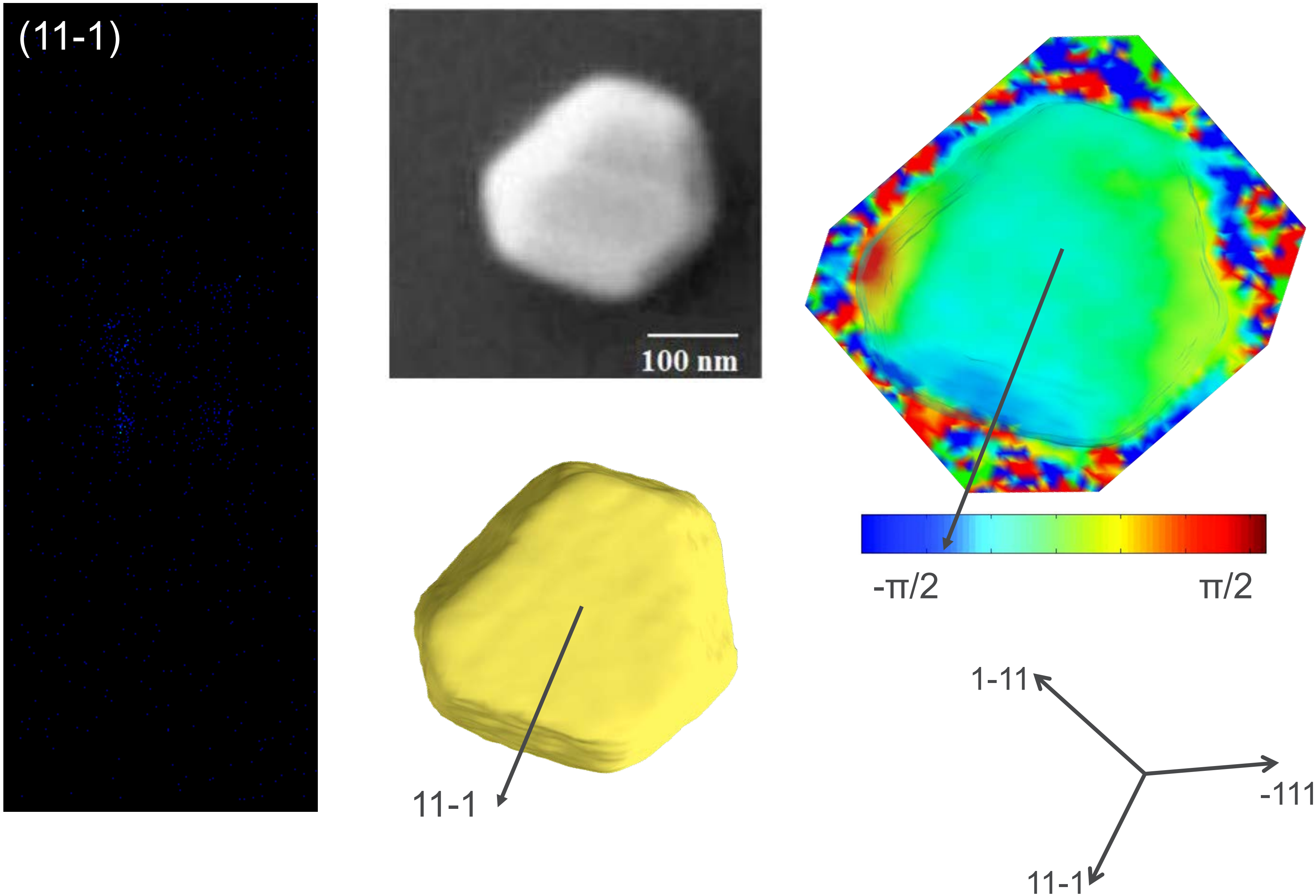

Multiple reflection reconstructions

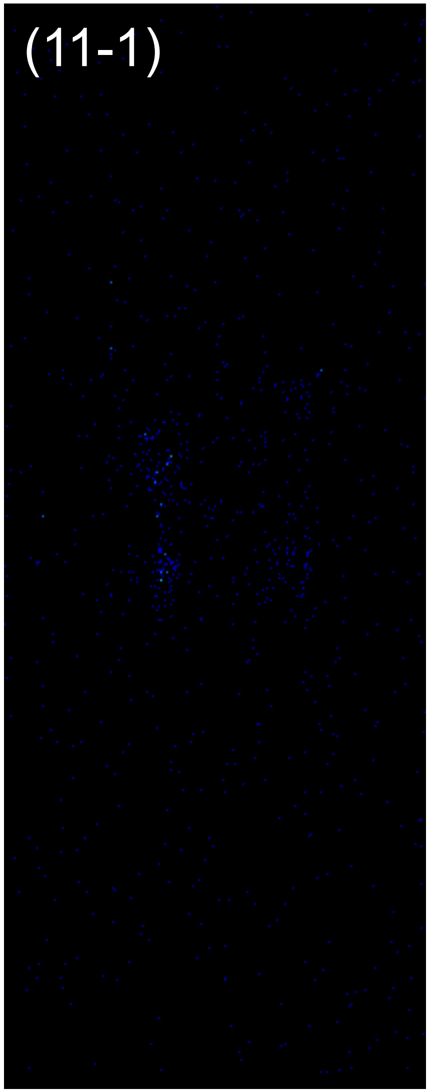

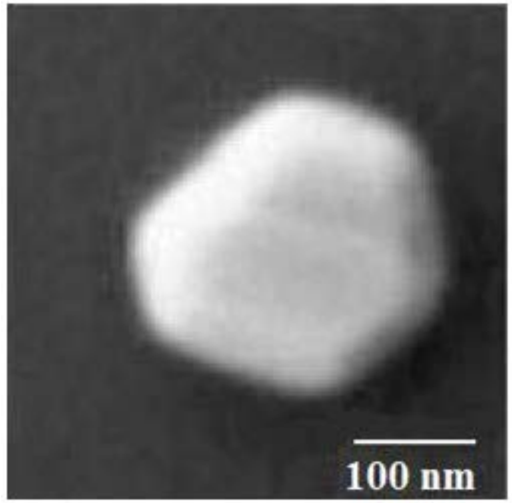

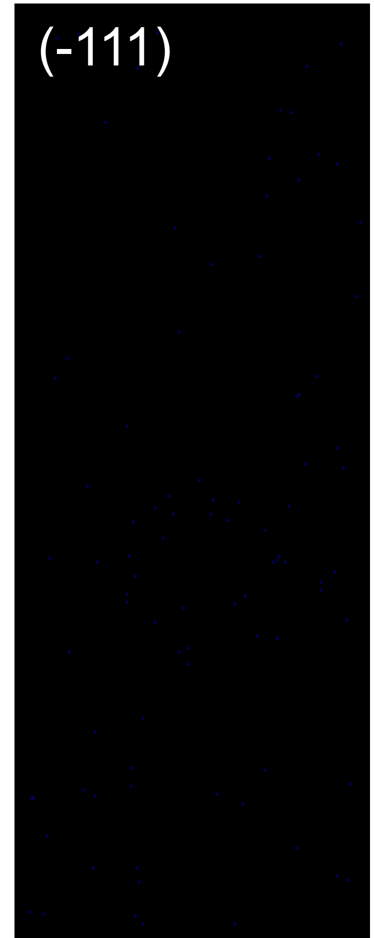

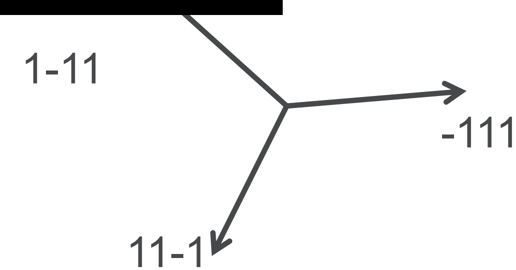

Multiple reflection reconstructions

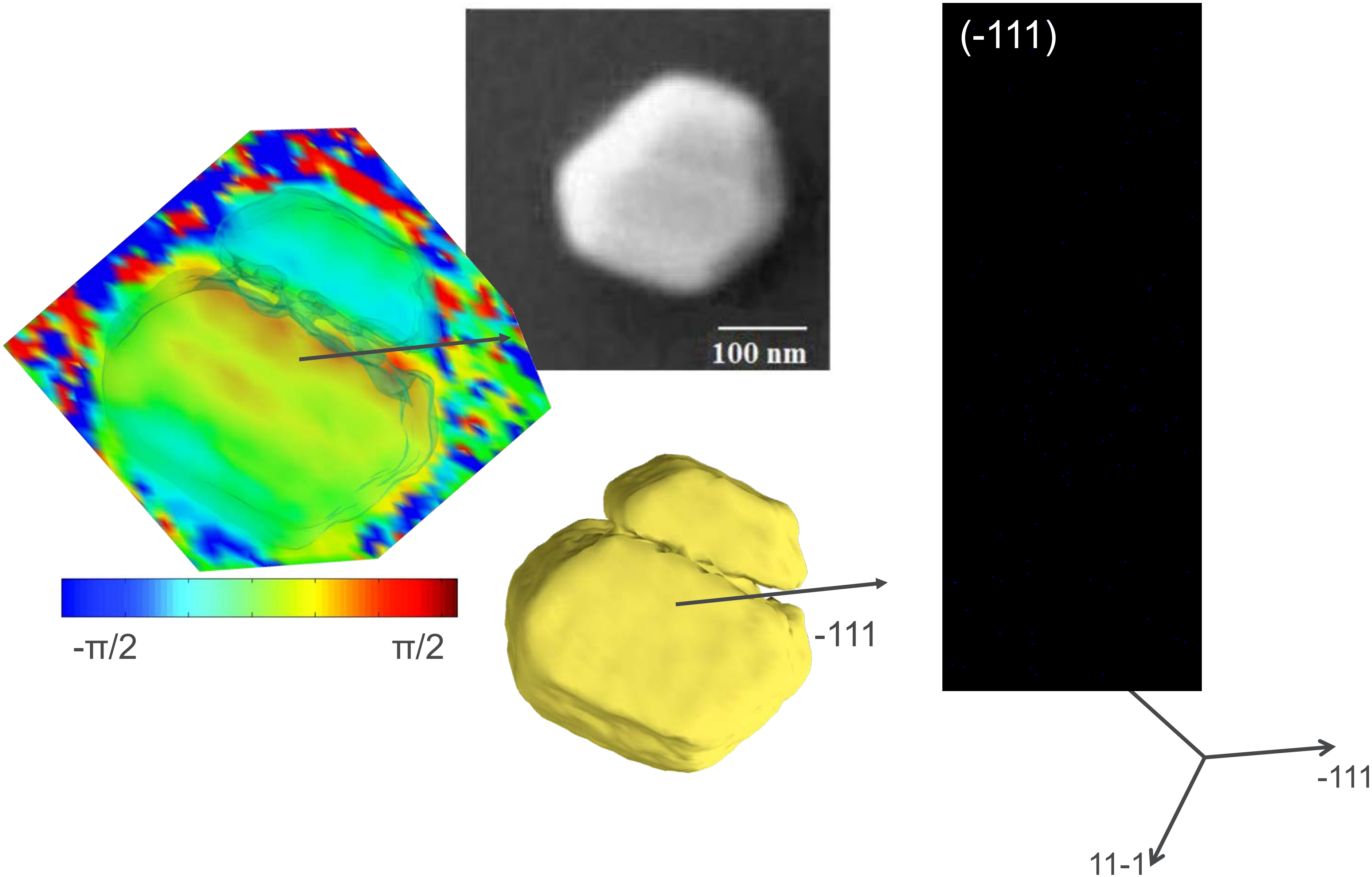

Multiple reflection reconstructions

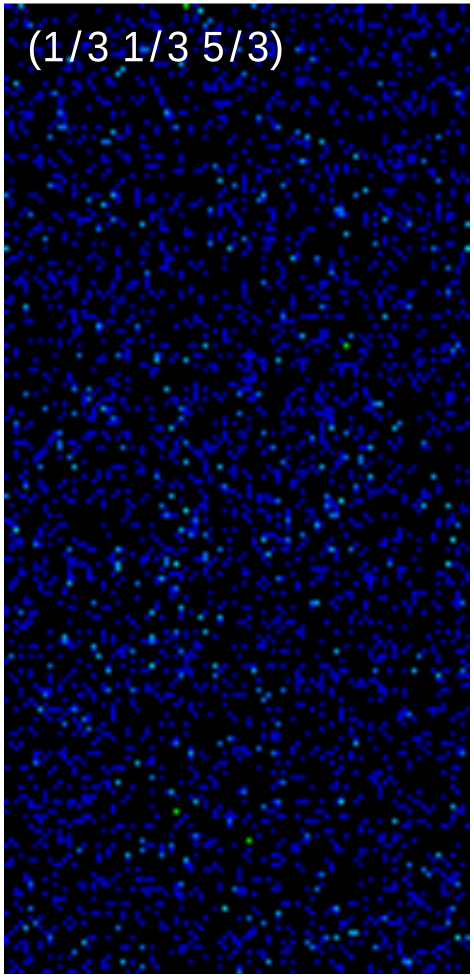

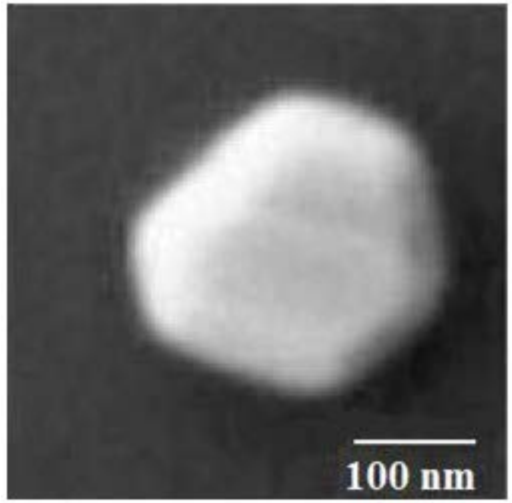

(1/3 1/3 5/3)

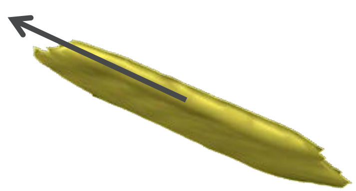

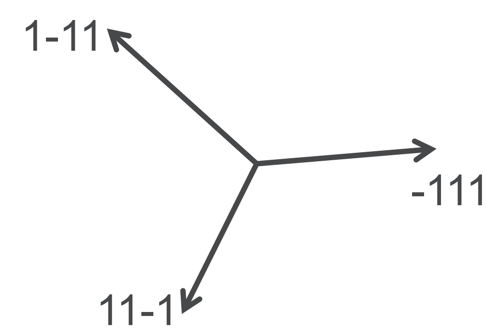

Multiple reflection reconstructions

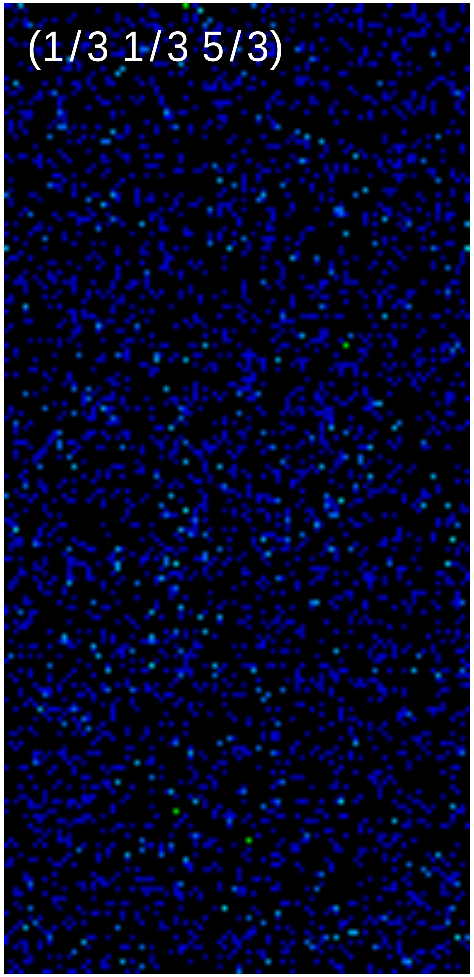

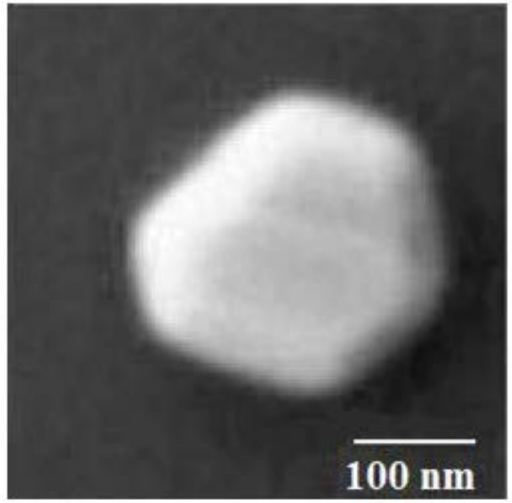

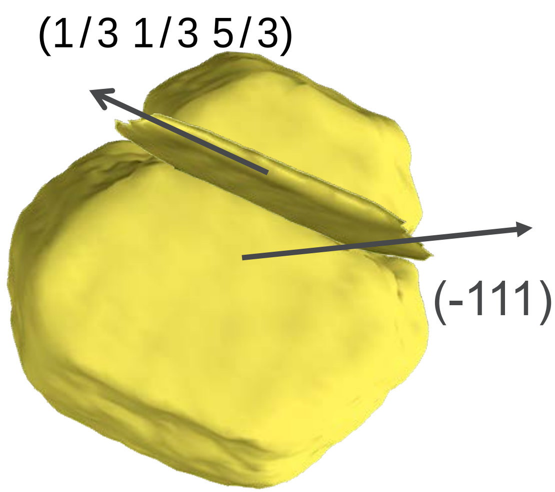

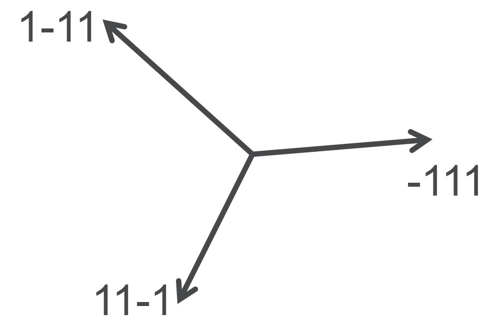

Multiple reflection reconstructions

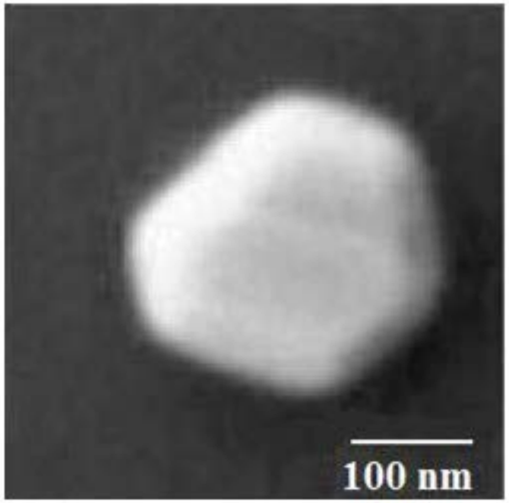

$$\varphi = q.u(r)$$

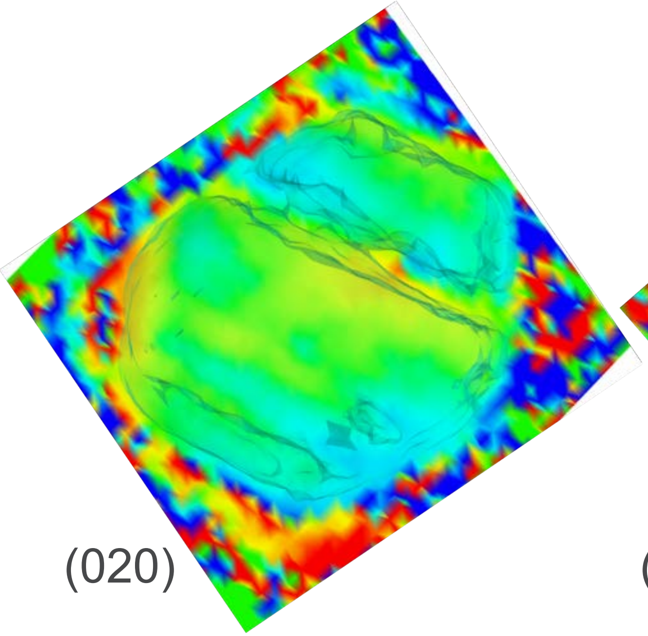

(020)

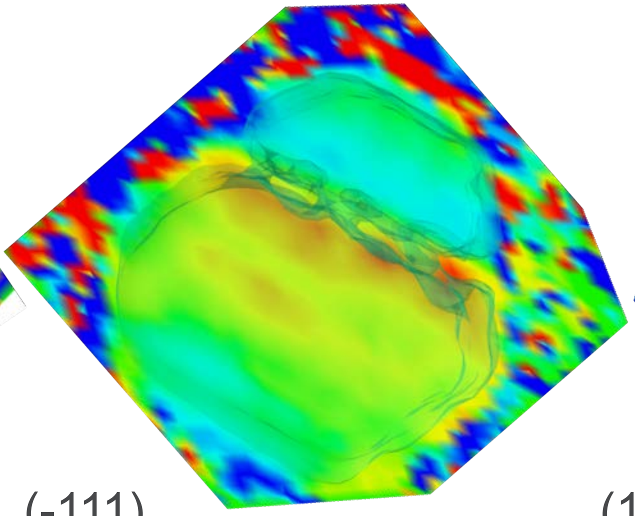

(-111)

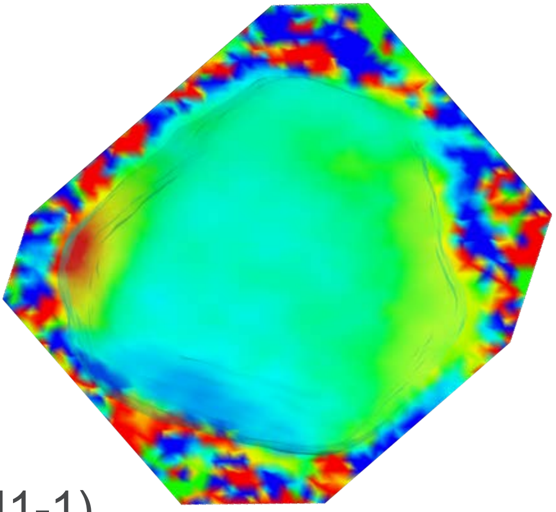

(11-1)

Vector Displacement Field of Gold lattice

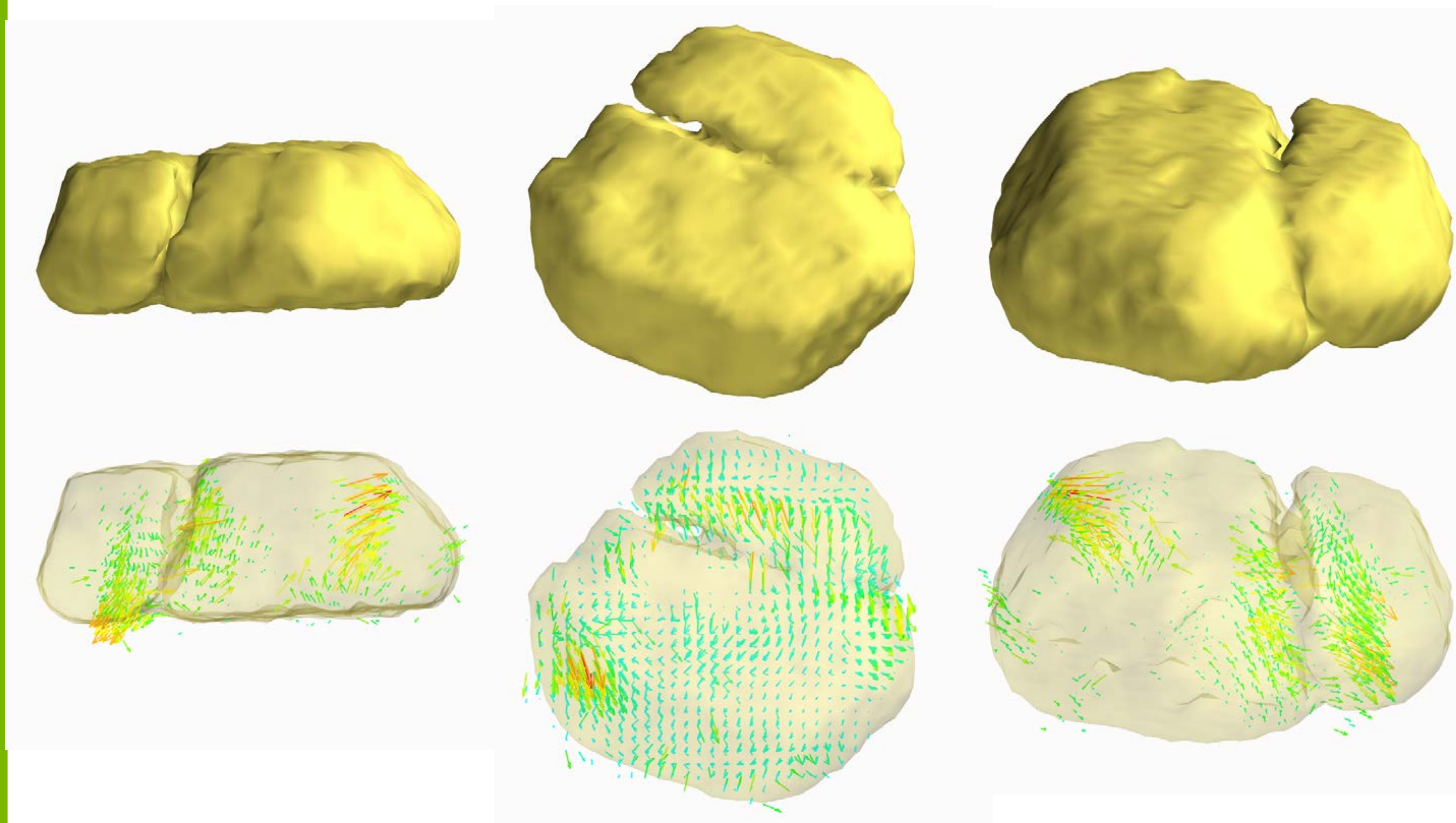

Produced by combining reconstructions from (11-1) (020) (-111)

BCDI TODAY

Operando Nanoscale Imaging

Dislocation dynamics in Li-Ion battery

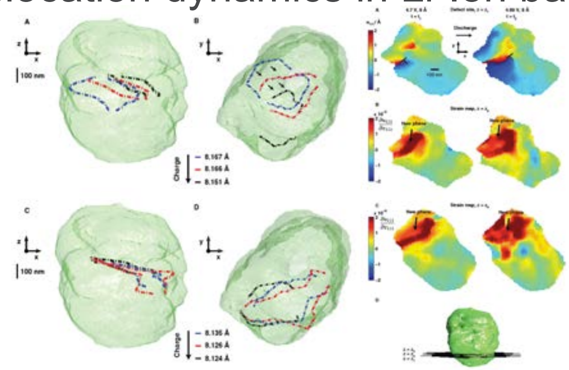

Ulvestad, A., et al. (2015). *Science*, *348*(6241), 1344–1347

Liquid Catalysis

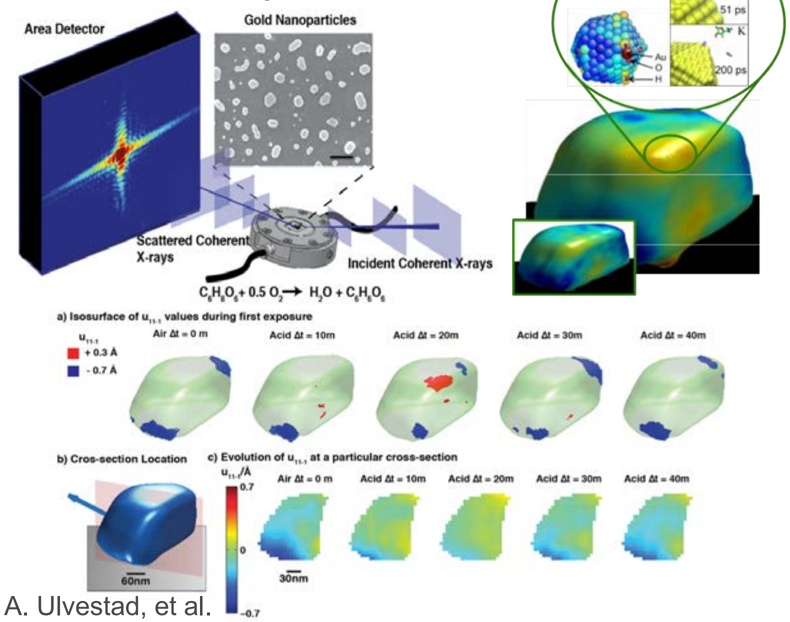

A. Ulvestad, et al.
J. Phys. Chem. Lett., vol. 7, no. 15, pp. 3008, Aug. 2016.

Strain Tensor Imaging

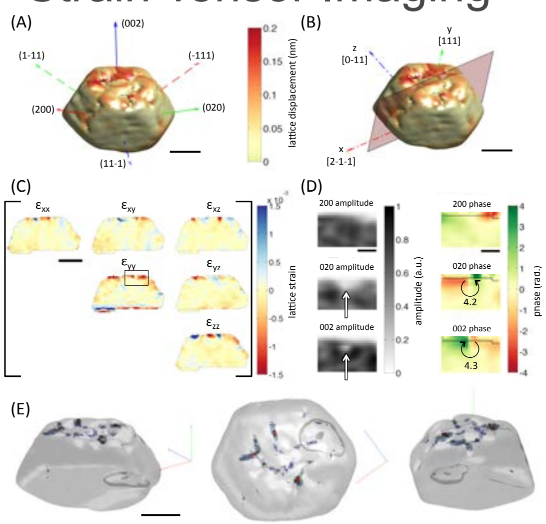

F. Hofmann, et al.
Sci Rep, vol. 7, p. 45993, Apr. 2017.

Dislocation dynamics in the hydriding phase transformations of Pd

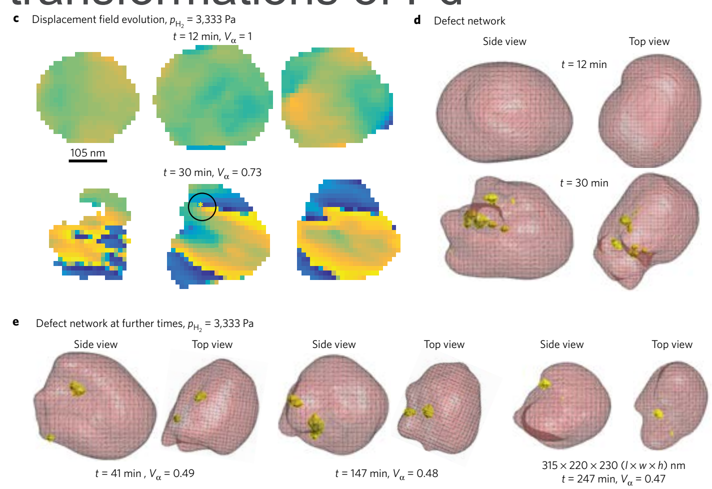

Ulvestad, et al.
Nature Materials, vol. 16, no. 5, pp. 565–571, Jan. 2017.

Argonne NATIONAL LABORATORY

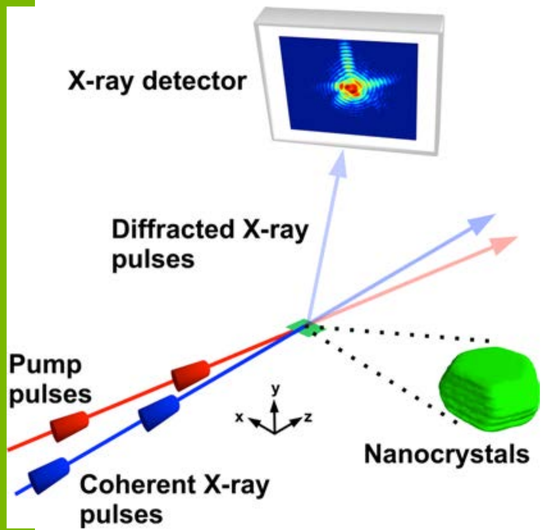

Imaging Lattice Dynamics
Laser Pump – CXD Probe@LCLS

$$S(\tau) = \sum_{n=1}^{N} A_n \exp\left[-\frac{\tau}{\tau_{d,n}}\right] \cos\left[\frac{2\pi}{T_n}(\tau + \tau_{0,n})\right] + C_n.$$

600 pm "breathing modes"

Crystal A
101 ps and 241 ps

Crystal B
90 ps and 256 ps

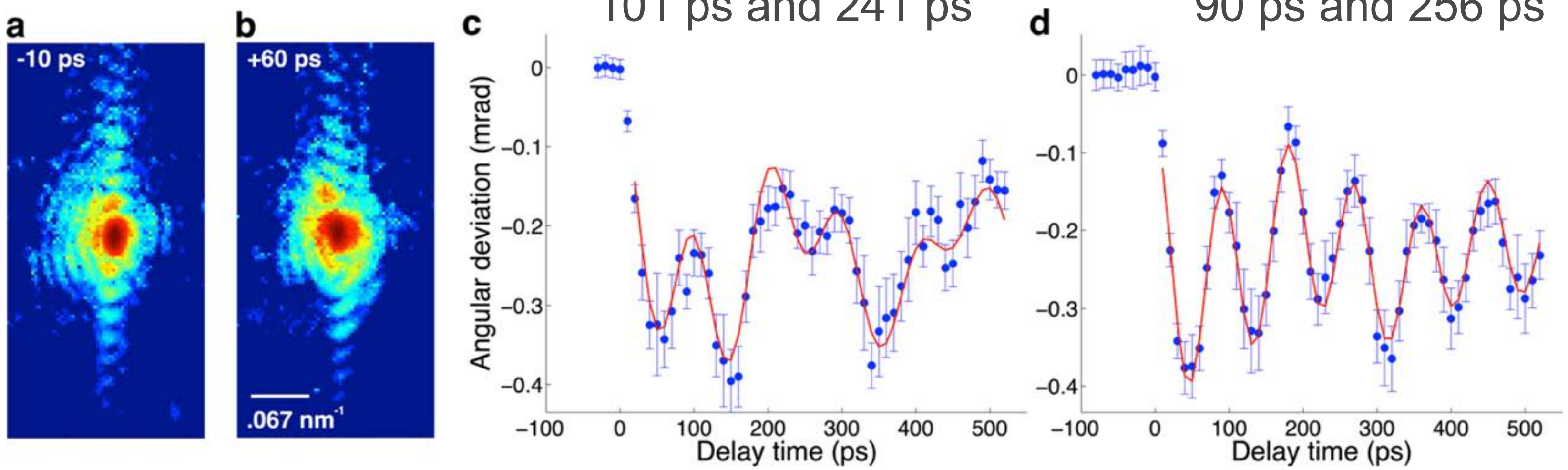

Ultrafast three dimensional imaging of lattice dynamics in individual gold nanocrystals
J. N. Clark, L. Beitra, G. Xiong, A. Higginbotham, D. M. Fritz, H. T. Lemke, D. Zhu,
M. Chollet, G. J. Williams, M. Messerschmidt, B. Abbey, R. J. Harder,
A. M. Korsunsky, J. S. Wark & I. K. Robinson. (2013). *Science*, *341*(6141), 56–59

Imaging Lattice Dynamics
Laser Pump – CXD Probe@LCLS

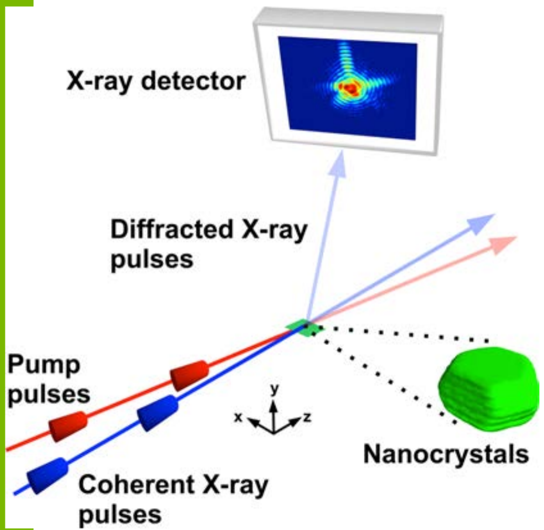

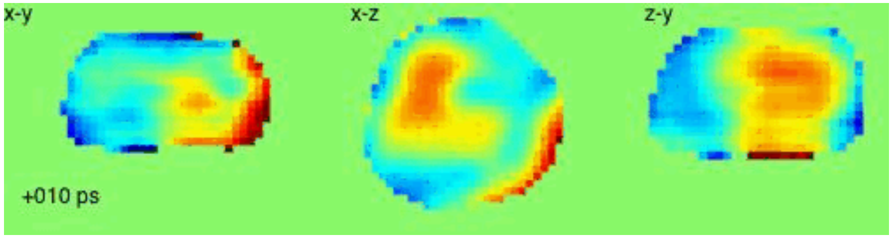

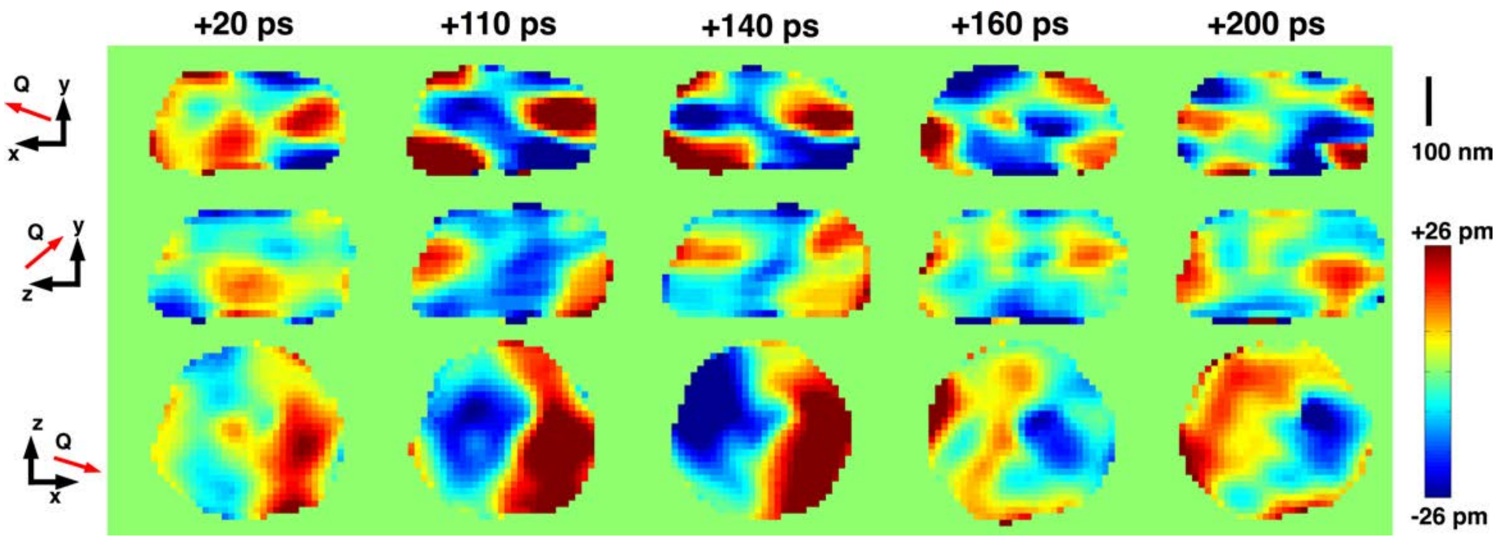

Ultrafast three dimensional imaging of lattice dynamics in individual gold nanocrystals
J. N. Clark, L. Beitra, G. Xiong, A. Higginbotham, D. M. Fritz, H. T. Lemke, D. Zhu, M. Chollet, G. J. Williams, M. Messerschmidt, B. Abbey, R. J. Harder, A. M. Korsunsky, J. S. Wark & I. K. Robinson. (2013). *Science*, *341*(6141), 56–59

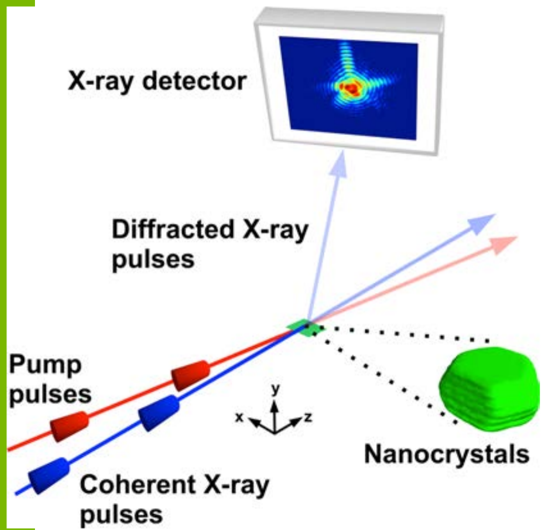

Imaging Lattice Dynamics
Laser Pump – CXD Probe@LCLS

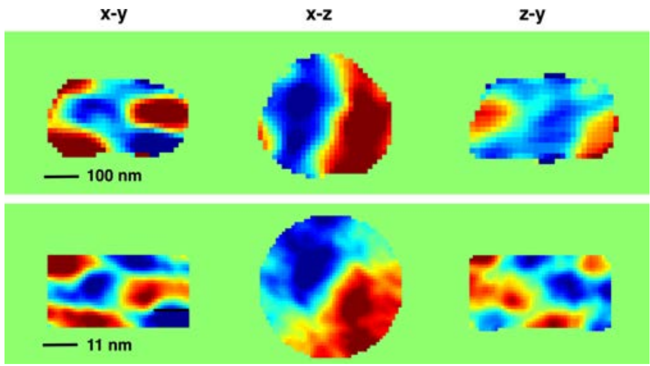

Orthogonal slices
Through crystal density

MD simulation
at +110ps

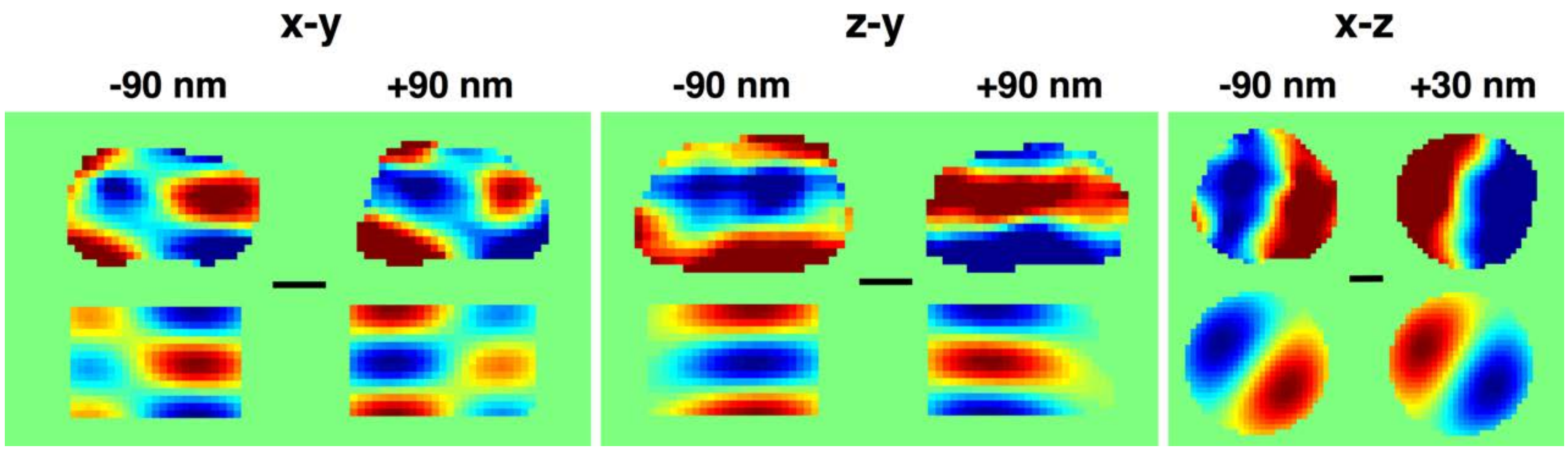

Ultrafast three dimensional imaging of lattice dynamics in individual gold nanocrystals
J. N. Clark, L. Beitra, G. Xiong, A. Higginbotham, D. M. Fritz, H. T. Lemke, D. Zhu,
M. Chollet, G. J. Williams, M. Messerschmidt, B. Abbey, R. J. Harder,
A. M. Korsunsky, J. S. Wark & I. K. Robinson. (2013). *Science*, *341*(6141), 56–59

Ptychography (to fold) - Scanning CDI for extended object

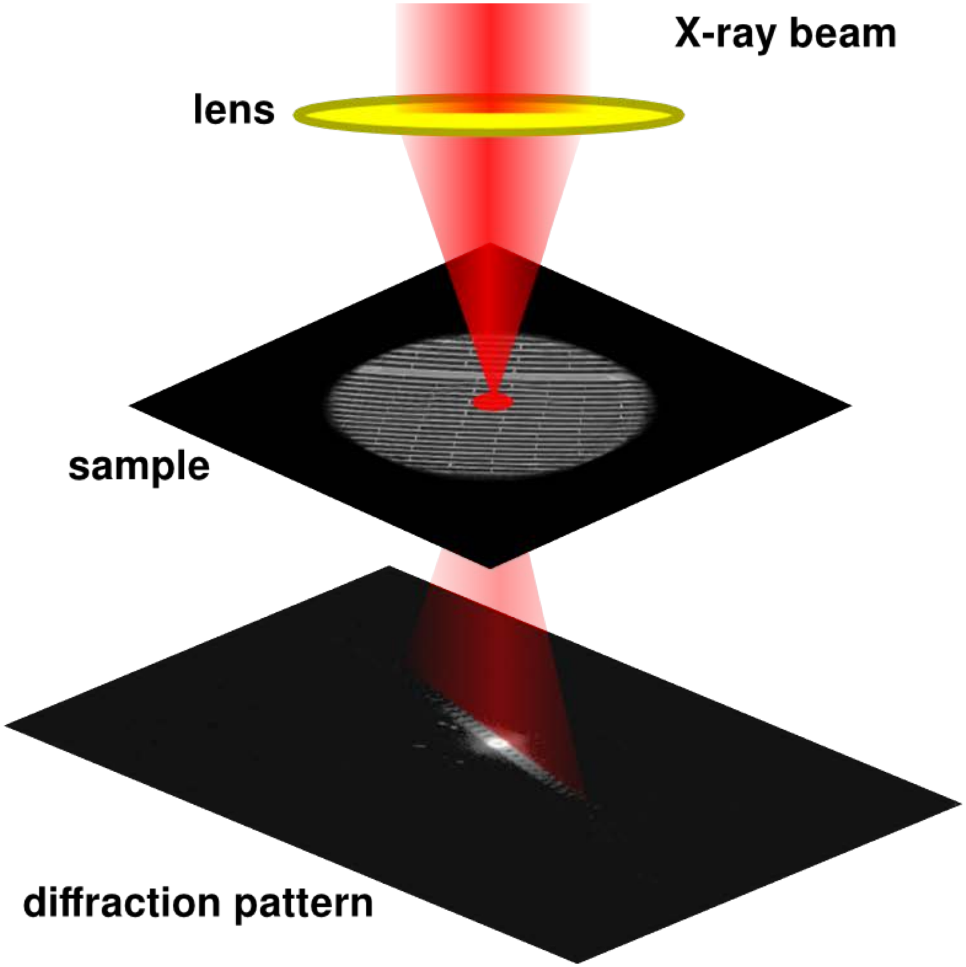

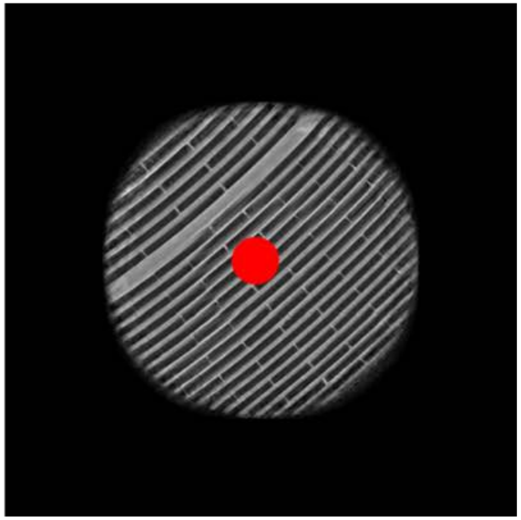

Courtesy Dr. Junjing Deng (APS)

Ptychography (to fold) - Scanning CDI for extended object

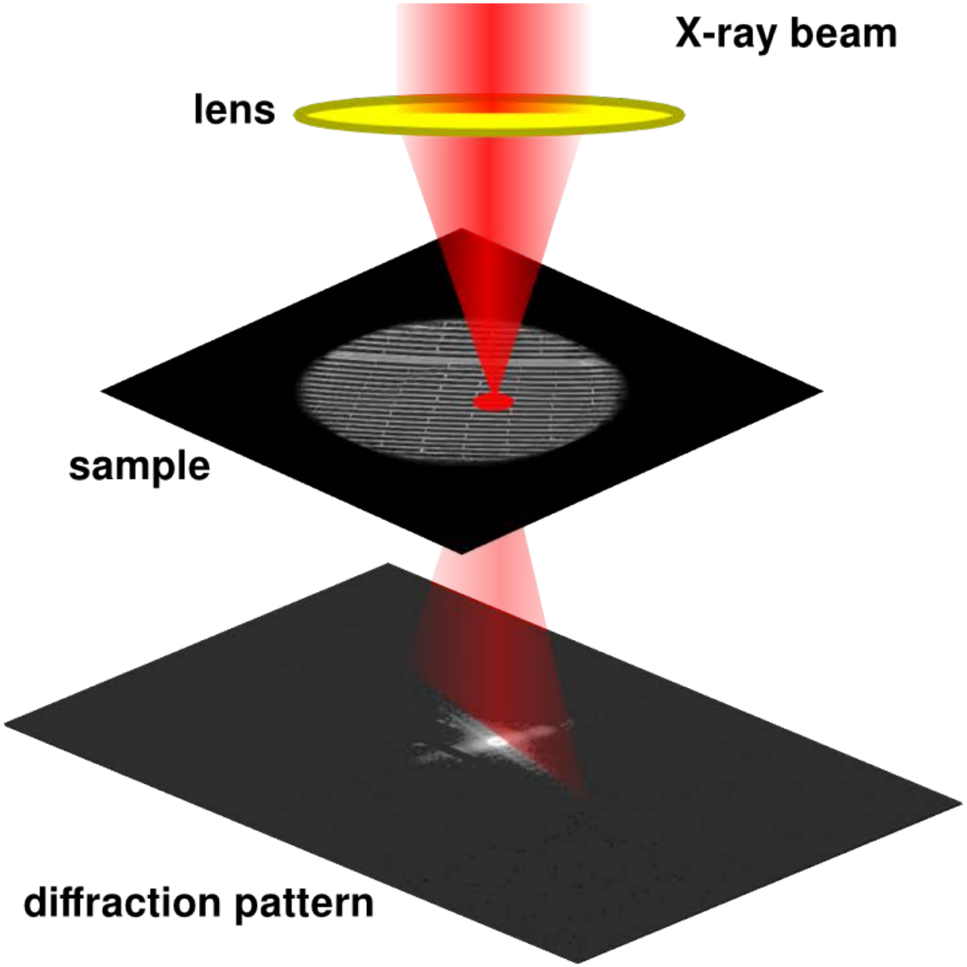

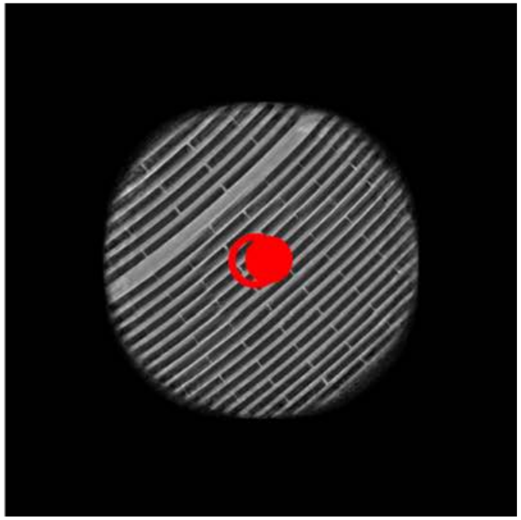

Courtesy Dr. Junjing Deng (APS)

Ptychography (to fold) - Scanning CDI for extended object

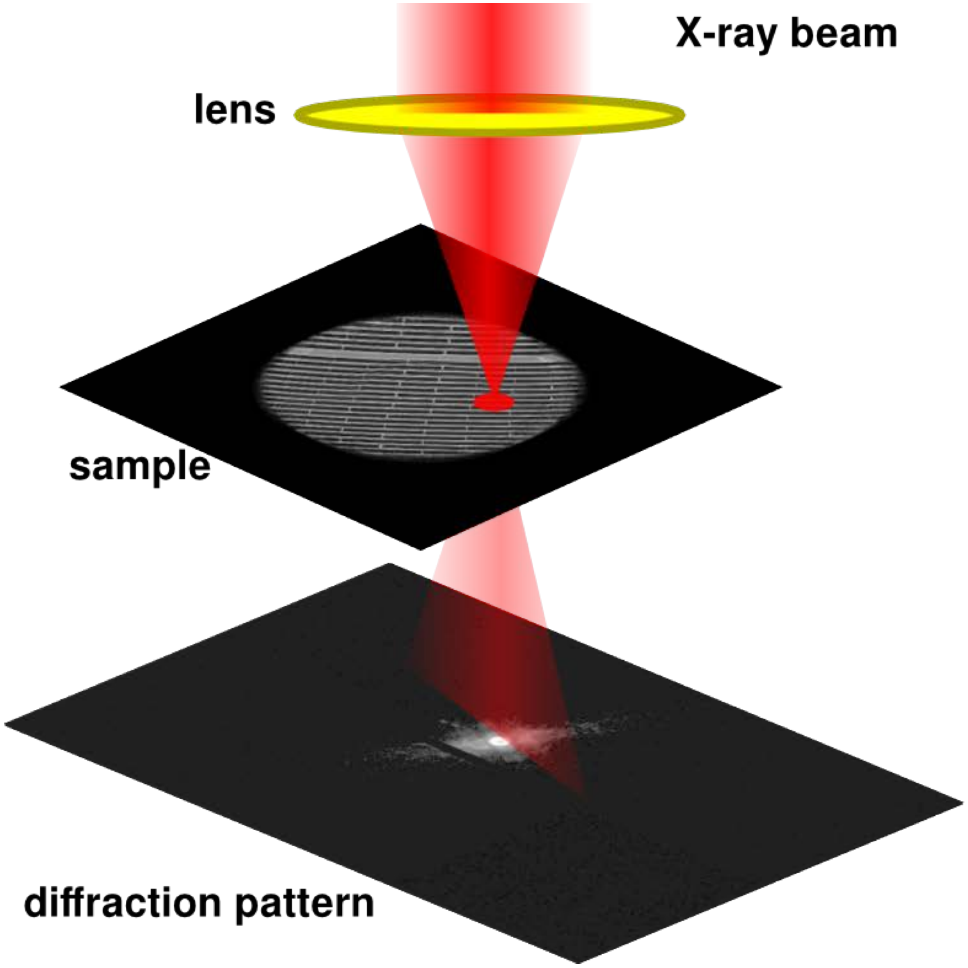

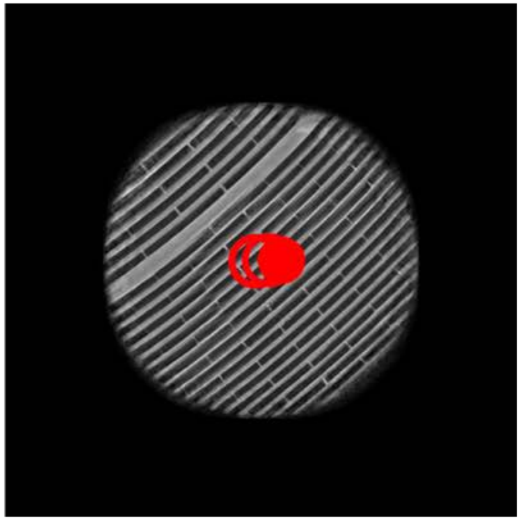

Courtesy Dr. Junjing Deng (APS)

Ptychography

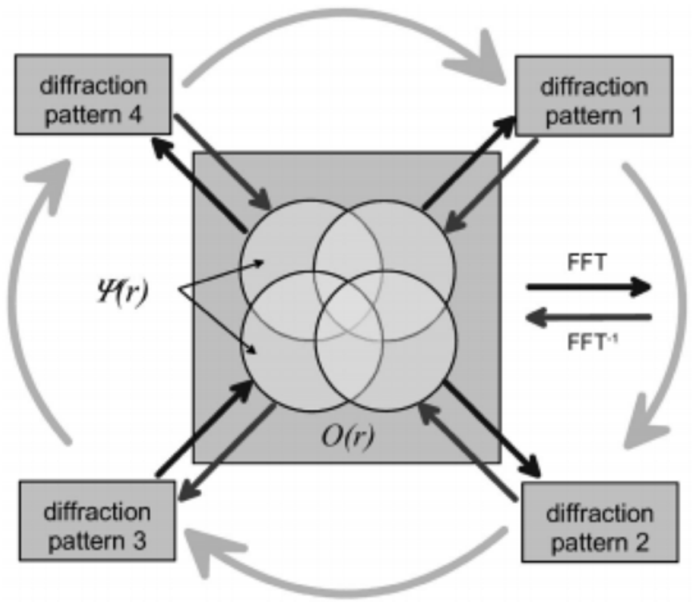

Ptychographic iterative engine (PIE)

J. Rodenburg *et al., PRL* **98** , 034801 (2007)

Platinum nanostructure

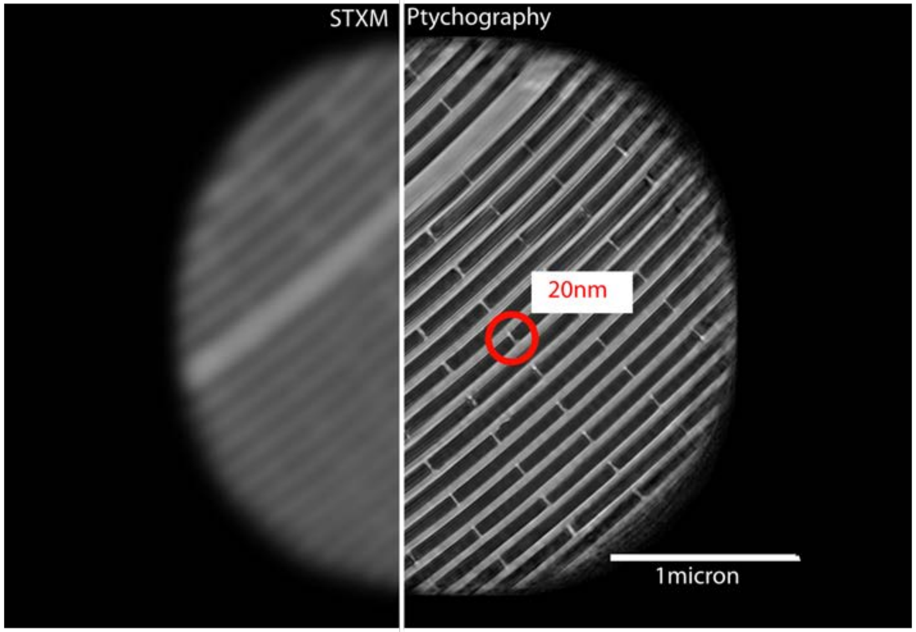

Spatial resolution: $\delta = \frac{\lambda}{\theta} = \frac{\lambda z}{N\Delta}$

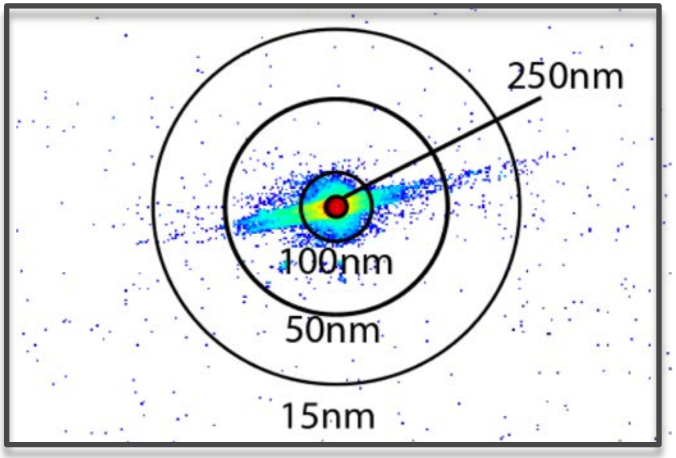

Exit surface wave field: $\psi(r) = P(r)O(r)$

$$O(\mathbf{r}) = \frac{\sum_j P^*(\mathbf{r}-\mathbf{r}_j)\psi_j(\mathbf{r})}{\sum_j |P(\mathbf{r}-\mathbf{r}_j)|^2} \qquad P(\mathbf{r}) = \frac{\sum_j O^*(\mathbf{r}+\mathbf{r}_j)\psi_j(\mathbf{r}+\mathbf{r}_j)}{\sum_j |O(\mathbf{r}+\mathbf{r}_j)|^2}$$

P. Thibault *et al., Science* **321**, 379 (2008)

Argonne NATIONAL LABORATORY

Courtesy Dr. Junjing Deng (APS)

At which plane ptychographic images are reconstructed

$$\psi(r) = P(r)O(r)$$

Ptychography always produces images at the sample plane.

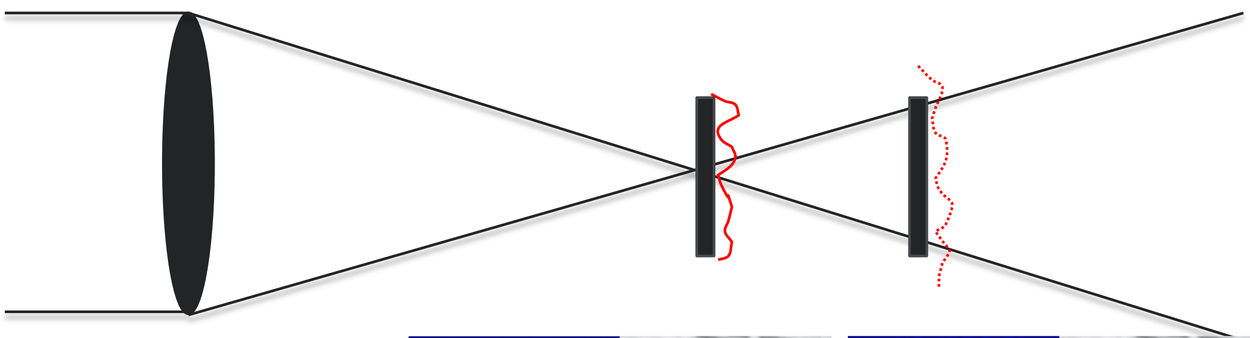

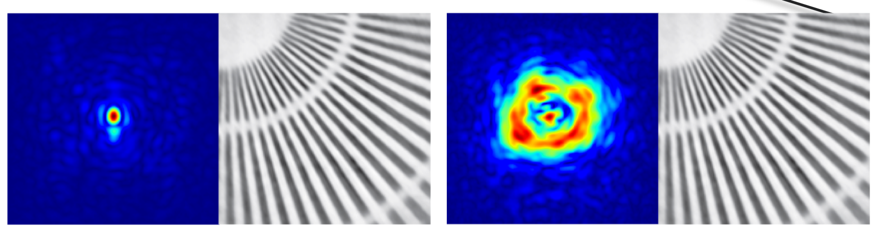

The resolution is not limited by the beam size.

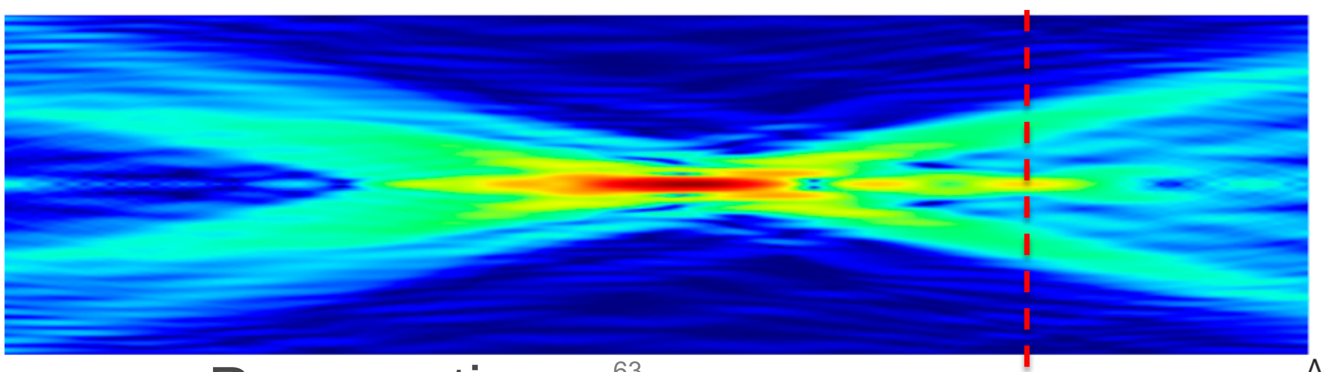

Characterization of focusing optics.

Propagation

Sample plane

Courtesy Dr. Junjing Deng (APS)

PTYCHOGRAPHY
MICROPROBES -> COHERENT IMAGING INSTRUMENT

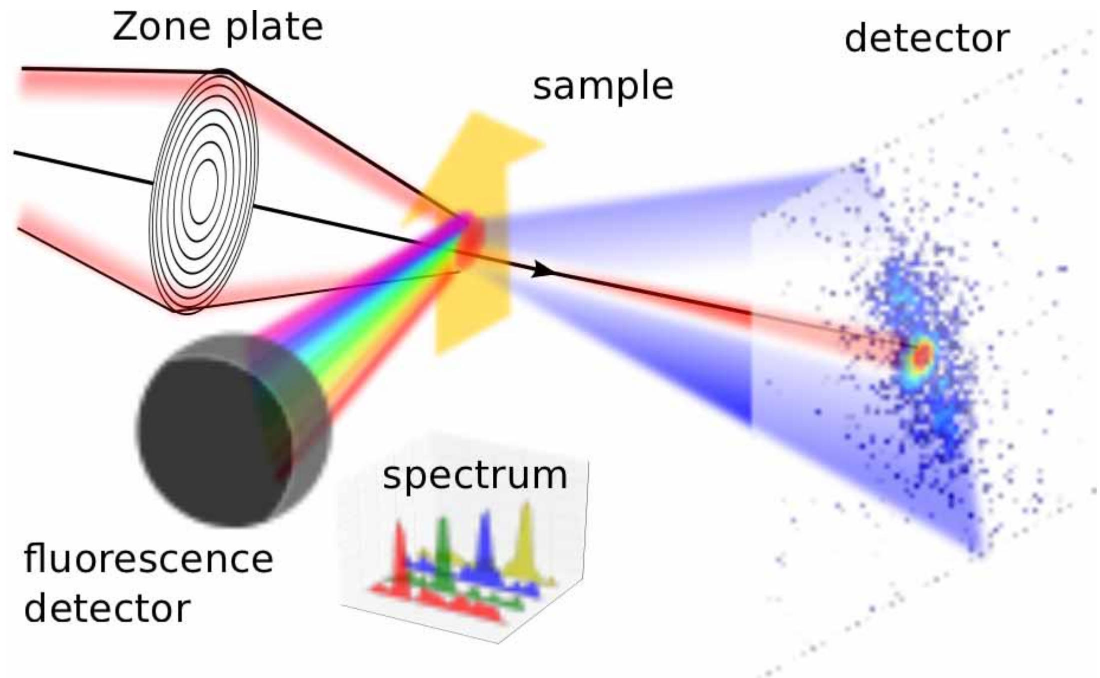

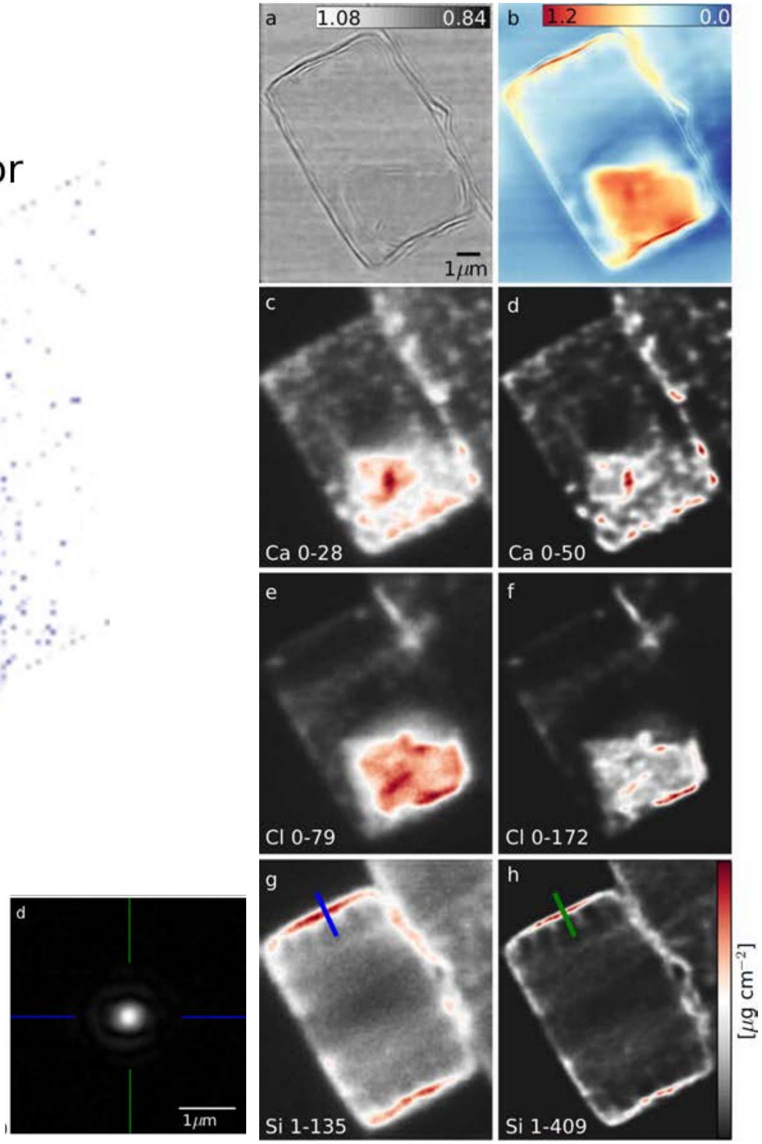

Vine, et al. (2012). *Opt. Express*, *20*(16), 18287–18296.

Making ptychography colorful

❖ **Combination of Ptychography & Fluorescence**

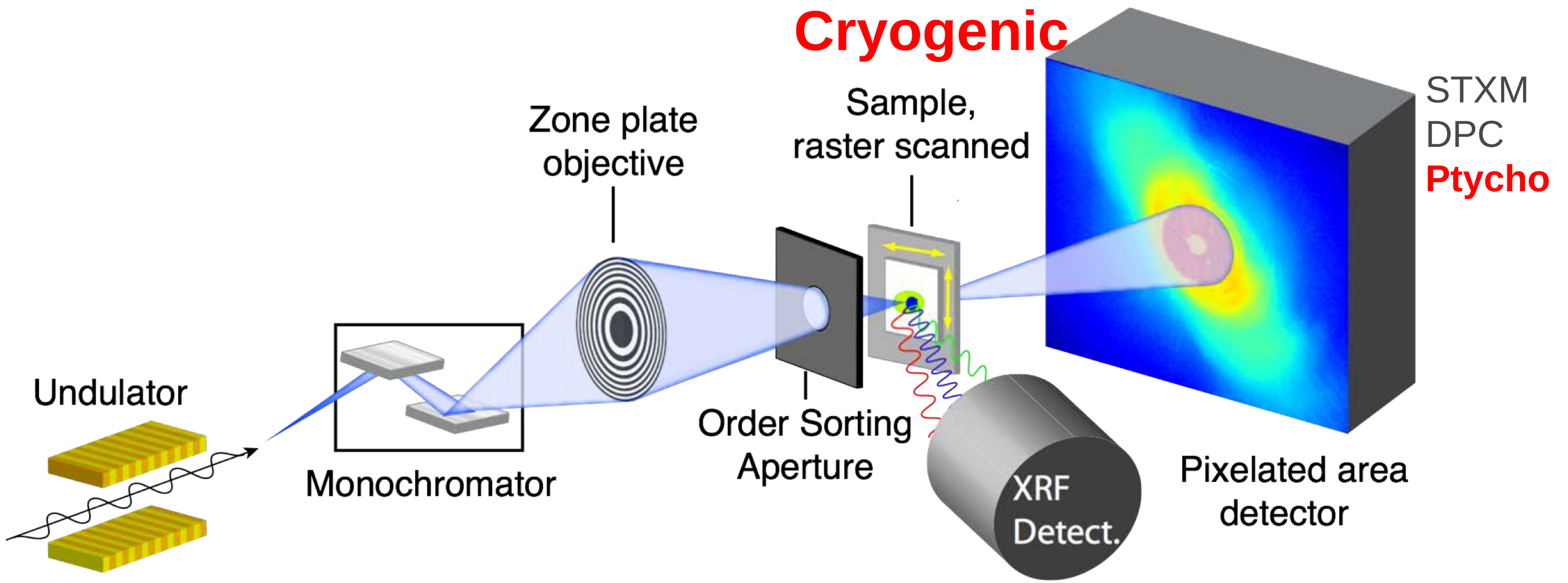

J. Deng, *et al. PNAS* **112**, 2314-2319 (2015)

- **Frozen-hydrated samples:** closer to natural state, reduce radiation damage
- **Fluorescence:** quantitative elemental composition
- **Ptychography:** structure information with high resolution

Courtesy Dr. Junjing Deng (APS)

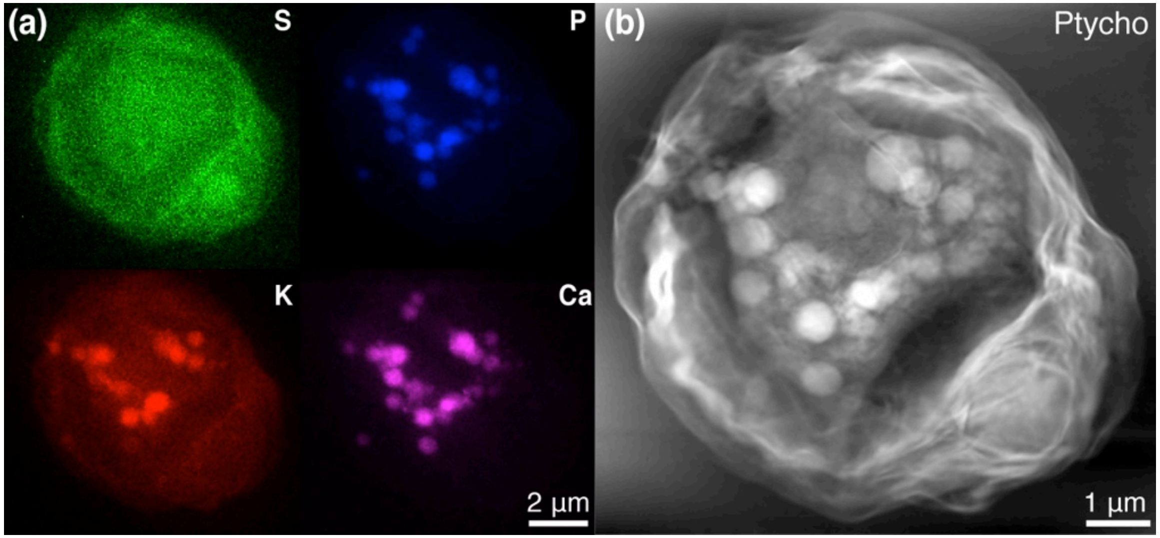

J. Deng, *et al. Sci. Rep.* (accepted)

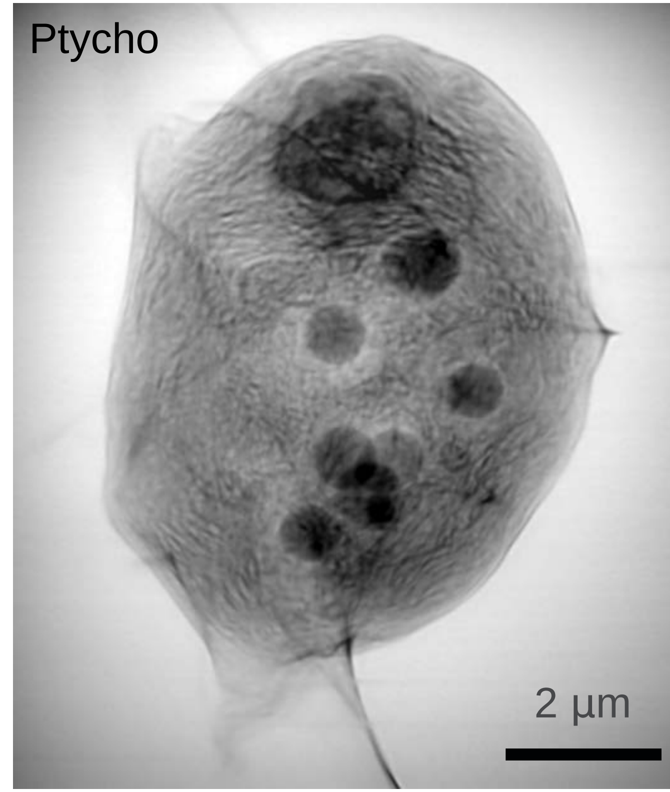

- Frozen-hydrated *Chlamy.* Alga
- Ptychographic image resolution: ~18 nm
- Fluorescence image resolution:~ 100 nm
- Complementary information helps with sample analysis

Courtesy Dr. Junjing Deng (APS)

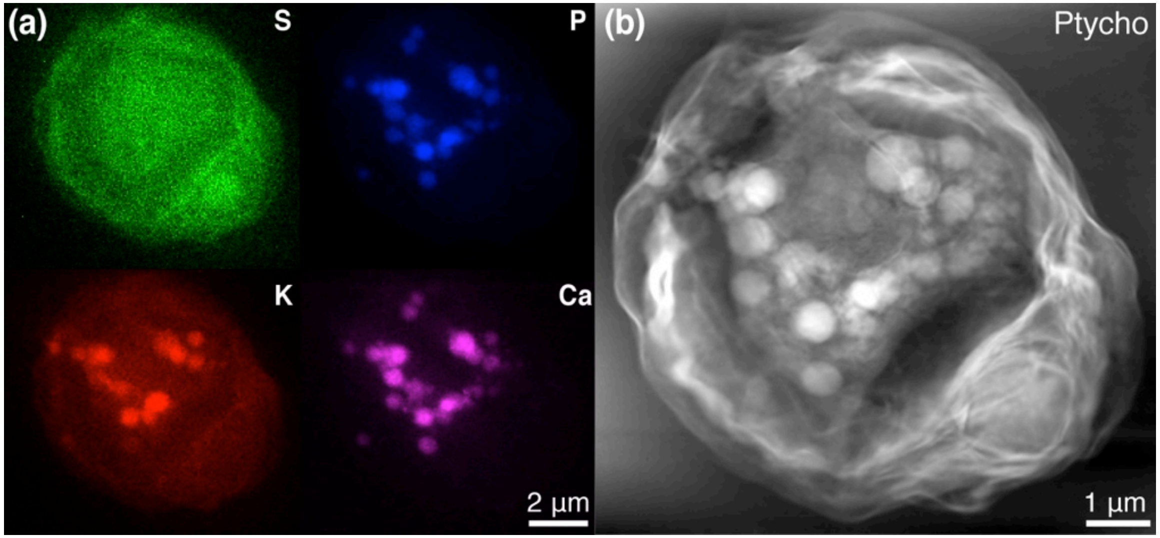

J. Deng, *et al. Sci. Rep.* (accepted)

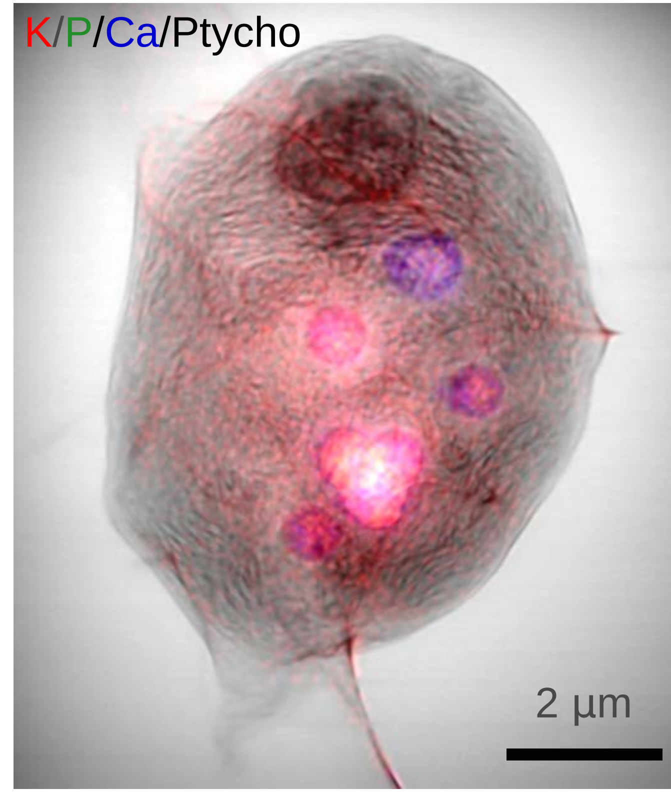

- Frozen-hydrated *Chlamy.* Alga
- Ptychographic image resolution: ~18 nm
- Fluorescence image resolution:~ 100 nm
- Complementary information helps with sample analysis

Courtesy Dr. Junjing Deng (APS)

Argonne NATIONAL LABORATORY

Extended to 3D

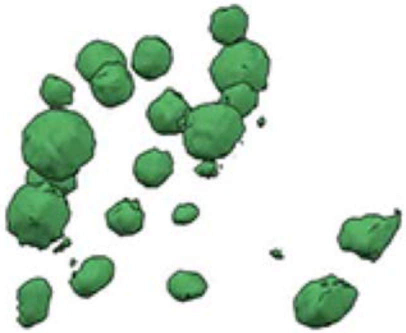

P

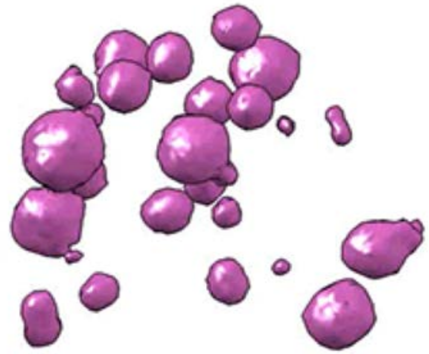

Ca

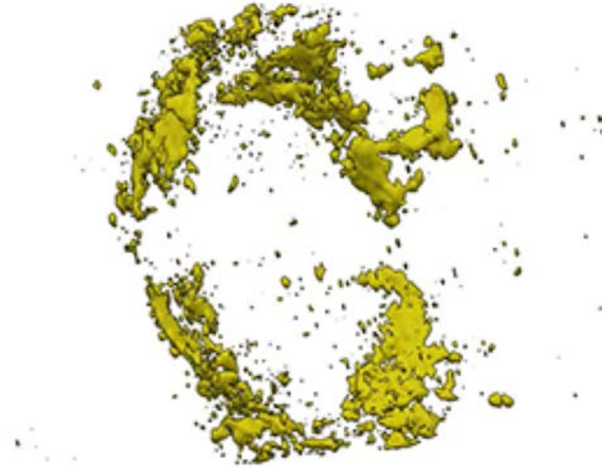

Cl

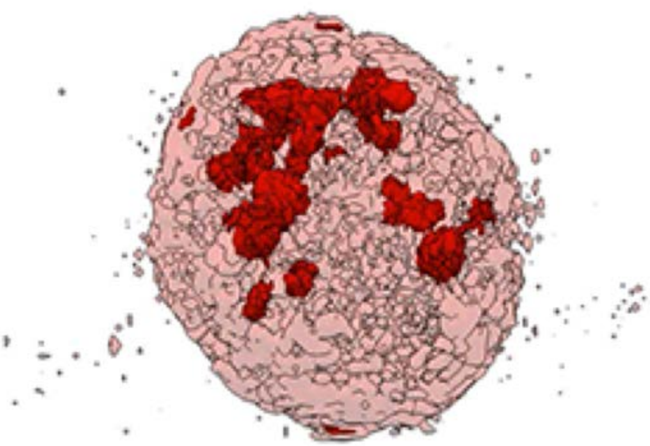

K

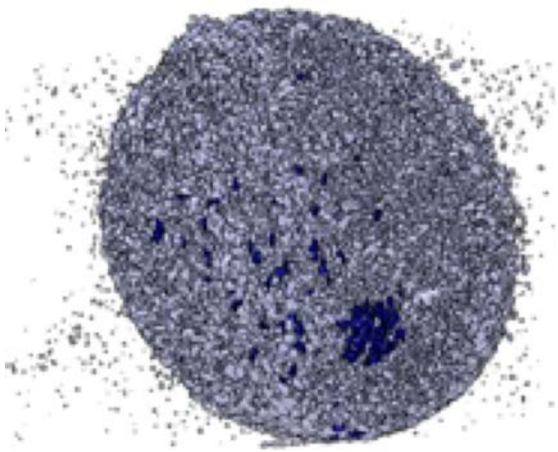

S

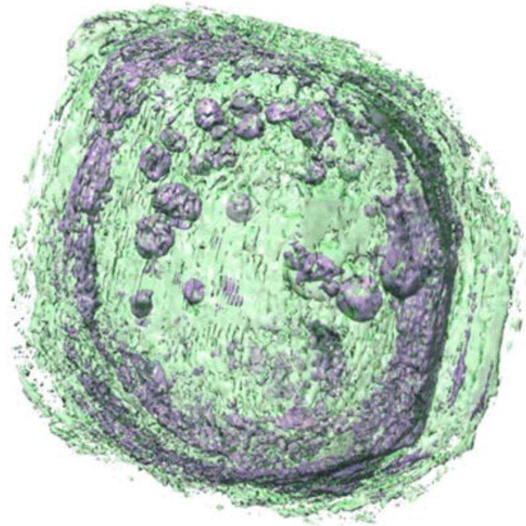

Ptycho

(In preparation)

Courtesy Dr. Junjing Deng (APS)

❖ Ptychographic spectroscopy

-- like STXM XNEAS analysis, but with higher resolution and more information (both absorption and phase) from refractive index

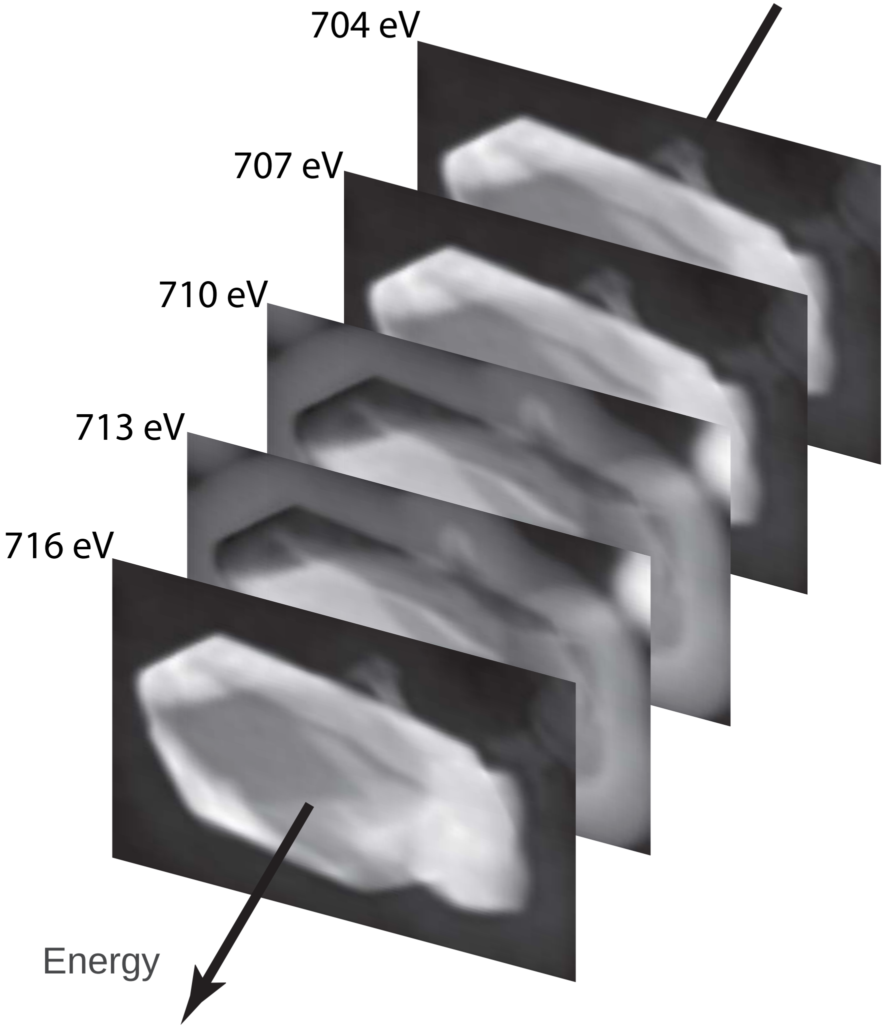

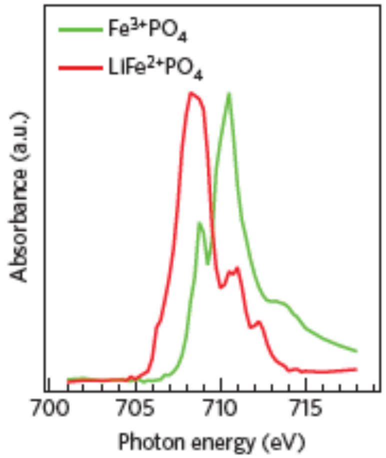

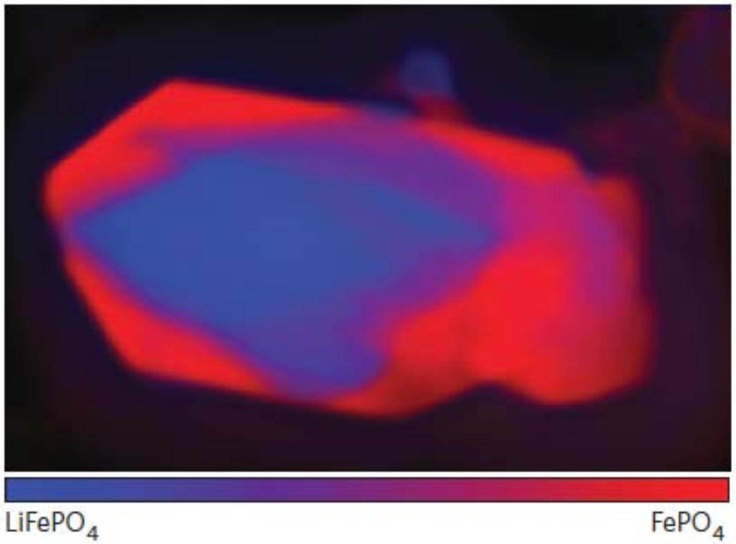

Adapted from D. Shapiro, *et al. Nat. Photon.* **8**, 765 (2014)

GDFE LAYERED MAGNETIC FILMS

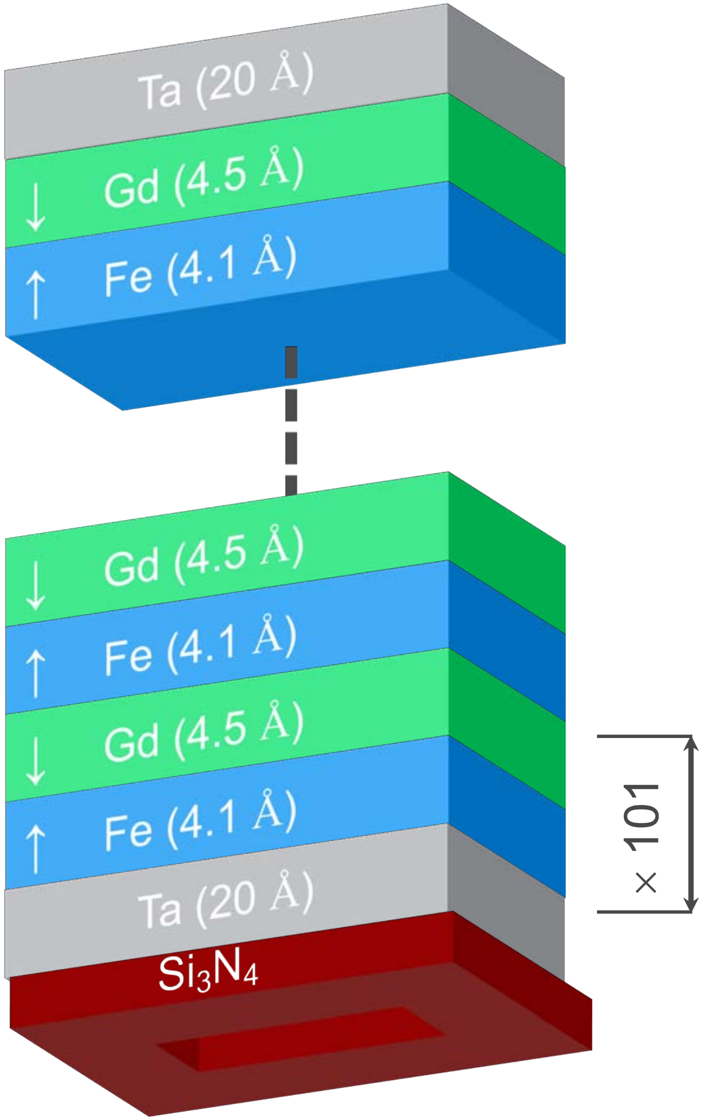

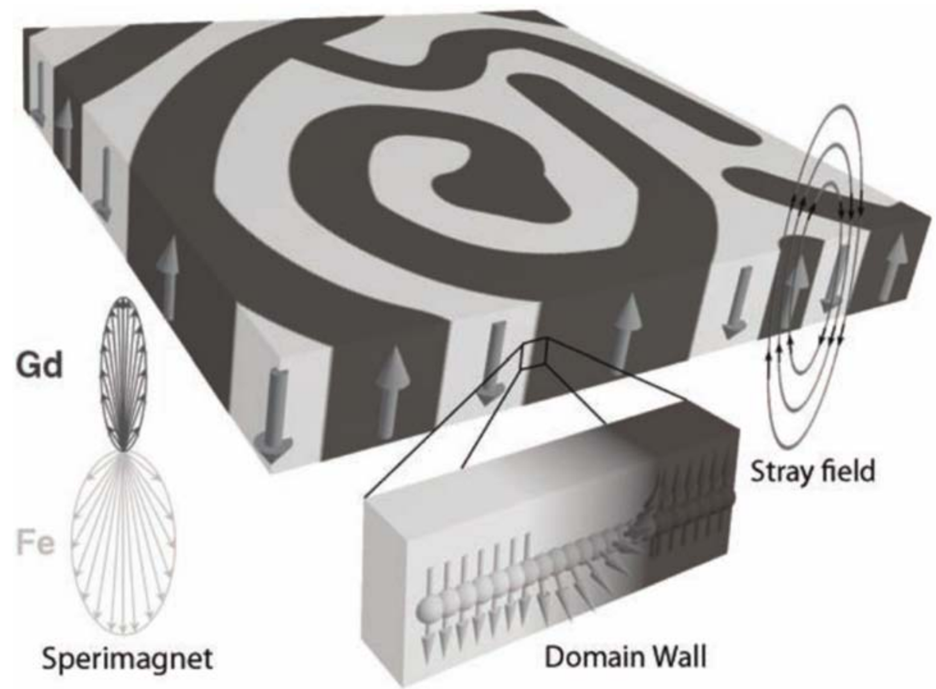

$$E_{tot} = \int [\, \underbrace{e_{ex}(\mathbf{m})}_{exchange} + \underbrace{e_{an}(\mathbf{m})}_{anisotropy} - \underbrace{\mu_0 \mathbf{H_{ex}} \cdot \mathbf{M}}_{ext.\, field} + \underbrace{\frac{1}{2}\mu_0 \mathbf{H_d^2}}_{stray\, field} \,]\, dV$$

A. Tripathi, O.S. et al., Proc Natl Acad Sci USA 108, 13393 (2011)

Argonne NATIONAL LABORATORY

MAGNETIC CONTRAST MECHANISM

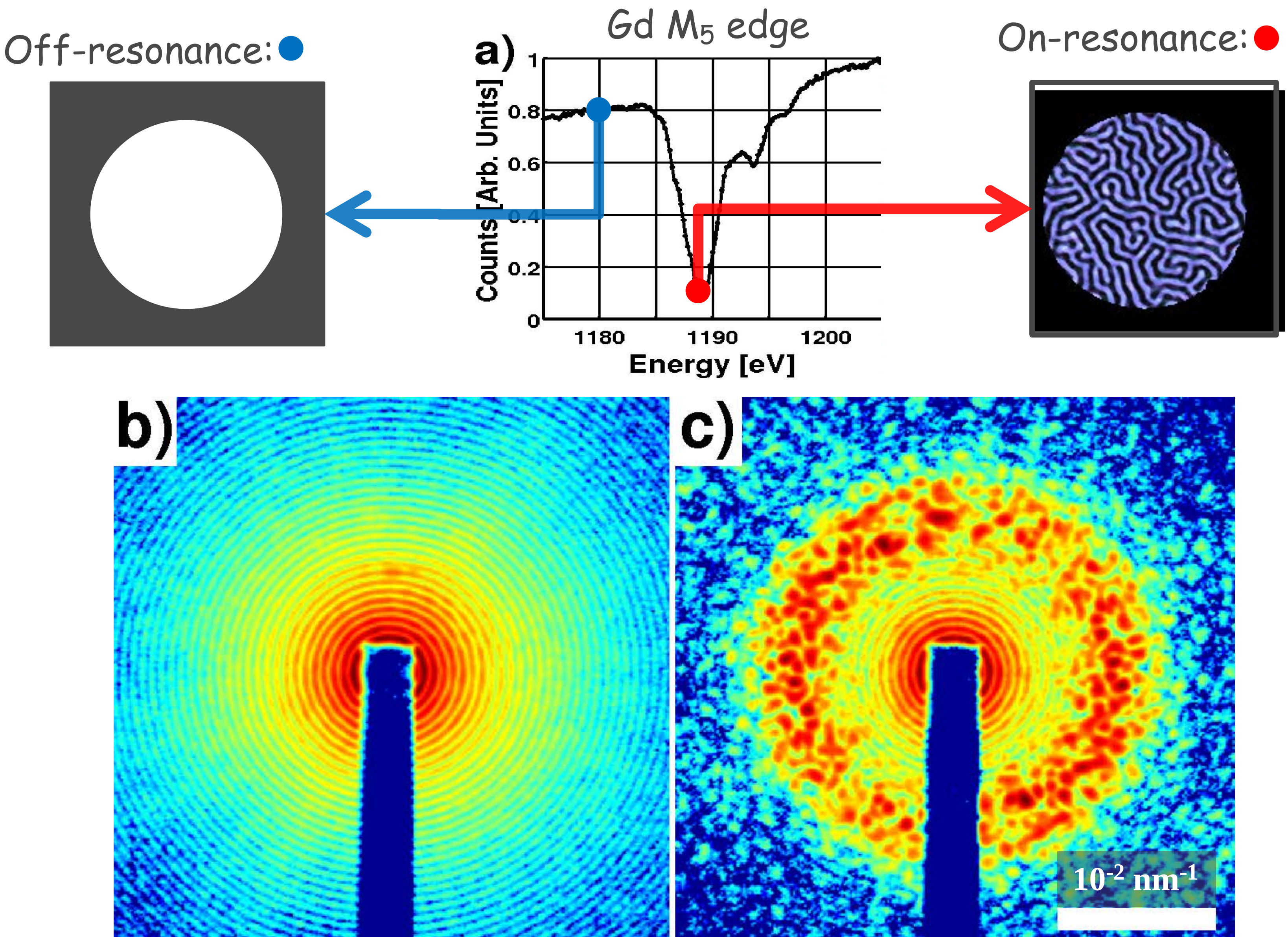

A. Tripathi, O.S. et al., Proc Natl Acad Sci USA 108, 13393 (2011)

REAL SPACE RECONSTRUCTION

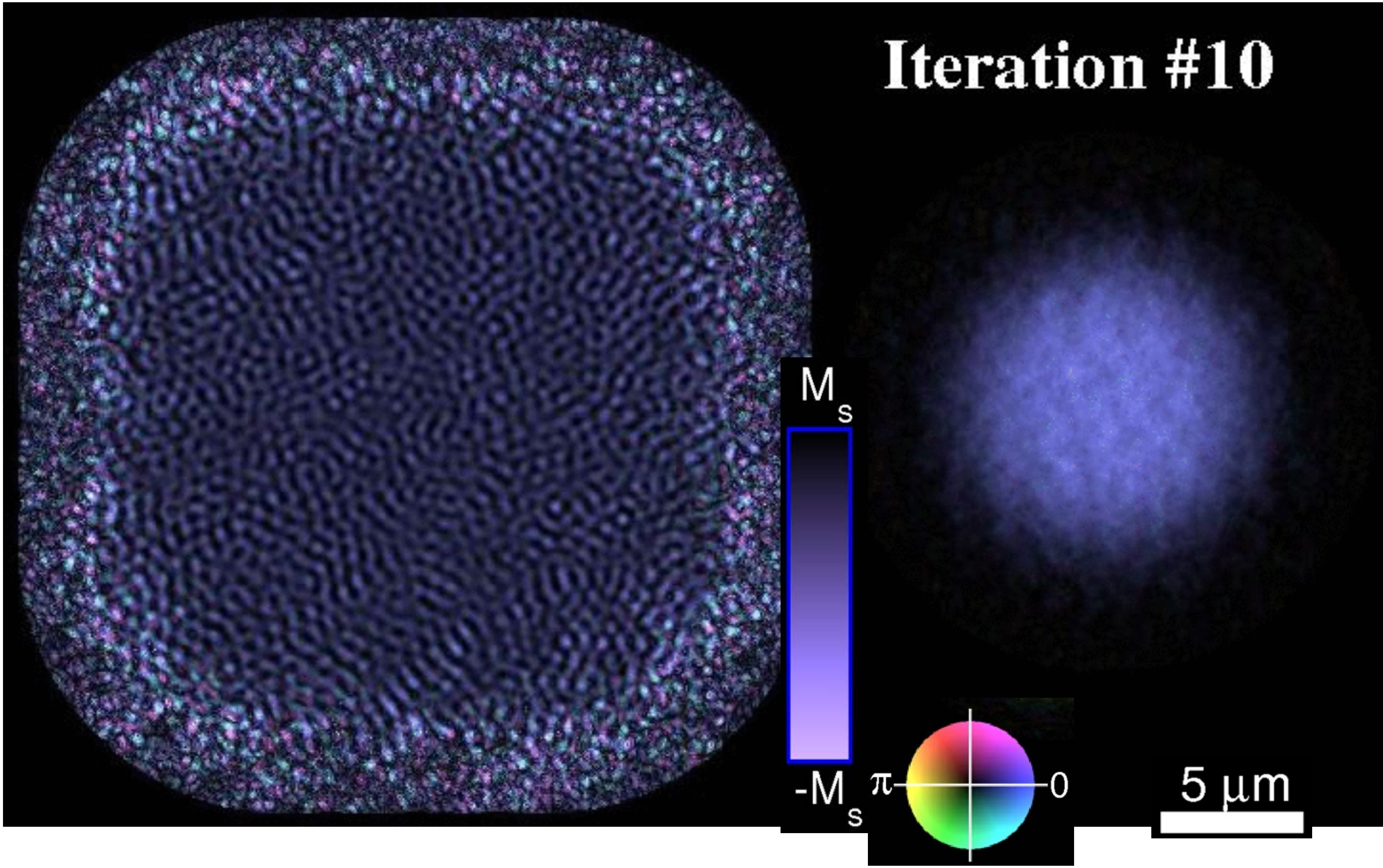

Magnetic structure (exit wave)

Illumination Function

A. Tripathi, O.S. et al., Proc Natl Acad Sci USA 108, 13393 (2011)

REAL SPACE RECONSTRUCTION

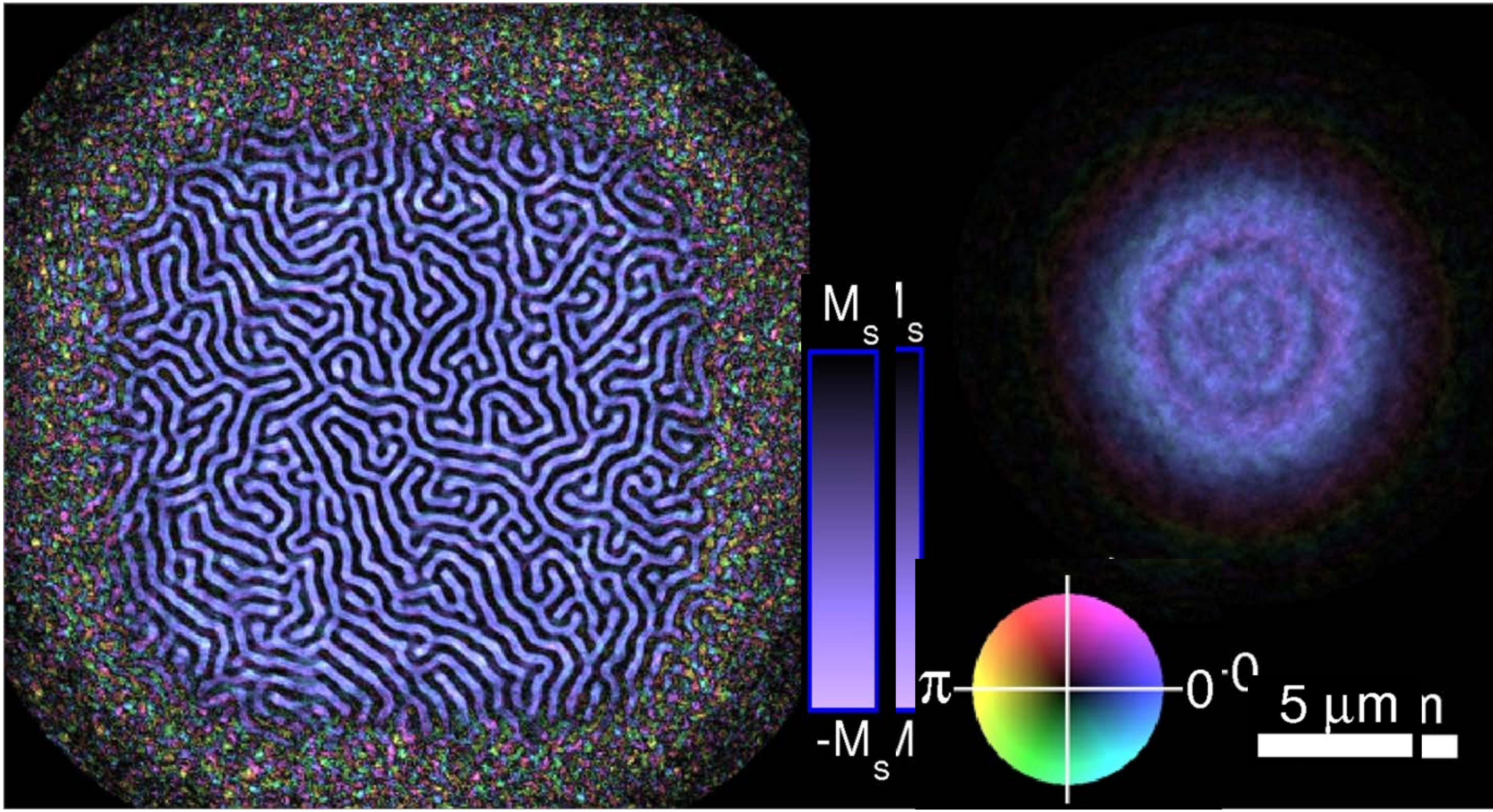

Magnetic structure
(exit wave)

Illumination Function

A. Tripathi, O.S. et al., Proc Natl Acad Sci USA 108, 13393 (2011)

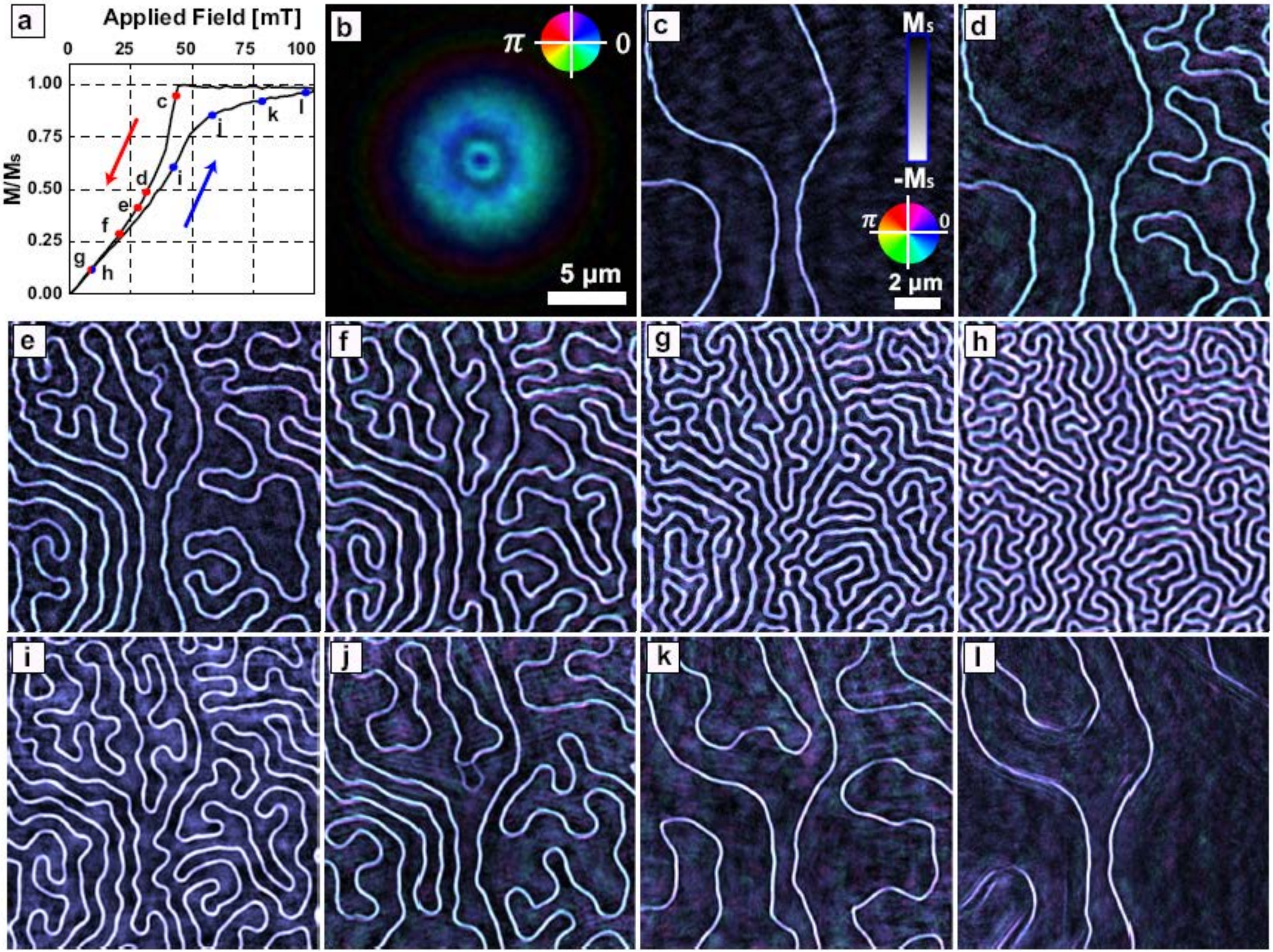

A. Tripathi, O.S. et al., Proc Natl Acad Sci USA 108, 13393 (2011)

INCREASING FIELD

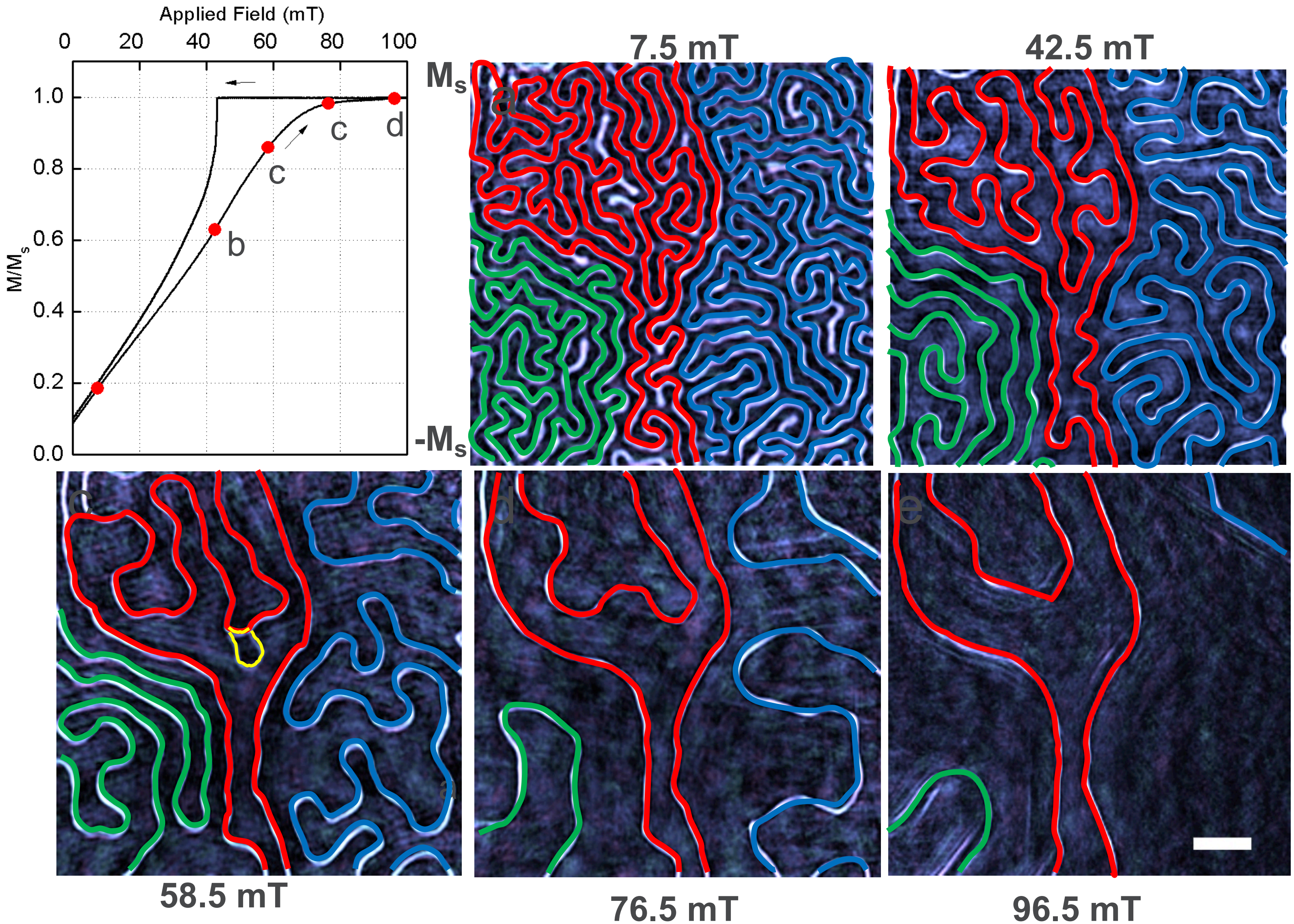

A. Tripathi, O.S. et al., Proc Natl Acad Sci USA 108, 13393 (2011)

Nanoscale Strain in SiGe film devices

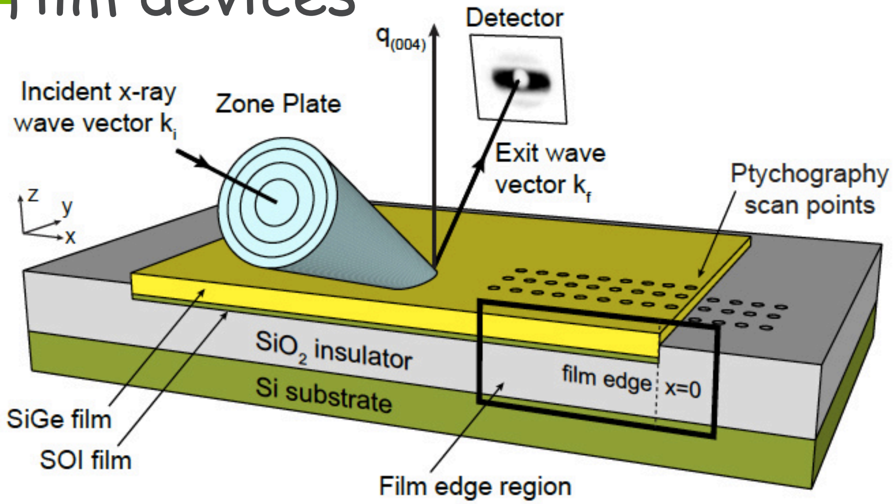

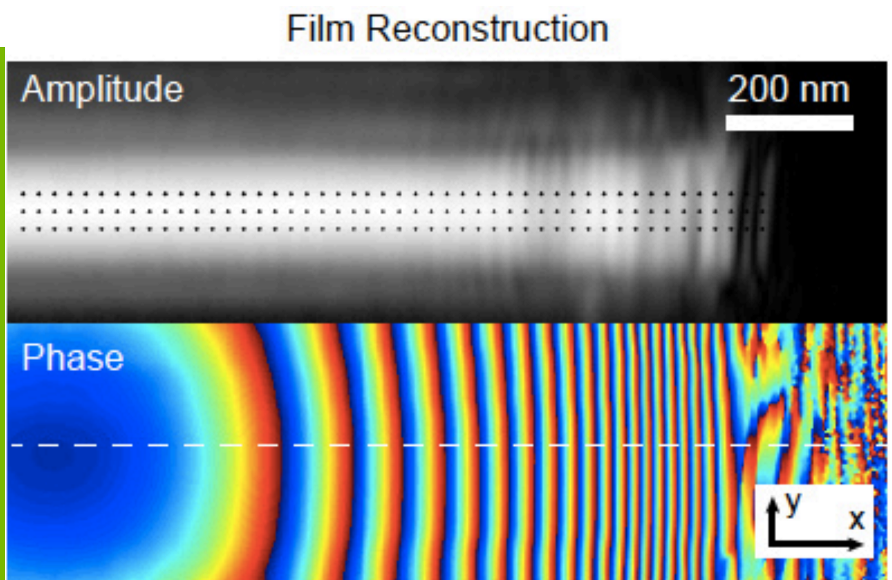

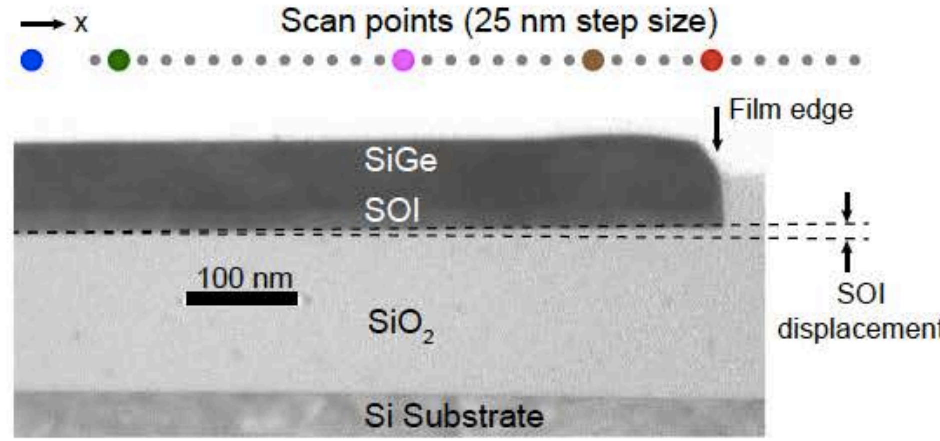

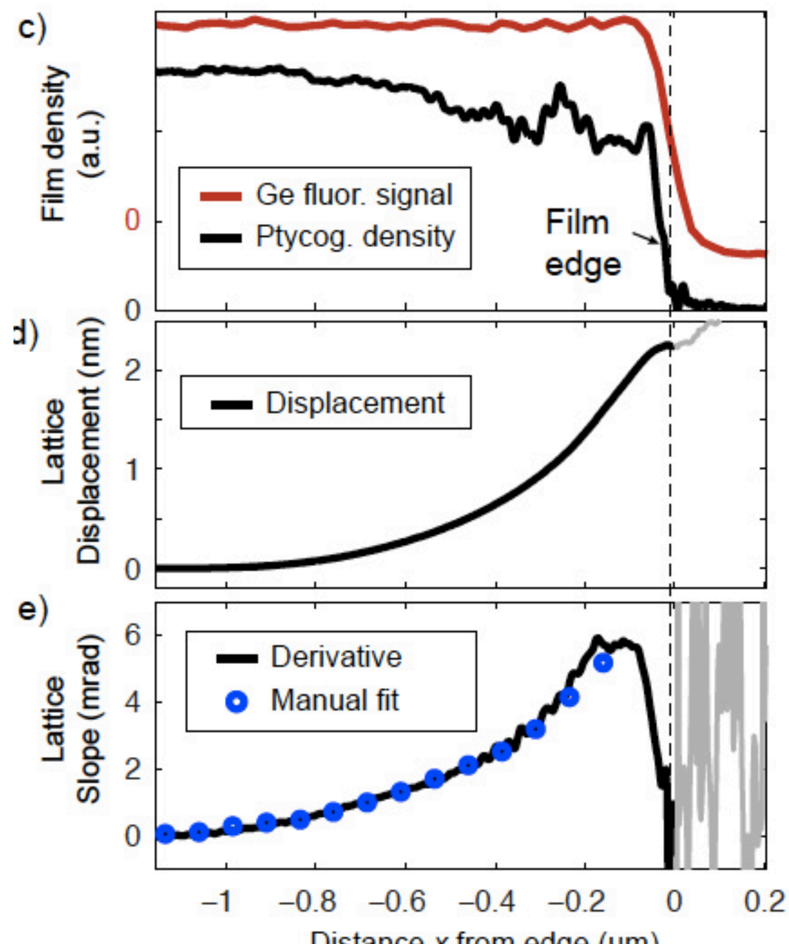

Hruszkewycz, S. O., Holt, M. V., et al. (2012). *Nano Letters*, *12*(10), 5148–5154.

SURFACE DIFFRACTION COHERENT IMAGING

- Image local surface structure
- Steps and step dynamics during film growth or interfacial reactivity
- Nanoparticle nucleation
- Defect distributions, particularly at interfaces
- Combined with x-ray micro fluorescence…..

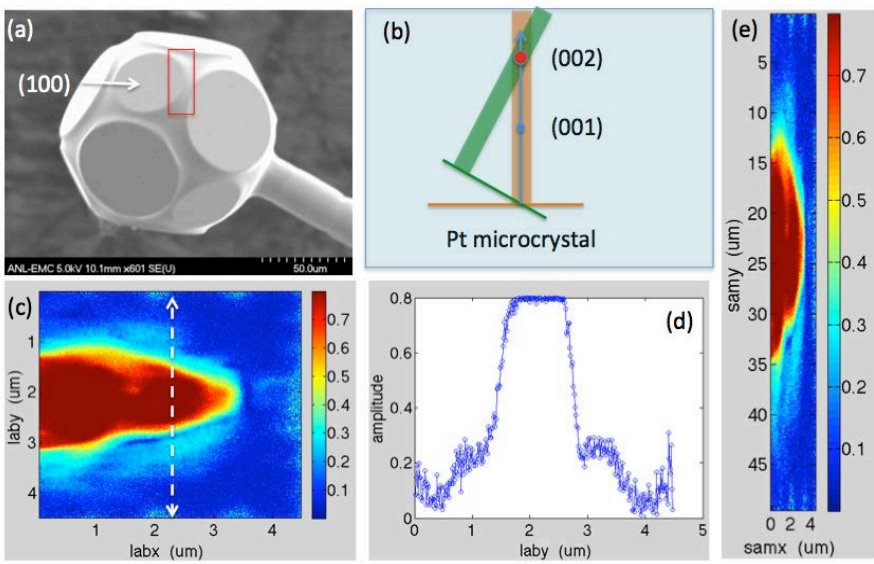

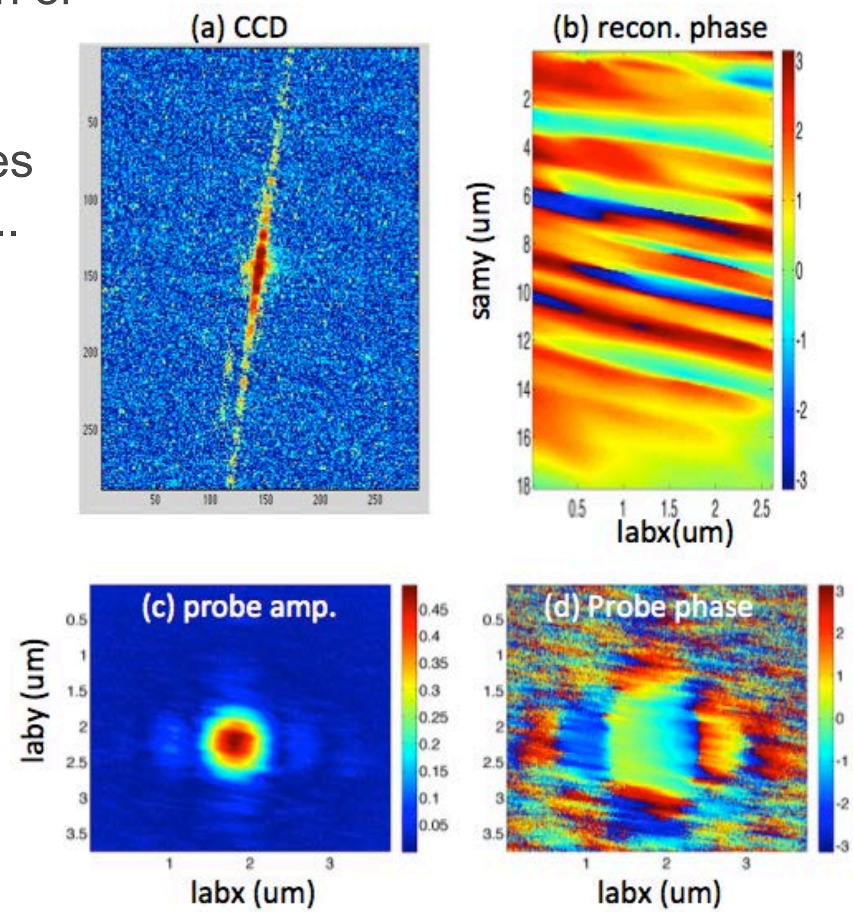

C. Zhu, et al. *Applied Physics Letters*, vol. 106, no. 10, p. 101604, Mar. 2015.

APPLY FOR COHERENT IMAGING BEAMTIME @ APS!

Bragg CDI

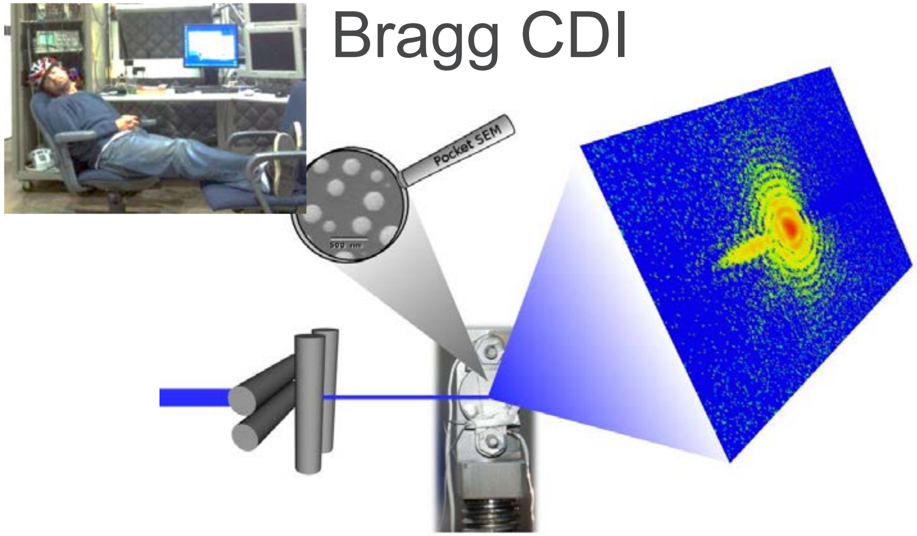

Email: Ross Harder rharder@aps.anl.gov
https://wiki-ext.aps.anl.gov/s34idc/index.php/34-ID-C

Ptychography Tomography

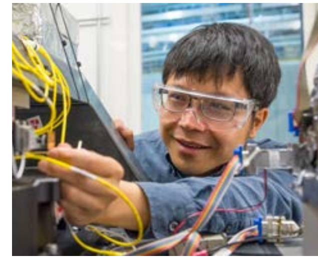

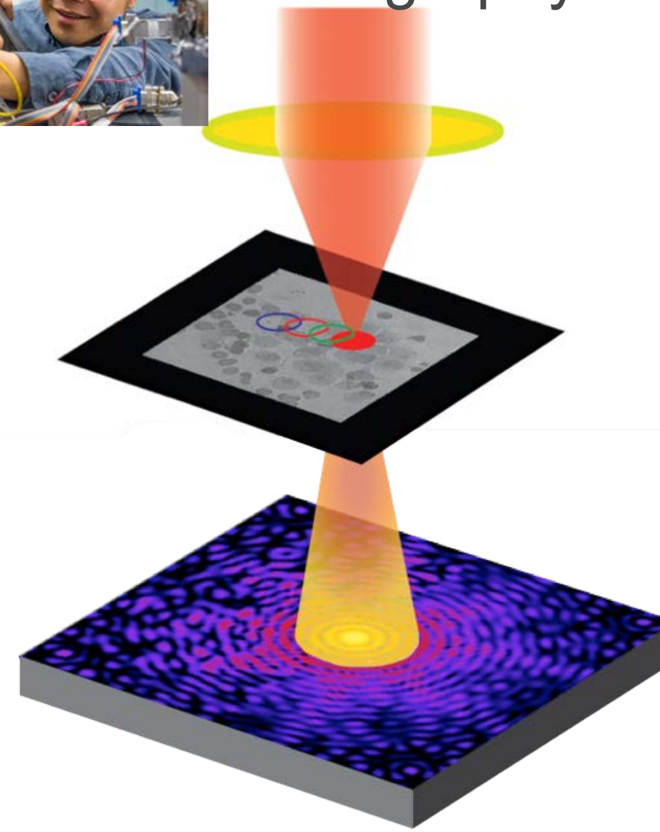

Email: Junjing Deng junjingdeng@aps.anl.gov

Bragg Ptychography

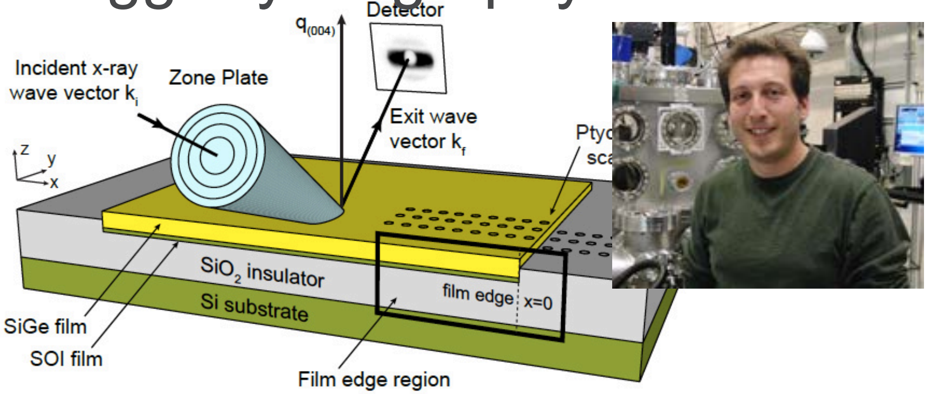

Email: Martin Holt mvholt@anl.gov
https://wiki-ext.aps.anl.gov/s26id/index.php/26-ID

https://www.aps.anl.gov/Users-Information